

QUANTIFICATION OF UNCERTAINTY IN RESERVOIR SIMULATIONS
INFLUENCED BY VARYING INPUT GEOLOGICAL PARAMETERS, MARIA
RESERVOIR, CAHU FIELD

A Thesis

by

KARINE CHRYSTEL SCHEPERS

Submitted to the Office of Graduate Studies of
Texas A&M University
in partial fulfillment of the requirements for the degree of

MASTER OF SCIENCE

May 2003

Major Subject: Geology

QUANTIFICATION OF UNCERTAINTY IN RESERVOIR SIMULATIONS

INFLUENCED BY VARYING INPUT GEOLOGICAL PARAMETERS, MARIA

RESERVOIR, CAHU FIELD

A Thesis

by

KARINE CHRYSTEL SCHEPERS

Submitted to the Office of Graduate Studies of
Texas A&M University
in partial fulfillment of the requirements for the degree of

MASTER OF SCIENCE

Approved as to style and content by:

Wayne M. Ahr
(Chair of Committee)

Duane A. Mc Vay
(Member)

Hongbin Zhan
(Member)

Andrew Hajash
(Head of Department)

May 2003

Major Subject: Geology

ABSTRACT

Quantification of Uncertainty in Reservoir Simulations Influenced by Varying Input
Geological Parameters, Maria Reservoir, CaHu Field. (May 2003)
Karine Chrystel Schepers, B.S., Institut Geologique Albert-de-Lapparent
Chair of Advisory Committee: Dr. W. Ahr

Finding and developing oil and gas resources requires accurate geological information with which to formulate strategies for exploration and exploitation ventures. When data are scarce, statistical procedures are sometimes substituted to compensate for the lack of information about reservoir properties. The most modern methods incorporate geostatistics.

Even the best geostatistical methods yield results with varying degrees of uncertainty in their solutions. Geological information is, by its nature, spatially limited and the geoscientist is handicapped in determining appropriate values for various geological parameters that affect the final reservoir model (Massonnat, 1999).

This study focuses on reservoir models that depend on geostatistical methods. This is accomplished by quantifying the uncertainty in outcome of reservoir simulations as six different geological variables are changed during a succession of reservoir simulations. In this study, variations in total fluid produced are examined by numerical modeling. Causes of uncertainty in outcomes of the model runs are examined by changing one of six geological parameters for each run.

The six geological parameters tested for their impact on reservoir performances include the following: 1) variogram range used to krig thickness layers, 2) morphology around well 14, 3) shelf edge orientation, 4) bathymetry ranges attributed for each facies, 5) variogram range used to simulate facies distribution, 6) extension of the erosion at top of the reservoir. The parameters were assigned values that varied from a minimum to a maximum quantity, determined from petrophysical and core analysis.

After simulation runs had been completed, a realistic, 3-dimensional reservoir model was developed that revealed a range of reservoir production data. The parameters that had the most impact on reservoir performance were: 1) the amount of rock eroded at the top of the reservoir zone and 2) the bathymetry assigned to the reservoir facies.

This study demonstrates how interaction between geological parameters influence reservoir fluid production, how variations in those parameters influence uncertainties in reservoir simulations, and it highlights the interdependencies between geological variables.

The analysis of variance method used to quantify uncertainty in this study was found to be rapid, accurate, and highly satisfactory for this type of study. It is recommended for future applications in the petroleum industry.

DEDICATION

This effort is dedicated to:

*Ma grand mère, qui s'est envolée lorsque je rédigeais cette thèse.
Que le succès de cette thèse soit une flamme au fond de tes yeux, tes ailes pour le
Paradis, et la preuve la plus pure de mon amour pour toi.
Love.*

ACKNOWLEDGMENTS

I would like to express my sincerest appreciation to Dr. Wayne Ahr, chair of my advisory committee, for his help not only in constructing and completing this thesis, but also in my professional formation.

I would like to thank Dr. Duane Mc Vay, member of my advisory committee, for his constant orientation and constructive discussions and opinions.

I address my gratitude to Dr. Zhan, for his service as member of my advisory committee, and to Dr. Hajash, Head of the Geology and Geophysics Department, for giving me the opportunity of being part of the best Geology program.

I am also grateful to the faculty and staff at the Halbouty Department of Geology and Geophysics, and at the Harold Vance Department of Petroleum Engineering for their support during my studies at Texas A&M University.

And finally, I want to thank my friends Ahmed and Zoon for their unconditional and permanent company and encouragement.

TABLE OF CONTENTS

	Page
ABSTRACT	iii
DEDICATION	v
ACKNOWLEDGMENTS.....	vi
TABLE OF CONTENTS	vii
LIST OF TABLES	x
LIST OF FIGURES.....	xii
 CHAPTER	
I INTRODUCTION.....	1
II BACKGROUND	4
2.1 Data Available for the Study.....	4
2.2 Previous Works	4
2.2.1 Geological Models	4
2.2.2 Reservoir Models	5
2.2.3 Sensitivity Analysis.....	5
III GEOLOGICAL SETTING OF FIELD AREA	6
3.1 Regional Setting.....	6
3.1.1 Middle Cretaceous	6
3.1.2 Upper Cretaceous	8
3.2 Structural Setting.....	9
3.2.1 Regional Characteristics.....	9
3.2.2 Field Characteristics.....	9
3.3 Stratigraphic Setting.....	13
3.3.1 Alban Formation	13
3.3.2 Cyclical Stratigraphic Units in the Maria Formation.....	13
3.3.3 Jose Formation	18
3.3.4 Cycle 1-Alban Limit: Sb1	18
3.4 Gocad Models	18

CHAPTER	Page
IV RESERVOIR SIMULATION.....	21
4.1 Model Input	21
4.1.1 Current Model	21
4.1.2 Upscaling.....	22
4.1.3 Reservoir Grid	23
4.1.4 Petrophysics.....	23
4.1.5 Rock Properties	30
4.1.6 Fluid Properties	30
4.1.7 Well Modeling and Production Constraints	32
4.2 Model Initialization	36
4.2.1 Compartments.....	36
4.2.2 WOC.....	36
4.2.3 Pressure Volume Temperature Data (PVT Data)	37
4.2.4 Pressure Regime	37
4.2.5 Simulation Results.....	37
V QUANTIFICATION OF UNCERTAINTY.....	39
5.1 Philosophy of Quantification of Uncertainty	39
5.2 Design of Experiment	40
5.2.1 Method Used to Build the Models Data Set.....	40
5.2.2 Method Used to Combine the 6 Parameters	41
5.3 Analysis of the Response Variables	52
5.3.1 Run Order Influence.....	52
5.3.2 Response Variable Distribution	58
5.4 Influence of Individual Parameters	64
5.4.1 Classification of Models	64
5.4.2 Influence of Individual Parameters	67
5.5 Quantification of Uncertainty	82
5.5.1 DEX Mean Slope Method.....	82
5.5.2 Analysis of Variance Method: Effects and Interactions	86
VI RESULTS AND DISCUSSION	96
6.1 Quantification of Uncertainty.....	96
6.1.1 Impact of Each Geological Factor on the Reservoir Performances	96
6.1.2 Discussion of the Impact of Each Factor	99
6.2 Discussion on the Different Methods of Quantification	110
VII CONCLUSIONS.....	114

	Page
REFERENCES CITED	116
APPENDICES.....	118
VITA	155

LIST OF TABLES

	Page
Table 1 Facies description (modified from Lodola, 2002a,).....	16
Table 2 Porosity range per facies	24
Table 3 Porosity permeability law for each facies	25
Table 4 Capillary pressure and relative permeability table.....	26
Table 5 Krg and Krog values, $Sw_i=6\%$	28
Table 6 PVT summary	31
Table 7 The complete PVT data set incorporated inside the reservoir model	32
Table 8 Well coordinates implemented in this study	35
Table 9 Matrix of the first coded 35 models	43
Table 10 Matrix of the last coded 31 models	44
Table 11 First 32 models reorganized, example of the RF: -1 level models.....	65
Table 12 Last 32 models organized, for OOIP: level +1models for all factors	66
Table 13 Effect of each factor on the OOIP	83
Table 14 Effect of each factor on the recovery	83
Table 15 Effect of each factor on the Np	84
Table 16 Effect of each factor on the Wp/Np	84
Table 17 Effect of each factor on the GP/Np	85
Table 18 Constant contrasts table.....	88
Table 19 OOIP factor coefficient effect, part 1	91
Table 20 OOIP factor coefficient effect, part 2.....	92
Table 21 Quantification of uncertainty for each factor and its interactions	94
Table 22 ANOVA coefficient effects.....	97
Table 23 Effect of each factor on all response variables.....	100
Table 24 Comparison mean slope and ANOVA methods for OOIP	110
Table 25 Comparison mean slope and ANOVA methods for recovery.....	111
Table 26 Comparison mean slope and ANOVA methods for Np.....	111

	Page
Table 27 Comparison mean slope and ANOVA methods for W_p/N_p	112
Table 28 Comparison mean slope and ANOVA methods for G_p/N_p	112

LIST OF FIGURES

	Page
Figure 1 Regional stratigraphy	7
Figure 2 Aerial picture of the field.....	11
Figure 3 A block diagram illustrating the main environments (after Guy et al., 2000) ...	15
Figure 4 Paleobathymetry profile, Maria Formation (modified from Lodola, 2002a) ...	17
Figure 5 Kr curves	27
Figure 6 Capillary pressure curve for the entire field	27
Figure 7 Relative permeability gas (Krg) and oil (Krog) curves	29
Figure 8 Previous well completions	33
Figure 9 Well completion implemented in this study	34
Figure 10 Np ranges vs time (from 66 models)	45
Figure 11 Recovery range vs time (from 66 models).....	46
Figure 12 GOR range vs time (from 66 models)	47
Figure 13 Fw range vs time (from 66 models).....	48
Figure 14 Gp range vs time (from 66 models)	49
Figure 15 Wp range vs time (from 66 models)	50
Figure 16 OOIP plot vs run order.....	53
Figure 17 Recovery factor vs run time.....	54
Figure 18 Cumulative oil produced vs run order	55
Figure 19 Wp/Np ratio versus run order	56
Figure 20 Gp/Np ratio versus run order	57
Figure 21 OOIP frequency histogram	59
Figure 22 Recovery factor frequency histogram.....	60
Figure 23 Cumulative oil production frequency histogram	61
Figure 24 Wp/Np ratio frequency histogram	62
Figure 25 Gp/Np ratio frequency histogram	63
Figure 26 OOIP DEX scatter plot	68

	Page
Figure 27 Recovery factor DEX scatter plot.....	70
Figure 28 Cumulative oil produced DEX scatter plot.....	71
Figure 29 Wp/Np ratio DEX scatter plot	72
Figure 30 Gp/Np ratio DEX scatter plot	73
Figure 31 OOIP DEX mean plot.....	75
Figure 32 OOIP DEX mean plot without erosion factor plotted.....	76
Figure 33 Recovery factor DEX mean plot.....	77
Figure 34 Cumulative oil produced DEX mean plot.....	79
Figure 35 Wp/Np ratio DEX mean plot	80
Figure 36 Gp/Np ratio DEX mean plot	81
Figure 37 2 ² factorial design.....	86
Figure 38 Gocad models: shelf edge orientation and facies repartition.....	102
Figure 39 Bathymetry range for levels -1 and +1 (after Lodola, 2002b)	103
Figure 40 Injector locations compared to reservoir elongation.....	108

CHAPTER I

INTRODUCTION

In petroleum exploration, even when abundant information is available from core and petrophysical data, some geological parameters remain unknown, creating a certain degree of uncertainty about the “true” geological model. For example, it is very difficult to reconstruct the paleo-water depth that existed at the time reservoir rocks were deposited. Without specific seismic data to pinpoint subsurface features, the degree of slope and orientation of shelf-slope break are also very difficult to determine.

On the other hand, it is the geoscientist’s job to build 3D geological models in spite of the uncertainties that may exist in data. In such cases, geostatistical methods are commonly utilized. These methods employ variograms to predict spatial distribution of geological properties in subsurface space. The three dimensional distribution of reservoir facies can be simulated using variograms enabling geologists to estimate the areal extent of the facies, but a level of uncertainty still exists.

In this thesis, a field that produces from a carbonate reservoir has been chosen for study. A geological model in three dimensions was constructed from available geological data using the geostatistical software GOCAD®. In this study, six geological - geostatistical parameters, called factors, were identified as key parameters that influence uncertainty. The following conditions had to be established to apply the geostatistical program and evaluate the degree of uncertainty imposed by each of the condition:

This thesis follows the style and format of American Association of Petroleum Geologists Memoir.

1. The range of the variogram used to obtain formation layer thickness and kriging residuals
2. The range of the variogram used to obtain spatial dimensions of reservoir facies by kriging.
3. The vertical thickness of each layer inside the reservoir zone in the Cretaceous Maria Formation.
4. The amount of rock thickness removed by erosion of the top of the reservoir zone.
5. The range of bathymetry attributed to each facies over the field.
6. The influence of platform slope-break orientation (N-S; E-W) on facies character.

Each of the six parameters could take only two values, a minimum and a maximum, determined from analogous field, regional setting and field data.

The objectives of this thesis are to identify and analyze quantitatively the impact of the uncertain geological and geostatistical parameters on hydrocarbon production in the field. To ascertain the impact on uncertainty caused by changes in the values of each parameter, different geological models were built. Each model includes specific values for each of the six parameters, resulting in the construction of 2^6 , or 64 models. Determinations had to be made on the influence of each of the six factors, called response variables, on the total liquid recovery, the proportion of oil in total liquids, the quantity of gas and water produced, and the amount of original oil in place. To achieve these objectives, a reservoir model was built using Eclipse® software.

A black oil model (only gas and oil are produced) was created based on data from previous studies conducted by Total engineers. The simulated reservoir model was programmed to “produce” for a period of 30 years with water injection beginning in 1999. As the reservoir simulation ran, different geological models were incorporated one at a time so that production and reservoir performance characteristics would vary

depending on which geological model was used. In turn, each geological model varied as the 6 key geological parameters, or “factors” were modified.

A data base was constructed for each response variable (factor) and it indicated that the data were arrayed in a bimodal distribution. A statistical analysis was then performed to rank the comparative impact of each geological and geostatistical factor. The method chosen was an analysis of variance (ANOVA) method in which a percentage effect was attributed to each factor. This percentage quantifies the impact on the response variables caused by the changing the value of the geological parameters. As a result, the affect of each factor on each response variable could be determined.

Finally, several predictive regression models were defined by identifying the equations that link the factors and the response variables. Knowing the value of each of the six factors, the ultimate recovery, the total fluid produced, and the OOIP could be predicted for the field over the 30-year time span.

CHAPTER II

BACKGROUND

2.1 Data Available for the Study

All the technical words and abbreviations are explained in Appendix 68. The study utilized geological data from a carbonate reservoir of Cretaceous age in the Middle East. The data were provided with the generous support of TotalFinaElf Oil Company (hereafter referred to as Total); which requested that proprietary information about the location coordinates of wells and field boundaries be excluded from the completed thesis. Geological data provided for the study include: 1) a field base map, 2) wireline log data on all field wells, 3) a limited amount of petrophysical data from core analyses, 4) a generalized, interpretive geological model of the field as interpreted by TFE engineers and synthesized by Lodola, 2002a; 5) a compendium of previous studies on the field. Reservoir data in this study are from previous work by Guy et al., 2000, Laroche, 2000.

2.2 Previous Works

2.2.1 Geological Models

A number of geological models were built from 1991 through 2000, all of which describe a carbonate ramp with a shoal barrier, lagoonal, fore-shoal, slope and basin facies. The reservoir facies are the shoal and fore-shoal deposits. Seal facies are the lagoonal and basinal facies. The updated model used in this study (Lodola, 2002a) is used to refine the geological description of the 14 different facies identified for this study. Previous works incorporated only 7 facies. Bathymetric (paleo-depth) ranges were assigned to each facies in order for the software (Gocad®) to function properly.

2.2.2 Reservoir Models

The reservoir models employed in this study were simplified as compared with those in previous work by Total engineers. This was done in order to facilitate rapid and accurate, multiple computer runs to test for the significance of each geological parameter on outcome uncertainty in reservoir simulations. The types of simplifications made to the original setup are as follows:

- 1) Structural configuration of the reservoir area was simplified to omit faults.
- 2) Reservoir compartmentalization by sealing faults divided the field in previous models, resulting in variable initial pressure, differing oil-water-contacts, and unnecessarily complex behavior of reservoir fluids, e.g., different PVT values were assigned to each compartment.
- 3) The development scheme in previous studies included vertical, horizontal and deviated wells. In this study only vertical wells were modeled.

2.2.3 Sensitivity Analysis

Sensitivity analyses were performed previously by Laroche, 2000. He employed parameters based on the order of their comparative influence on reservoir performance, e.g., recovery factor, OOIP, and N_p . These parameters he chose include a structural description including the number and sealing quality of faults, the amount of stratigraphic section removed by erosion from the top of the reservoir, the total thickness of the reservoir, and a porosity cutoff.

Other conditions in Laroche's procedure included establishing a net-to-gross ratio (percent reservoir to non-reservoir rock) for stratigraphic cycle 2, a porosity map of the reservoir, a permeability map of the entire reservoir, and whether or not the OWC is tilted, the depth to the OWC in cycles 1 & 2, water saturation curves attributed for each rock type, and net formation volume factor for the reservoir. He did not perform quantification of uncertainty; therefore, the effect of each variable on uncertainty of outcome in simulation runs was not known.

CHAPTER III

GEOLOGICAL SETTING OF FIELD AREA

3.1 Regional Setting

The studied field is located on a stable shield where a thick sedimentary prism was deposited on the underlying Precambrian basement. The sedimentary prism thickens to the NE, where much of the sedimentary column is made up of Mesozoic and Cenozoic sediments (Leparmentier, 1981).

Most of the area was affected by halokinesis that created diapirs and domes. During Middle and Upper Cenomanian times, five main sedimentary formations were deposited in the area. They are, from the oldest to youngest, Manuello, Ivan, including the Alban, Marta, and Maria members, Jose and Rene formations (Figure 1). The Maria Formation is the reservoir studied in this thesis (from Leparmentier, 1981).

3.1.1 Middle Cretaceous

3.1.1.1 Manuello

The Manuello Formation was deposited during a transgression in Albian time and consists mainly of marl and shale that are interpreted to represent a low energy depositional environment.

3.1.1.2 Ivan Formation

The Ivan Formation was deposited during Albo-Cenomanian time and is divided into two members: the Alban-Marta and the Maria.

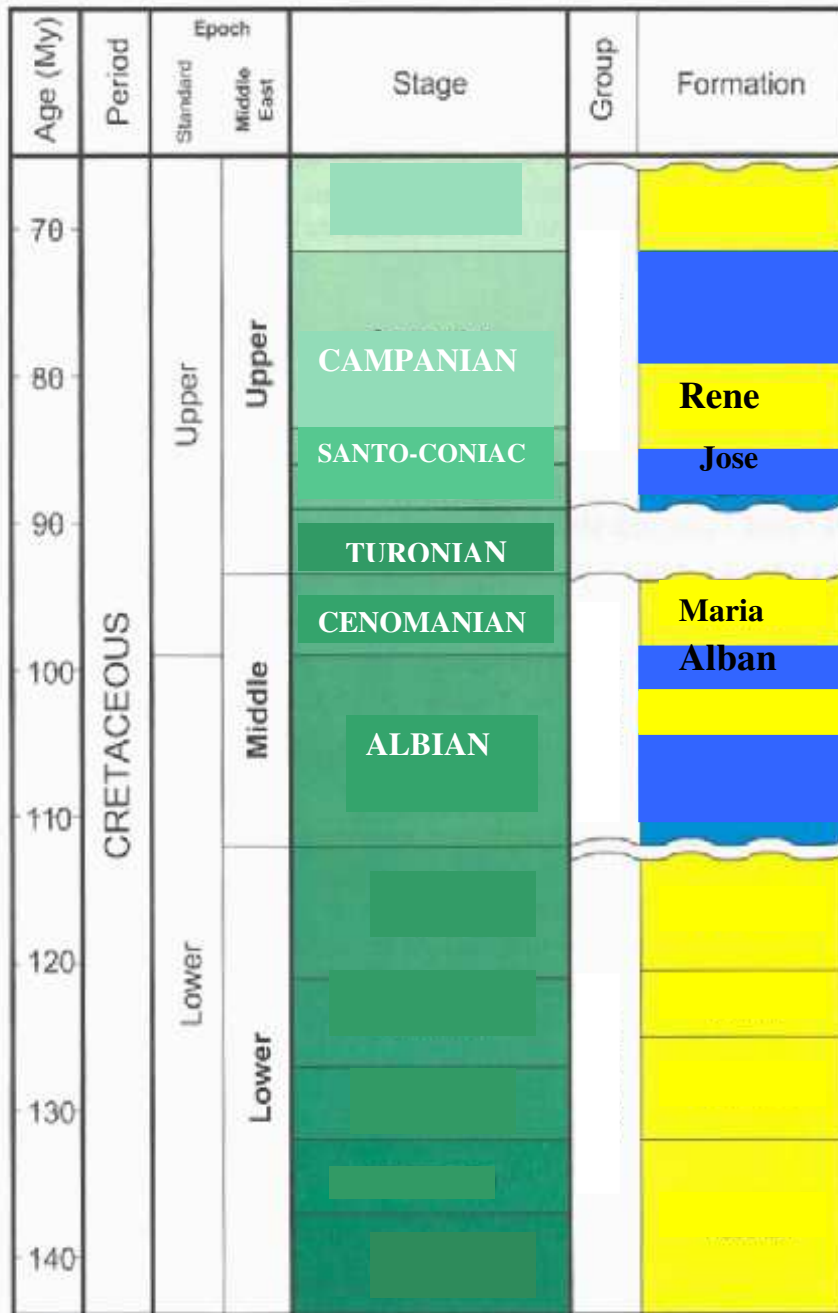


Figure 1: Regional stratigraphy

3.1.1.3 Alban-Marta

The Alban-Marta Formation is mainly a bituminous, lime mudstone-wackstone with abundant organic matter that suggests deposition in a restricted, euxinic basin.

3.1.1.4 Maria

The Maria Member was deposited during upper Cenomanian time as a grainstone-reef interval that developed on the shallow part of the Cenomanian ramp. The Maria Member passes laterally to the Alban Formation. The Maria Member can be divided into two zones, an upper packstone-grainstone unit containing abundant shell debris and coarse nummulitid foraminifera. This zone, called Maria cycle 2, is interpreted to have been deposited without erosion or reworking but in a “high energy” depositional environment. A lower, packstone to grainstone interval called Maria cycle 1 consists of shell hash similar to that in cycle 2. The contact between the Alban and Maria Members grades upwards from shelly packstones to mudstones and wackstones.

The cycle 2 reef is actually a biostrome composed of fine skeletal hash; consequently, one can draw a North- South barrier across the Alban ramp, separating the Alban gulf. Deposition of the Maria Member represents a shallowing-up of the Alban gulf accompanied by the development of shallow subtidal reefs and grainstones. Shallowing resulted in subareal exposure and regionally extensive erosion that produced a readily identifiable disconformity between Upper and Middle Cretaceous.

3.1.2 Upper Cretaceous

3.1.2.1 Jose Formation

The Jose Formation consists of thin bedded marine shales that were deposited during the Early Santonian transgression.

3.1.2.2 Rene Formation

The Rene Formation of Santonian-Campanian age is characterized by monotonous mudstones to wackestones. It overlies and succeeds the Jose Formation shales of the Santonian transgression.

3.2 Structural Setting

This paragraph was extracted from Guy et al., 2000.

3.2.1 Regional Characteristics

The study area is located in a foreland basin with the following characteristics:

- a. An inherited NNE-SSW and WNW-ESE structural grain
- b. Infra-Cambrian Helena salt that influenced the formation of domes and diapirs
- c. A foredeep basin that formed as the result of subduction and ophiolite obduction during Upper Cretaceous times. The attendant formation of a regional unconformity started during mid-Turonian time, during which much of the Maria Member rocks were removed by erosion. The Jose and Rene Formations were deposited in this foreland basin.
- d. A second tectonic event that occurred during Oligocene to Holocene times and which resulted in uplift, thrusting, and fault related folding.

3.2.2 Field Characteristics

The main characteristics of the field are:

- 1) anticline structure, NNE-SSW elongated, 7km large x 14 km long (Figure 2).
- 2) Top Rene at -2750mss and top Maria (base Jose unconformity) at -2670mss

- 3) Erosional toplaps on the crest of the structure in Maria, that is a Maria thickness varying from 15m to more than 100m from crest toward flanks; but conformable Jose (1-5m thick) and Rene (75-85m thick)
- 4) N30-N170-N80-N120 complex fault network with limited vertical throws (less than 25m)
- 5) Actual structure framework, anticline shape and fault network, results from a relatively complex structural history corresponding to two major structural events at the end of Maria deposition and during Miocene. As a consequence, throws of faults as observed at top Rene are related to different structural events at different times and structural closure was probably evolving through time.

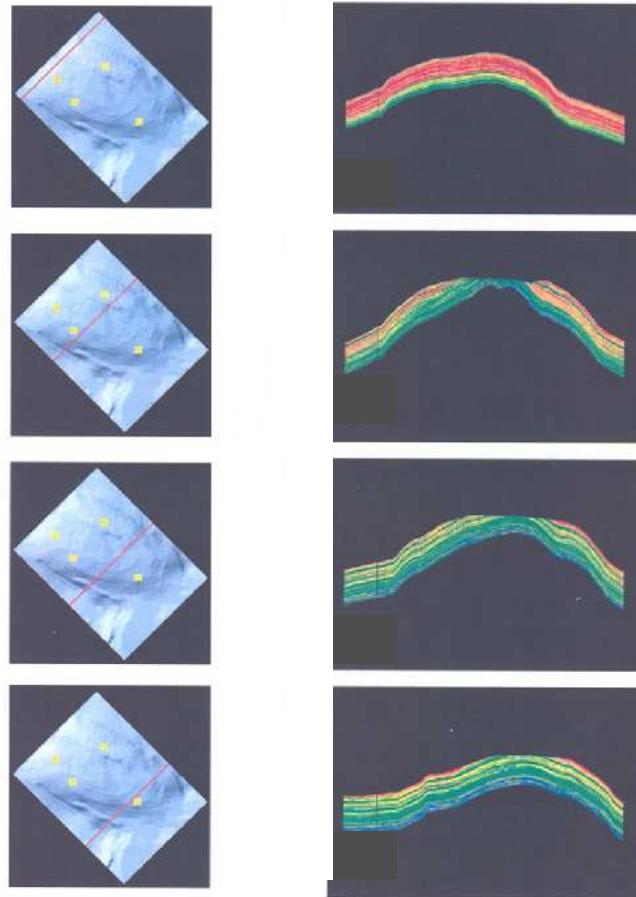


Figure 2: Aerial picture of the field

The combination of structural seismic interpretation, regional background and field analog leads to propose the following structural history of the field.

3.2.2.1 Structure Initialization, End Cenomanian to Turonian

This field is a 7 X 14 km sized anticlinal structure oriented NNE-SSW (Figure 2). The principal reservoir horizons designated as Rene and Maria are at 2750 and 2670 feet below present sea level respectively. In addition, erosion on the crest of the structure has removed from 15m to more than 100m of the Maria horizon. The structural configuration of the field is the result of a long structural history related to two major structural events during Miocene times.

3.2.2.2 Origin of the Structures

The structure underlying this field formed as elongate salt dome on which subsequent erosion removed varying amounts of the stratigraphic column in or near the reservoir horizon. This event is interpreted to have occurred near the end of the Maria depositional cycle 2. The erosional events occurred during regional eustatic sea level fall in mid-Turonian times. From a regional point of view, the field located on the forebulge of the andine foredeep. Later, during a period of tectonic quiescence from Eocene to Oligocene time, the Rene, Grego and Pablo Formations (Figure 1) were deposited.

3.2.2.3 Structural Characteristics During Miocene to Present Times

Field structure during this time can be characterized by the following characteristics: 1) the lower Flavio Formation is marked by tectonic tilting toward the NE; 2) the lower Flavio Formation was influenced by reactivation of the Cenomanian-Turonian anticline and 3) from deposition of the Grego Formation to the present, anticline growth has continued. Although structural growth has been more or less continuous since lower

Flavio deposition, the anticlinal shape was changed. From the deposition of the Grego Formation to the present, there has been additional tilting toward the NW. Anticline growth has been associated with reactivation of strike slip faults and attendant creation of “en echelon” faults and related positive flower structures. From a regional point of view, this structural event is linked to the second andine event, that is to Andine folded belt formation.

3.3 Stratigraphic Setting

Three formations are represented in the this field, the Alban, Maria and Jose Formations. The geological model of Lodola, 2002a forms the basis for this stratigraphic interpretation.

3.3.1 Alban Formation

Only a few meters of this formation were taken in borehole cores in the study area. The facies found in the cores include pelagic limestones with black shale intervals. Planctonic foraminifera such as *Rotalipora appenninica* are abundant and form the basis for establishing the age of the rocks as Albian.

3.3.2 Cyclical Stratigraphic Units in the Maria Formation

3.3.2.1 Cycle 1

Cycle 1 varies in thickness from 60 to 70 m and was deposited during Lower to Middle Cenomanian time. This sequence consists of hemipelagic facies, beach, and reef facies. Cycle 1 is the only one modeled with Gocad® software and used in the Eclipse® reservoir simulations. Lodola, 2002a identified 5 main facies in the Maria Formation; they are: well bedded, coarsening upward bioclastic packstones with abundant burrowing bivalves and echinoids that are interpreted to be deeper water “slope” deposits; massive bedded bioclastic packstones and grainstones with whole and

fragmented nummulites, corals, echinoderms, and foraminifera, interpreted to be calcarenite sandwaves (shoals) and patch reefs; cumulated biostromes, and bioclastic wackstones - packstones interpreted to be a semi-continuous reefs along the shelf edge, coarse to fine bioclastic packstones - grainstones on the inboard side of the reef trend and interpreted to be back-reef calcarenites; and foraminiferal to peloidal mudstones and wackstones interpreted to be lagoonal deposits. Figure 3 shows the three dimensional repartition of the 5 main facies in the Maria Formation. The shoals formed a barrier, parallel to the shelf edge (red color in figure 3). The lagoonal facies are in green, and slope facies, in blue in the Figure 3.

The sedimentological study of Lodola, 2002a identified 14 facies in cycle 1. They are listed in the Table 1. To facilitate Gocad® simulation, facies F0a, b, c and d were finally regrouped in facies F0. The range of bathymetric depths were interpreted from core and thin sections analyses. The facies array on the Cretaceous ramp in the study area is shown in Figure 4.

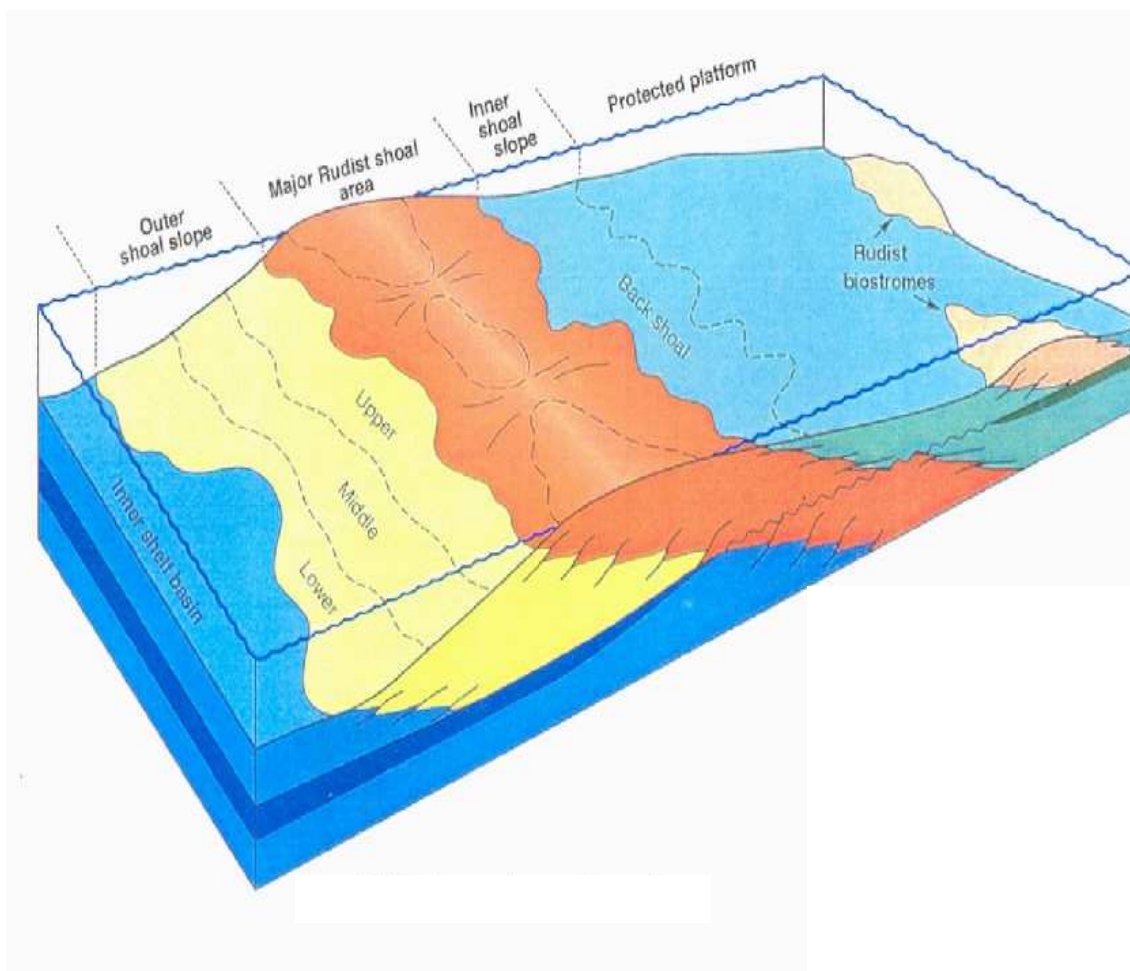


Figure 3: A block diagram illustrating the main environments (after Guy et al., 2000)

Table 1: Facies description (modified from Lodola, 2002a,)

FACIES	TEXTURE	LITHOLOGY	ENVIRONMENT	BATHYMETRY		
F5a,b	G(P)	Rounded elements, and coarse bivalv debris	SHOAL	infralitt	0	-4
F8b	WP	Infralittoral debris and external platform microfauna	lagoon	infralitt	-2	-8
F8a	G/P	Peloids and mainly Nummulits debris	foreshore	infralitt	-2	-9
F8	WP	Nummulits	outershelf	infralitt	-3	-12
F3	G	Peloids	outershelf	circalitt	-5	-15
F2a,b,c	WP	Echinoderms, Bivalvs debris, peloids	outershelf	circalitt/hemipelagic	-8	-45
F1	W	Bivalvs, Oysters, Ammonits, Gastropods	outershelf	hemipelagic	-25	-55
F0a,b,c,d	W	Calcispheres, Radiolairs, Planktonics	outershelf	hemipelagic	-35	-100

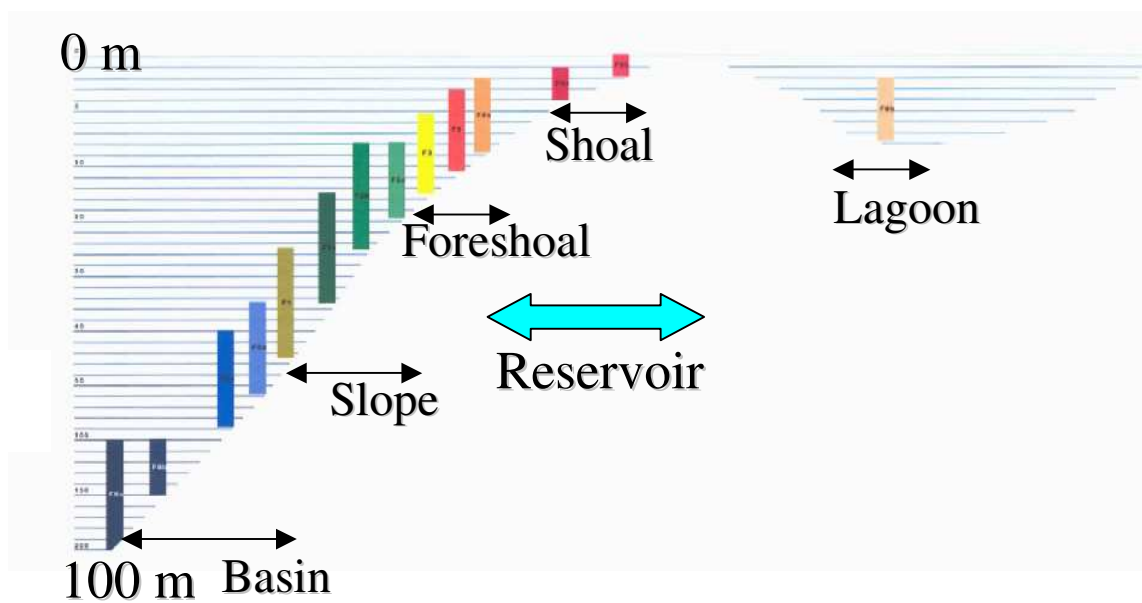


Figure 4: Paleobathymetry profile, Maria Formation (modified from Lodola, 2002a)

3.3.2.2 Cycle 2

Maria Formation Cycle 2 varies in thickness from few centimeters to 32 meters, alveolinid forminifera are abundant, and the cycle is Middle Cenomanian in age. The principal rock types are interpreted to have been deposited in lagoonal environments, and the rocks are interpreted to have been fractured early in their burial history.

3.3.3 Jose Formation

The Jose Formation is Coniacian in age according to Alsharhan and Nairn, 1993. This age for this formation indicates that the Upper Cenomanian and Turonian stratigraphic section has been removed by erosion, or was not deposited, in the study area.

3.3.4 Cycle 1-Alban Limit: Sb1

The Sb1 is located at the limit Alban-Maria limit. Indeed, facies environment change drastically, from anoxic and pelagic to hemipelagic. A strong sea level fall appears here. Furthermore, some early and late dolomites appear at the bottom of Maria formation, just above the Sb1. Due to the presence of dolomite along this surface, its location was difficult to determine. The location of this surface represents one of the uncertain geological parameters analyzed in this study.

3.4 Gocad Models

Once the two-dimensional stratigraphic and structural models had been established, the next step was to simulate the platform characteristics in 3-dimensions using commercial software. This was accomplished by building a geological model on a 3D grid using GOCAD[®] commercial software. Parameters in this model, such as facies, bathymetric range for each facies, aquifer size for reservoir water drive, reservoir petrophysical parameters such as porosity, permeability, were defined so that for each cell of the model, one value for each parameter was assigned.

Limitations on amount of information available at all well locations prevented entering a uniform set of data into the software. To offset this limitation, variograms were used to establish the confidence limits with which the geological parameters can be extrapolated in space. This is known as the correlation distance and it represents the maximum distance between two data points along which there is statistical certainty that an interaction between the two points will exist. In this study, variograms were used to simulate the thickness of each layer, the morphology of the platform, and the facies distribution. The effective “range” over which the variograms are applied is arbitrarily chosen because of a lack of information. For this reason the variogram ranges in this study were considered as uncertain parameters.

The ranges of bathymetric depths assigned to facies were assigned on a facies by facies basis. Ranges of bathymetry were attributed on a facies per facies basis. For that reason, sensitivity analysis of bathymetric depth range was made in this study. In addition, the orientation of the platform was also uncertain. That is, the azimuth along which the shelf-slope break existed was not known; consequently, the “windward” and “leeward” orientation of facies could not be identified with certainty. Finally, uncertainty exists about reservoir thickness owing to the presence of the erosional unconformity at the top of the reservoir formation. In short, 6 parameters in the study have “uncertain” values and each of them were assigned one of two values, or *levels*: 1) a variogram used to synthetically map thickness of strata over a varying lateral distance designated as short range: 5km*3.3 km: level -1 or long range: 45km*30km: level +1.

Bathymetry was designated as a high or low around well 14 where the low (deep) was assigned a value of -1 and the high a value of +1. Azimuthal orientation of the shelf edge was assigned N-S orientation = level -1 and E-W orientation = level +1. The lateral extent to which bathymetric depth values could be assigned was designated as

short range = original extension *0.6: level -1 and long range = original extension *1.4: level +1.

The variogram ranges used to simulate facies juxtaposition over lateral distances were designated as short range = 3km*2km: level -1; and long range = 12km*8km: level +1. The amount of erosion at the top of the reservoir formation was assigned the following values: top reservoir map at -5m compared to the reference case depth map = level -1 and top reservoir map at +5m compared to the reference case depth map: level +1.

These parameters are the six which will be studied in the quantification of uncertainty. For the first model, average values of these six parameters have been used: this is the *reference case*. The average values are determined from analogous fields or log/core mean values. Geological models are sometimes called *static models*. Once they are constructed they may include different values for the six parameters previously mentioned. Then the reservoir model is constructed and it is known as a dynamic model. This step is presented in the quantification of uncertainty chapter.

CHAPTER IV

RESERVOIR SIMULATION

4.1 Model Input

4.1.1 Current Model

The geological model used in this thesis was constructed by Lodola, 2002b. The model has been simplified and no history matching was performed. This study differs from earlier attempts to evaluate uncertainty in simulations of this reservoir by including only the uppermost stratigraphic cycle in the Cretaceous Maria Formation in the commercial Gocad® and Eclipse® computer programs. The model in this thesis was built with ECLIPSE® software, in which data from exploration wells, pilot holes designated as wells, and data from 10 producing and injection wells were used.

The following assumptions were employed in the reservoir model:

- 1) Sequence stratigraphic boundaries were used as dynamic layer limits, meaning that no *dynamic layering* (segregation of the entire reservoir in several *layers*) was defined. A *dynamic layer* is one which has a identical reservoir quality all along the field.
- 2) Petrophysical properties (Phi, K) were attributed on a facies by facies basis
- 3) Geological model updates confirmed that an emersive phase existed at the top of the reservoir and was accompanied by erosion and diagenesis, particularly at the top of cycle 1 where facies-selective dissolution is abundant. It is also confirmed by DST measurements (DST well 13) that permeability is higher in the top layers
- 4) For these reasons, an individual diagenetic drain layer was incorporated at the top of the reservoir in the computer model.

- 5) Only one capillary pressure and one relative permeability curves were considered to be representative of the entire reservoir, and one rock type was defined for the entire reservoir
- 6) One set of PVT values was employed, along with one oil-water contact depth for the field
- 7) All wells are assumed to be vertical
- 8) No dynamic barriers exist between northern and southern parts of the field

4.1.2 Upscaling

Originally, Gocad® geological models were formed by 75,000 cells. The upscaling phase consists of grouping fine cells from the geological model together in order to obtain a grid with larger cell size, available for the reservoir model.

A variogram range defines the maximum distance along which data points (here facies) are correlated together, that is the distance between points along which the value (facies) defined at point 1 will influence the determination of facies at point 2, and vis versa. Here, the variogram range for the facies was equal to 800m, which represented the length of 3 fine cells of geological model. This distance of correlation served to group geological model cells together (each cell having its own size). Cells from geological models were grouped 3*3*4 in X,Y and Z directions respectively.

In this study, a total of 65 models were generated with Gocad® software, and each one was upscaled. The fine grid of each model was first upscaled, merging several fine cells together (3cells merged together in X and Y directions, 4 in Z direction). A coarse grid was obtained this way. As well, horizontal permeability in X and Y directions were assumed to be equal. At this stage, porosity, and horizontal permeability were arithmetically averaged.

Finally, vertical permeability was calculated using the harmonic average of the four cells merged previously. These upscaled properties were then incorporated in the coarse simulation grid.

4.1.3 Reservoir Grid

The coarse grid, also called *reservoir grid*, is a *Corner Point Grid*, which means that the cells are trapezoidal and not squared, composed by 21,025 cells. The large side of the grid is oriented NNE-SSW (N45), as the axis of the anticline structure. The grid covers a total area of 300 km² including 200 km² of aquifer area on the flanks of the anticline on which the field is located.

4.1.4 Petrophysics

4.1.4.1 Porosity and Permeability

Porosity and permeability values were obtained from wireline log data and core analyses, respectively. Once the range of measured porosity and permeability were known, a range of porosity was assigned to each facies in the simulation model. Porosity and permeability were assumed to be normally distributed. Porosity ranges are presented in Table 2.

We assumed that permeability along the x axis was equal to permeability in Y direction, it means homogeneous permeability in the horizontal direction. Horizontal permeability will be referred as Kh in next pages. Applying a *phi/log K correlation*, a curve fitting regression model relating porosity with permeability, a range of Kh was determined for each facies. Phi/K correlation laws are presented in Table 3.

Table 2: Porosity range per facies

Facies	Mean	standard deviation	Max	Min
F5b	0.181	0.052	0.263	0.055
F5a	0.208	0.035	0.27	0.087
F8b	0.149	0.031	0.203	0.128
F8a	0.185	0.03	0.243	0.132
F8	0.195	0.04	0.279	0.134
F3	0.209	0.025	0.293	0.143
F2c	0.150	0.038	0.205	0.055
F2b	0.179	0.039	0.263	0.043
F2a	0.121	0.065	0.233	0.017
F1	0.028	0.026	0.09	0.003
F0d	0.045	0.044	0.135	0.006
F0c	0.028	0.032	0.098	0.002
F0b	0.020	0.014	0.037	0.005
F0a	0.018	0.017	0.068	0.005

Table 3: Porosity permeability law for each facies

Rock Type	Gocad region	Facies	Phi/K law
PG 1	F01	F5a	$K=0.0124*e(34.933*Phi)$
PG 2	F00	F5b	$K=0.105*e(26.008*Phi)$
PG 3	F03+F04	F8+F8a	$K=0.077*e(23.843*Phi)$
PG 4	F05+F07	F3+F2b	$K=0.0655*e(23.338*Phi)$
PG 5	F02+F06+F08	F2a+F2c+F8b	$K=0.945*e(7.9964*Phi)$
PG 6	F09+F10+F11	F1+F0c+F0d	$K=0.0443*e(22.027*Phi)$

PG: Petrophysical group

The Gocad regions are zones of the field where facies were present. The facies names refer to the geological profile, Figure 4, in the geological model chapter. For the diagenetic layer, a permeability value K_h stemming from DST test was included. From DST WELL 13, $K=29.6$ mD. In accordance with previous studies (Guy et al., 2000, Laroche, 2000), $K_v/K_h = 0.5$.

4.1.4.2 Capillary Pressure and Relative Permeability Curves

For this simplified case, one value of Rock Type was defined for the simulation model. Capillary pressure (or “ P_c ”) curves were used from previous studies, and one value of relative permeability was also taken from earlier work. These values were assumed to be representative of the entire field. Earlier works assigned one P_c curve to each reservoir compartment and each rock type. In this study, an average reservoir quality RT was attributed for the entire field, with $S_{wi}=10$ %. Table 4, Figure 5 and Figure 6 illustrate these data.

Table 4: Capillary pressure and relative permeability table

Sw	Krw	Krow	Pc (Psia)
0.1	0	1	42.674
0.11	0.001	0.967	28.449
0.12	0.002	0.936	22.759
0.13	0.003	0.907	19.914
0.15	0.005	0.852	17.069
0.17	0.008	0.799	14.225
0.21	0.013	0.7	11.38
0.26	0.021	0.579	8.535
0.35	0.038	0.373	5.69
0.41	0.053	0.255	4.267
0.47	0.07	0.161	2.845
0.51	0.085	0.115	1.422
0.56	0.107	0.073	0.1
0.6	0.129	0.05	0.084
0.65	0.165	0.028	0.068
0.7	0.21	0.008	0.052
0.72	0.23	0	0.036
0.995	0.986	0	0.019
1.00	1.00	0	0

Krw represents the relative permeability of water,

Krow is the relative permeability of oil relatively to water one.

Pc is the capillary pressure, in Psia

Sw is the water saturation of the reservoir.

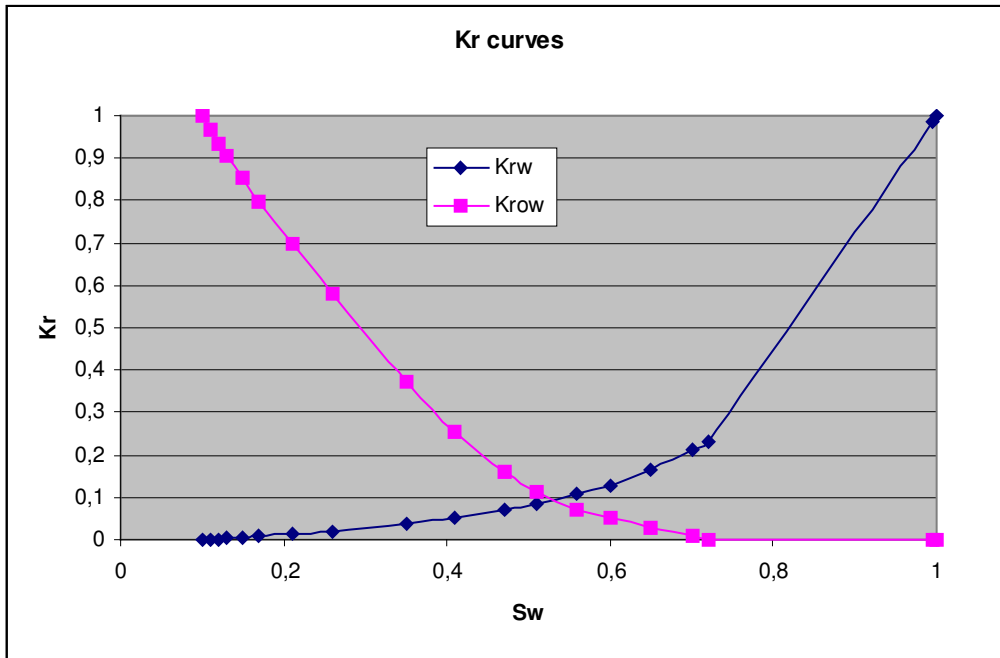


Figure 5: Kr curves

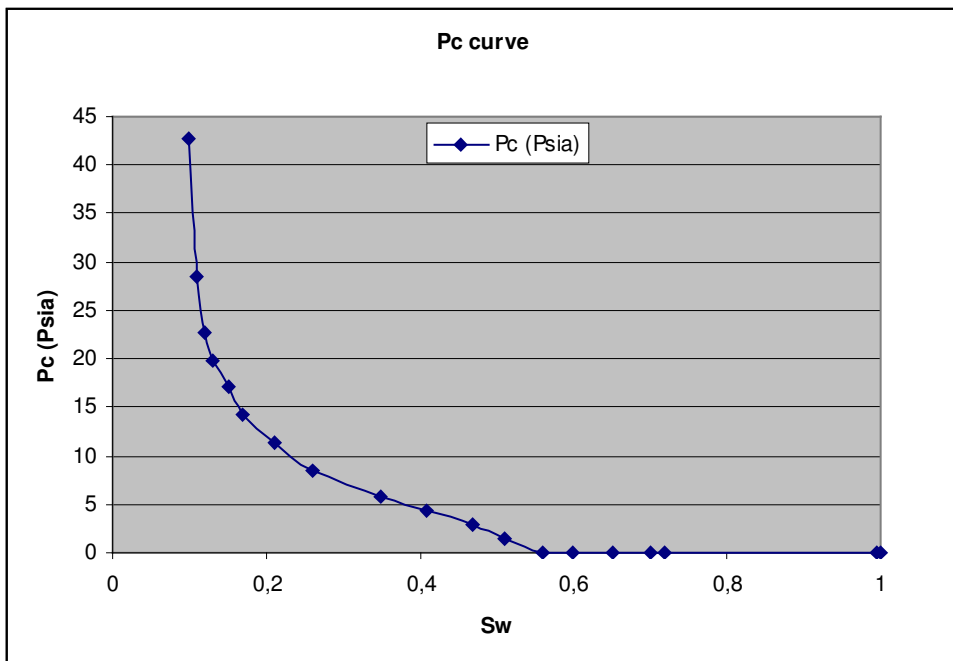


Figure 6: Capillary pressure curve for the entire field

Table 5: Krg and Krog values, Sw_i=6%

S_g	K_{rg}	K_{rog}	P_c
0	0	1	0
0.025	0	0.849	0
0.035	0.001	0.768	0
0.074	0.005	0.623	0
0.11	0.014	0.499	0
0.147	0.026	0.388	0
0.184	0.042	0.297	0
0.221	0.058	0.2338	0
0.258	0.082	0.185	0
0.294	0.111	0.143	0
0.331	0.145	0.114	0
0.368	0.181	0.095	0
0.405	0.219	0.074	0
0.442	0.261	0.054	0
0.478	0.308	0.035	0
0.515	0.37	0.019	0
0.57	0.47	0	0
0.644	0.526	0	0
0.736	0.596	0	0
0.91	0.727	0	0
0.94	0.75	0	0

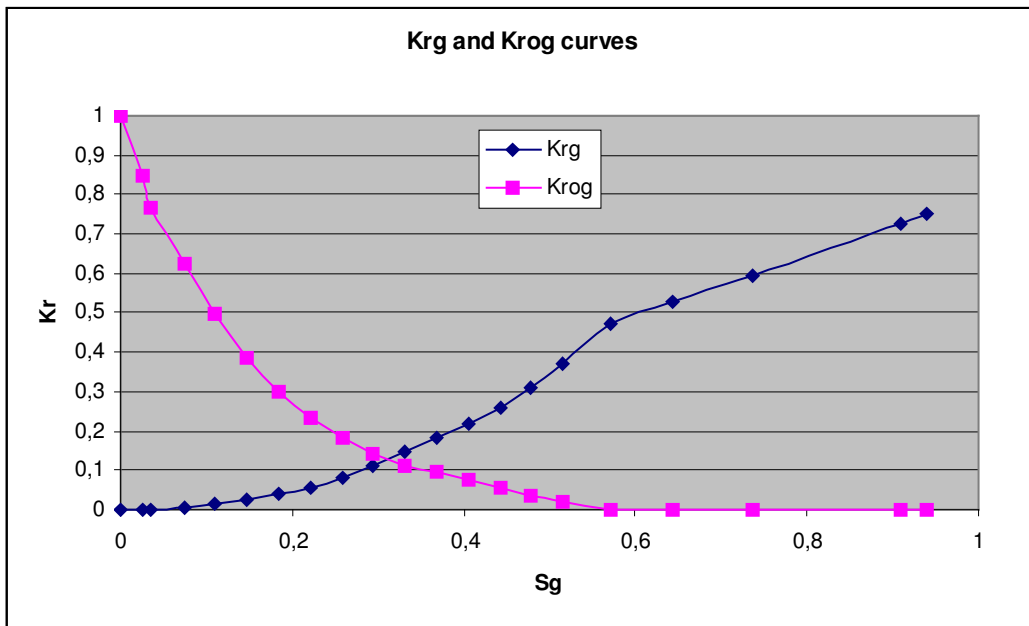


Figure 7: Relative permeability gas (K_{rg}) and oil (K_{rog}) curves

The relative permeability curves come from May 1997 reservoir model (Elf Aquitaine Company, 1997, Total, 1997). They were calculated from water sweep tests run on plugs at ambient conditions with synthetic fluids (Elf Aquitaine Company, 1975). Similar rock samples were used for unsteady state gas-oil relative permeability flow study. Gas-Oil set of relative permeability curves are presented in Table 5 and Figure 7.

4.1.5 Rock Properties

Rock compressibility in Maria reservoir was determined to be $4.4 \times 10^{-6} \text{ psi}^{-1}$. However, because the field is undergoing water, rock compressibility is considered to be negligible as a drive mechanism.

4.1.6 Fluid Properties

4.1.6.1 Choice of the PVT Set

PVT data from 5 wells were available from bottom hole samples on wells 19, 8, 11, 13 and 14. All were determined from experiments on. The PVT data are given in Table 6. From Guy et al., (2000) and Laroche, (2000) studies, different PVT values were assigned to different compartments in the field. Oils from well 11 and well 13 have similar composition but different B_o and GOR. According to earlier work, these differences resulted from errors in measurements at well 11. Both wells 8 and 19 exhibit non uniform PVT measurements; therefore, the PVT set from well 13 is used here as the reference data set.

4.1.6.2 PVT Description

Well 13 PVT is the reference data set in this full field reservoir model, as in previous models (Elf Company, 1997, Laroche, 2000). Table 7 shows the complete data set used in Eclipse. No correction between differential and flash measurements was done.

Table 6: PVT summary

Date	SIE-3 Jul-75	SIE-5 Dec-96	SIE-6 Spet-96	E3-P4P Feb-98	E3-P5 Aug-99
Pb (psia @ res cond.)	4090	3843	3366	3669	3342
Differential GOR (scf/stbo)	1081	1208	979	1067	1082
Differential Bo (rb/stb)	1.614	1.721	1.568	1.615	1.593
Oil density (Diff.) (kg/m3/API)	873-30.6	865-32.1	870-31.2	877-30	873-30.6
Flash GOR (number of stages)	967 (3)	1012 (5)	824 (5)	872 (5)	913 (5)
Flash Bo (rb/stb)	1.56	1.602	1.498	1.511	1.522
Oil density (Flash) (kg/m3/API)	862-32.7	841-36.8	851-34.8	860-33	861-32.8
PVT validity	Bo and GOR measurements not representative	Referenc e PVT	Oil for Mishrif cycle 2	Composition in between SIE-3 and SIE-5. No mixture with cycle 2 oil: Reference 2 (PVT)	Well probably isolated in a separated compartment
GOR @ test separator cond.	-	926	-	772	-
GOR @ PPE separator cond.	-	971	-	812	-

Table 7: The complete PVT data set incorporated inside the reservoir model

Pressure (psia)	OIL					GAS	
	Bo diff. eq. (rb/stb)	Bo compo. (rb/stb)	Rs diff.eq. Mscf/bbl	Rs compo. (Mscf/bbl)	Viscosity (cP)	Bg (rb/Mscf)	Viscosity (cP)
15	1.0778	1.0	0	0	1.343	229.601	0.007437
100	1.1788	1.08	0.097	0.081	1.078	34.169	0.009845
465	1.2695	1.163	0.221	0.185	0.794	7.109	0.01235
915	1.325	1.214	0.332	0.278	0.637	3.488	0.013817
1515	1.3915	1.275	0.48	0.402	0.51	2.032	0.015371
2115	1.4638	1.341	0.636	0.533	0.429	1.424	0.016922
2915	1.5755	1.443	0.864	0.724	0.361	1.026	0.019231
3515	1.6722	1.532	1.068	0.895	0.331	0.861	0.021218
3843	1.7497	1.603	1.208	1.012	0.331		
4215	1.7359	1.59	1.208	1.013	0.337		
4515	1.7264	1.581	1.208	1.014	0.342		
4685	1.7213	1.577	1.208	1.015	0.346		
5114	1.7092	1.566	1.208	1.016	0.355		
5417	1.7011	1.558	1.208	1.017	0.362		
5735	1.6931	1.551	1.208	1.018	0.369		
6015	1.6862	1.544	1.208	1.019	0.376		

4.1.7 Well Modeling and Production Constraints

The *development scheme*, that is the installation and location of wells among the field, was also simplified in this study. But the well locations remain the same as in the Guy et al. study. In this study, all the wells were assumed to be vertical. This choice was based on:

- Absence of completion report, and it was not possible to obtain it on time for this study,
- information about deviation was absent from previous reports; only the X,Y and Z coordinates of the intersection between the wells and the top layers defined in the December 2000 study were available during this study.

- those coordinates were missing for 9 injectors and 1 producer

So, for each well, the coordinates of the intersection between the upper layer of the cycle 1 and the well tubing were taken, and these coordinates are assumed to be those of the vertical well. Figure 8 and Figure 9 illustrate this procedure. Using only vertical wells avoided the additional uncertainty linked to well deviation, and changes of horizontal drain location (skin factor, in which layer the drain is located, etc.). Wells coordinates available for this study are summarized in the Table 8 below (from Guy et al., 2000).

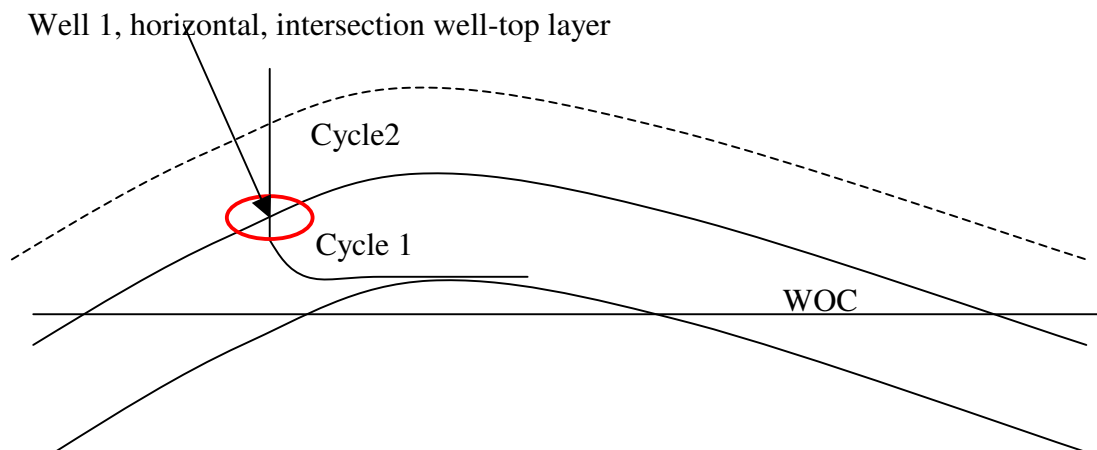


Figure 8: Previous well completions

Well 1, vertical, X, Y, and Z actual coordinates

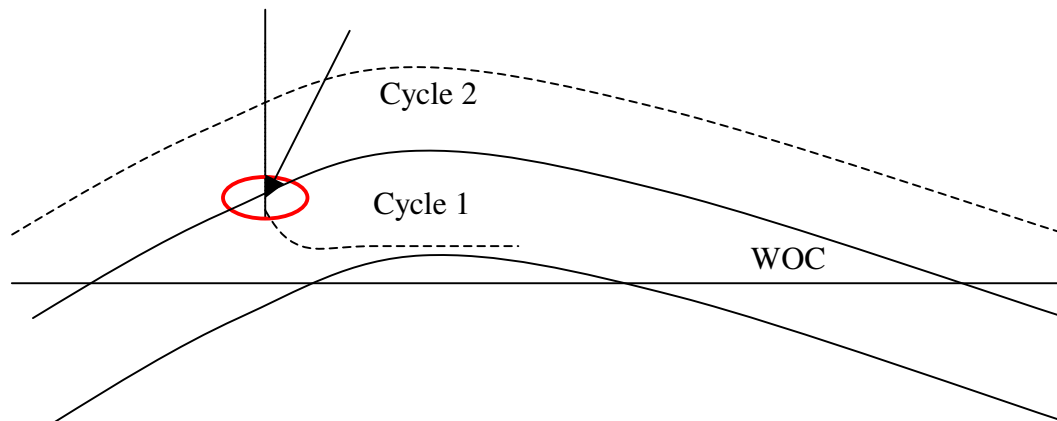


Figure 9: Well completion implemented in this study

Table 8: Well coordinates implemented in this study

Wells	I	J	K
1	17	14	5-18
2	17	17	9-20
3	20	18	1-14
4	21	19	1-8
5	23	11	8-23
6	28	13	12-25
7	11	15	1-8
8	12	16	1-20
9	17	19	1-5
10	21	15	10-21
11	14	15	1-23
12	30	9	4-25
13	24	18	1-25
14	24	8	2-24
15	16	13	1-4
16	29	15	9-22
17	12	17	1-14
18	14	20	1-12

Rem: some wells don't perforate the top layers (1 to 12): those layers were eroded at this location, so they are absent from well location.

4.1.7.1 Producers

14 producers were implemented here. Producer characteristics are as follow:

- tubing size: 4 ½ inch = 0.375 ft
- skin: 0

Well production constraints were the same as in Laroche, 2000:

- Maximum well water cut : 0.95 %
- Minimum well economical oil production rate: 250 Bbl/D
- Maximum well oil production rate: 15,000 bbl/D

Neither well head constraints nor VFP curves were implemented in this model (Eclipse® options).

4.1.7.2 Injectors

Compared to Laroche, 2000, 6 injectors are missing, making water injection less efficient compared to previous studies (Guy et al., 2000, Laroche, 2000). Only 4 injectors are present in this study. Injector characteristics are similar to Laroche, 2000 report ones:

- Tubing size: 0.375 ft
- Skin: 0

Well injection constraints are as follow:

- Maximum injection BHP: 6500 psia
- Maximum water injection rate: 20,000bb/D

As a conclusion, even if the number of wells differ from other previous models, it doesn't affect at all the objectives of this study.

4.2 Model Initialization

4.2.1 Compartments

In previous studies (Guy et al., 2000, Laroche, 2000) 2 or 3 compartments were individualized for the reservoir model, separated by sealing faults. By compartments, we mean reservoir compartments: in previous models, sealing faults were present in the field. These faults cut the field in different units, where oil quality and pressure behaviors were different. In this study, no fault was implemented in the geological model or in the reservoir simulation. So, the field is not compartmentalized.

4.2.2 WOC

In Laroche, 2000 study, two different WOC depth were considered, one for the North compartment, one for the south part. In this study, one WOC depth was implemented for the entire field: WOC located at 9511 ft sub sea (WOC depth of the north compartment of previous studies).

4.2.3 Pressure Volume Temperature Data (PVT Data)

As mentioned previously, WELL 13 PVT set was applied to the entire field.

4.2.4 Pressure Regime

Virgin pressure used here is: $P_i=4700$ psia at datum: 9350 ft sub sea. Data come from RFT of pilot wells.

4.2.5 Simulation Results

Some of the simulation results are presented in Appendix 1 to Appendix 67. The reservoir behavior is described as follows:

For the entire field, oil and gas rates drop continuously until the end of the production. The *Gas Oil Ratio* decreases at first, then increases and ultimately decreases at the end of the designated production time interval. The Water cut increases continuously during production but remains low and the water injection rate is constant.

For individual well plots, reservoir pressure drops quickly until the minimum bottom hole pressure is reached, below the *bubble point*, for wells far away from the injectors (well 7 and Well 11). A consequence of this is that a large amount of free gas is liberated at the beginning of the production. This free gas creates an early secondary gas cap, which can be observed on most of the wells near the top of the anticline structure. During the first year, pressure maintenance of the secondary gas cap and solution gas drive contribute to maintain reservoir pressure. Later, wells far from injectors produced by solution gas drive, during the 30 years of production. For wells close to injectors, pressure maintenance is accomplished by water injection and pressures are to be maintained to keep the Gas Oil Ratio (GOR) low at minimum (example of wells 5, 6 or 7). For injectors, Bottom Hole Pressures (or BHP) are at maximum value at the start of the simulation to hold injection rates constant and low (wells 16, 18 for example).

The small number of injection wells are not sufficient to maintain required pressure above the bubble point pressure (or P_b) in any wells for the 30 year simulation. This is revealed by the decline in BHP below the P_b during the entire production time, accompanied by formation of a secondary gas cap. Both cumulative oil produced and recovery are affected by the pressure drop.

Completion of vertical well instead of horizontal ones tends also to decrease the amount of both oil produced, and the recovery by as much as $\frac{1}{2}$ according to Laroche, 2000, and by 20% of the estimates given in Guy et al., 2000. Finally, the *water cuts* obtained in this study are much lower than those obtained in the previous studies, owing to the low pressures and the smaller number of injectors.

CHAPTER V

QUANTIFICATION OF UNCERTAINTY

5.1 Philosophy of Quantification of Uncertainty

Quantification of uncertainty is a statistical procedure designed to the range of values that a parameter can take in mathematical or physical model without the model undergoing failure to produce reasonable results. For example, if porosity is a parameter in a reservoir simulation model, it could vary between a low 1% to a high of 75%. The low and high ends are unrealistic based on experience with a wide variety of reservoirs; therefore the object of the study on uncertainty is to determine which values of the parameter will produce the more realistic result in the reservoir simulation model without knowing the value in advance. The lack of prior knowledge is the “uncertainty”. The degree of uncertainty imposed on the model outcome by variability in the parameter is the quantity to be identified, or “quantified”.

It is implicit in the procedure that an experiential factor or “common knowledge” will allow choice of a “reasonable range” for each parameter examined in the quantification process. In this study, the parameters, or factors, are geological characteristics that are supposed to have major influence on reservoir performance. These factors have already been listed. In some instances, for reservoir factors essentially, it is not necessary to know a “realistic” range of values for each factor because a process of “history matching” can be used as a first approximation of these values. With history matching, the principle involved is to assign values to each factor for which the “real” range of variation is uncertain. The test for whether or not the chosen values are “realistic” is then made by testing in a numerical reservoir simulator, as Eclipse®: the numerical simulation results have to be close to observed production data. At best, the simulation results even when they closely matched observed reservoir performance, are not unique

solutions, but are estimates, or approximations. For this reason, multiple model simulations must be created in this study. In the final analysis, it will be the goal of this study to assess the differences obtained between these models, and to define the impact of each individual factor (geological parameter) on the development of the field. In this study, history matching was not performed, but rather, ranges of values were assigned to each factor based largely on experience from the previous studies on the field done by Total geologists and engineers

5.2 Design of Experiment

5.2.1 Method Used to Build the Models Data Set

The method used to generate the 66 variants of the reservoir model begins with establishing the three- dimension grid as built in the geological static model discussed earlier in chapter II. The grid allows for spatial subdivisions with individually-assigned reservoir parameters in each grid subdivision, or block cell. Reservoir parameters and well locations are keyed into the grid along which reservoir data as PVT information, initial reservoir pressure, depth to oil-water contact, reservoir rock capillary pressure, relative permeability, and production constraints. These characteristics define reservoir description and its performance (OOIP, Fluid produced, recovery).

Once the model factors and grid characteristics have been established, iterative runs are made with the reservoir model. In this study, 66 iterations were required to test each of the 6 different geological factors and their impact on reservoir performance, also called *response variables* (OOIP, N_p , W_p/N_p , G_p/N_p , Recovery). In summary, the geological parameters will be called “*factors*”. The reservoir performance, OOIP, N_p , W_p/N_p , G_p/N_p and recovery, will be referred as “*response variables*”. In the quantification of uncertainty chapter, the term “*model*” will define a geological model which has been included into a reservoir simulator, and production was simulated during 30 years.

5.2.2 Method Used to Combine the 6 Parameters

In statistics, the input data, here the 6 geological parameters are called the *factors*, whereas the output data, here the reservoir performances, are called the *response variables*. A first procedure in a quantification of uncertainty is to design the experiment. That is determining the way in which all factors will be combined inside each model. In some techniques one parameter at a time is changing. This process is time consuming and generates a large number of outcomes, even if you are just testing 2 or 3 parameters. A quicker approach is the multi realization method (Corre et al., 2000). This method is intended to generate a large number of outcomes by changing several parameters simultaneously, in order to obtain a normal distribution of all your reservoir performance, to determine which is the most probable case. Then, this most probable geological model will be used to test the variation of reservoir parameter. This is the method used in Total Company.

When several factors are considered in a single experiment, a *factorial design* should be used. There are designs of co-varying factors. By factorial experiment, we mean that in each complete trial (one in this study) of the experiment all the possible combinations of the *levels* (range of values) of the factors are investigated. There are certain special types of factorial designs that are very useful (Hines et al., 2003). One of these is a factorial design with k factors, each at two levels. This is the case of this study. Because each complete trial of the design has 2^k runs, or *treatment combinations*, the arrangement is called a 2^k *factorial design*. Here, a 2^6 full factorial design was defined: you have 6 parameters and they will be combined together. Each model will have a particular combination of the 6 parameters. And the entire set of models will represent all the possible combinations of the six parameters. Each factor will have two levels in this case study: each parameter has two possible values, a high one, and a low one. For convenience, the low value is called the “-1” value for the X parameter, the high value, the “+1”. Each of those two values are considered to be the extremes, the limits, of the possible range that each parameter can take in reality.

So, the set of data (the geological models) represents all the combination of your 6 parameters, for which a high or a low value will be attributed: $2^6=64$ models available. To check the validity of your data set, it is useful to have at least one center point value for your parameters: it is a model in which all the parameters will take an average value, the most probable value, or the arithmetic mean of the high and the low value for this parameter. Here, just one center point was present. The symbol of a center point value is “0”. This is the reference case. Finally, a last model was created in this study, using a different upscaling size, grouping $4*4*5$ cells together in the geological model, instead of $3*3*4$ in X, Y, and Z directions. The parameters values are also center ones. It is called the *coarse* model.

The matrices Table 9 and Table 10 represent the $2^6 = 64$ combinations of geological parameters, the center case, called the reference case, the upscaled center case, the coarse model, and their coding. It means $64 + \text{reference case} + \text{coarse model} = 66$ runs.

Performance results of the 66 runs are presented Figure 10 to Figure 15.

Table 9: Matrix of the first coded 35 models

Name	Param 1	Param 2	Param 3	Param 4	Param 5	Param 6
CAS MOYEN	0	0	0	0	0	0
COARSE	0	0	0	0	0	0
AEIMQU	-1	-1	-1	-1	-1	-1
AEIMQV	-1	-1	-1	-1	-1	1
AEIMRU	-1	-1	-1	-1	1	-1
AEIMRV	-1	-1	-1	-1	1	1
AEINQU	-1	-1	-1	1	-1	-1
AEINQV	-1	-1	-1	1	-1	1
AEINRU	-1	-1	-1	1	1	-1
AEINRV	-1	-1	-1	1	1	1
AEJMQU	-1	-1	1	-1	-1	-1
AEJMQV	-1	-1	1	-1	-1	1
AEJMRU	-1	-1	1	-1	1	-1
AEJMRV	-1	-1	1	-1	1	1
AEJNQU	-1	-1	1	1	-1	-1
AEJNQV	-1	-1	1	1	-1	1
AEJNRU	-1	-1	1	1	1	-1
AEJNRV	-1	-1	1	1	1	1
AFIMQU	-1	1	-1	-1	-1	-1
AFIMQV	-1	1	-1	-1	-1	1
AFIMRU	-1	1	-1	-1	1	-1
AFIMRV	-1	1	-1	-1	1	1
AFINQU	-1	1	-1	1	-1	-1
AFINQV	-1	1	-1	1	-1	1
AFINRU	-1	1	-1	1	1	-1
AFINRV	-1	1	-1	1	1	1
AFJMQU	-1	1	1	-1	-1	-1
AFJMQV	-1	1	1	-1	-1	1
AFJMRU	-1	1	1	-1	1	-1
AFJMRV	-1	1	1	-1	1	1
AFJNQU	-1	1	1	1	-1	-1
AFJNQV	-1	1	1	1	-1	1
AFJNRU	-1	1	1	1	1	-1
AFJNRV	1	1	1	1	1	1
BEIMQU	1	-1	-1	-1	-1	-1
BEIMQV	1	-1	-1	-1	-1	1

Table 10: Matrix of the last coded 31 models

Name	Param 1	Param 2	Param 3	Param 4	Param 5	Param 6
BEIMRU	1	-1	-1	-1	1	-1
BEIMRV	1	-1	-1	-1	1	1
BEINQU	1	-1	-1	1	-1	-1
BEINQV	1	-1	-1	1	-1	1
BEINRU	1	-1	-1	1	1	-1
BEINRV	1	-1	-1	1	1	1
BEJMQU	1	-1	1	-1	-1	-1
BEJMQV	1	-1	1	-1	-1	1
BEJMRU	1	-1	1	-1	1	-1
BEJMRV	1	-1	1	-1	1	1
BEJNQU	1	-1	1	1	-1	-1
BEJNQV	1	-1	1	1	-1	1
BEJNRU	1	-1	1	1	1	-1
BEJNRV	1	-1	1	1	1	1
BFIMQU	1	1	-1	-1	-1	-1
BFIMQV	1	1	-1	-1	-1	1
BFIMRU	1	1	-1	-1	1	-1
BFIMRV	1	1	-1	-1	1	1
BFINQU	1	1	-1	1	-1	-1
BFINQV	1	1	-1	1	-1	1
BFINRU	1	1	-1	1	1	-1
BFINRV	1	1	-1	1	1	1
BFJMQU	1	1	1	-1	-1	-1
BFJMQV	1	1	1	-1	-1	1
BFJMRU	1	1	1	-1	1	-1
BFJMRV	1	1	1	-1	1	1
BFJNQU	1	1	1	1	-1	-1
BFJNQV	1	1	1	1	-1	1
BFJNRU	1	1	1	1	1	-1
BFJNRV	1	1	1	1	1	1

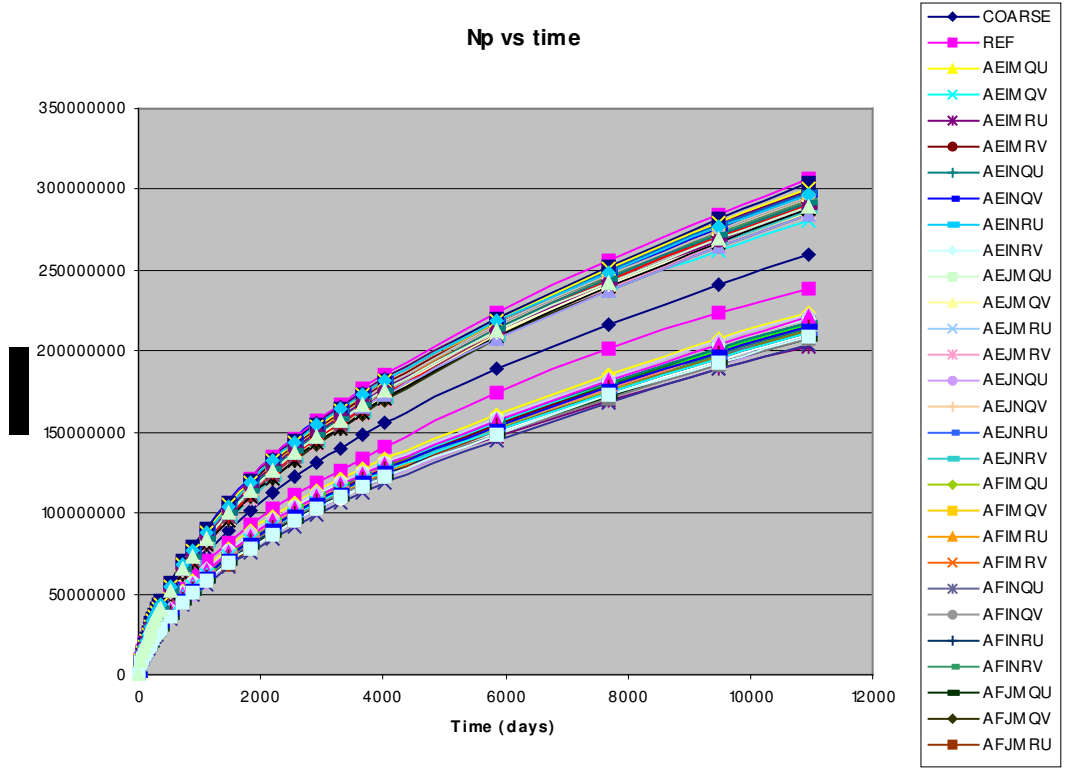


Figure 10: Np ranges vs time (from 66 models)

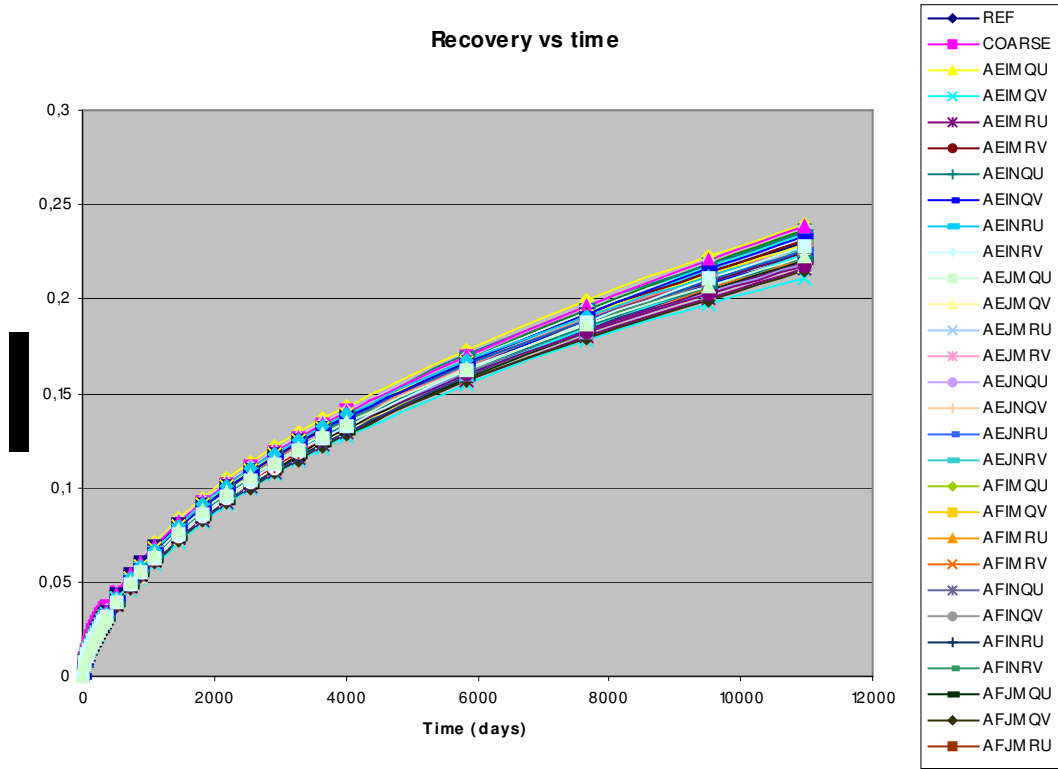


Figure 11: Recovery range vs time (from 66 models)

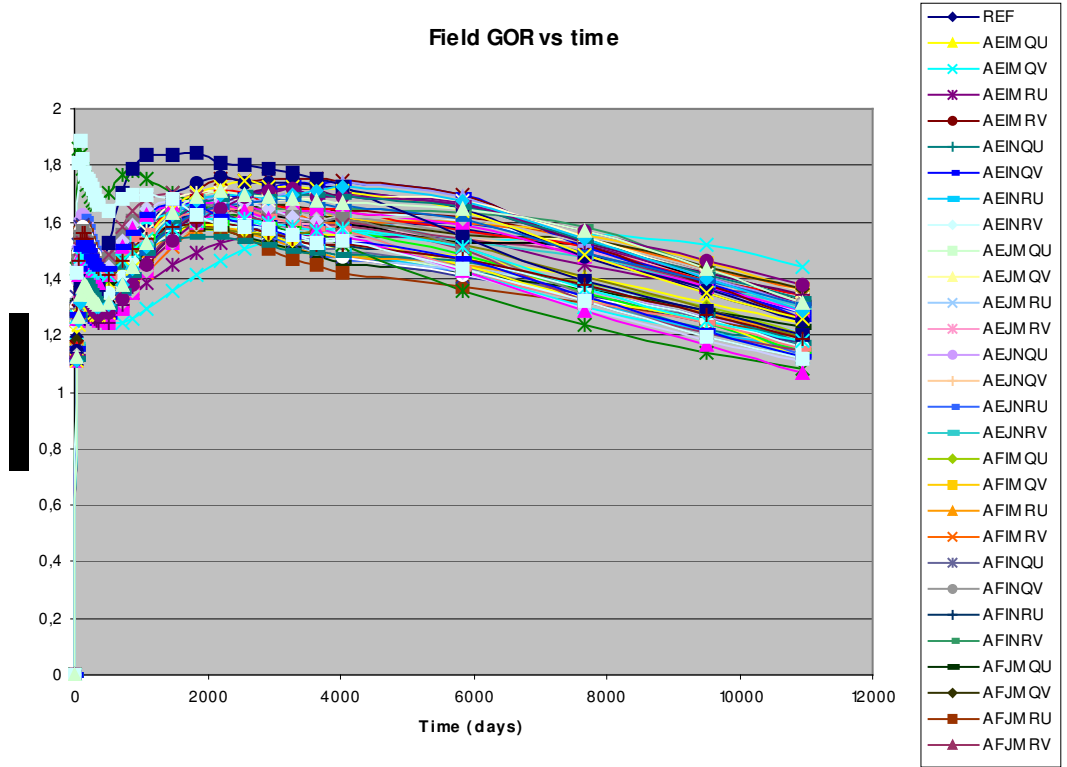


Figure 12: GOR range vs time (from 66 models)

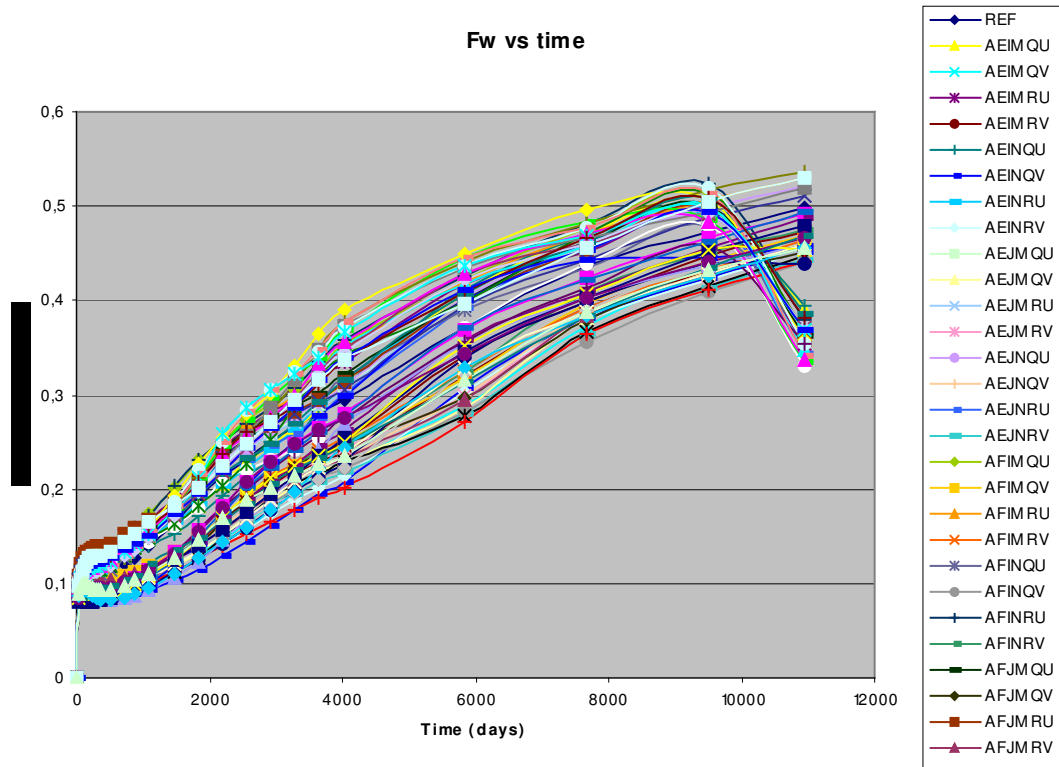


Figure 13: Fw range vs time (from 66 models)

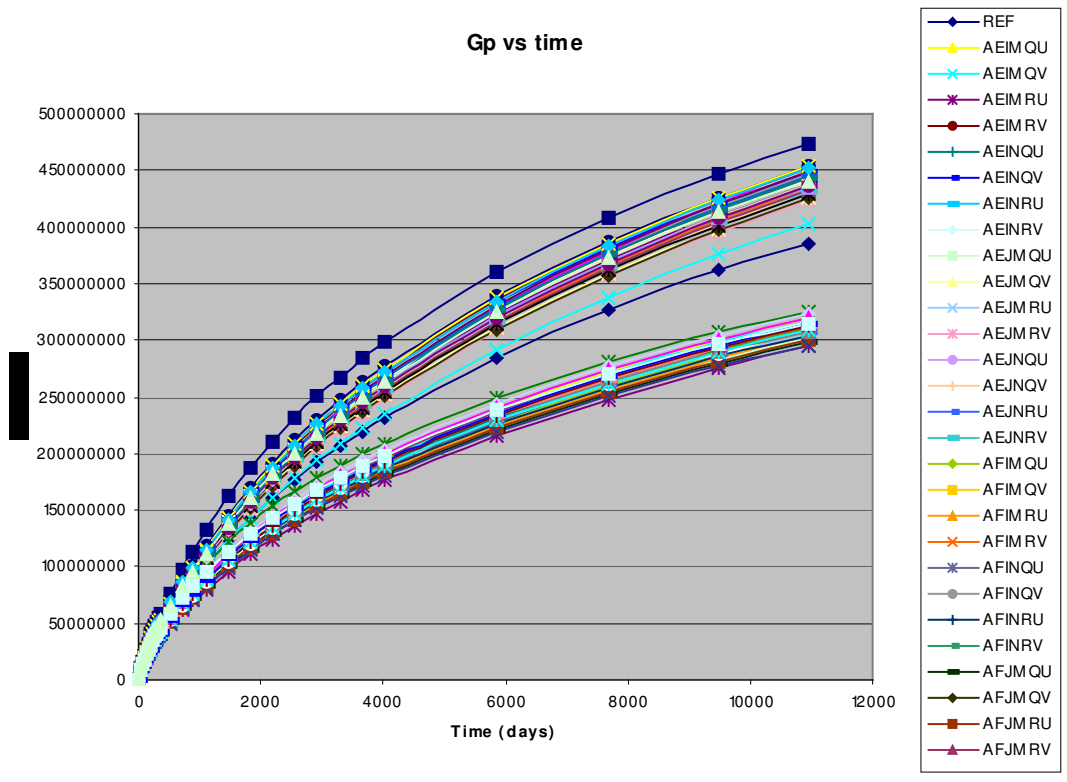


Figure 14: Gp range vs time (from 66 models)

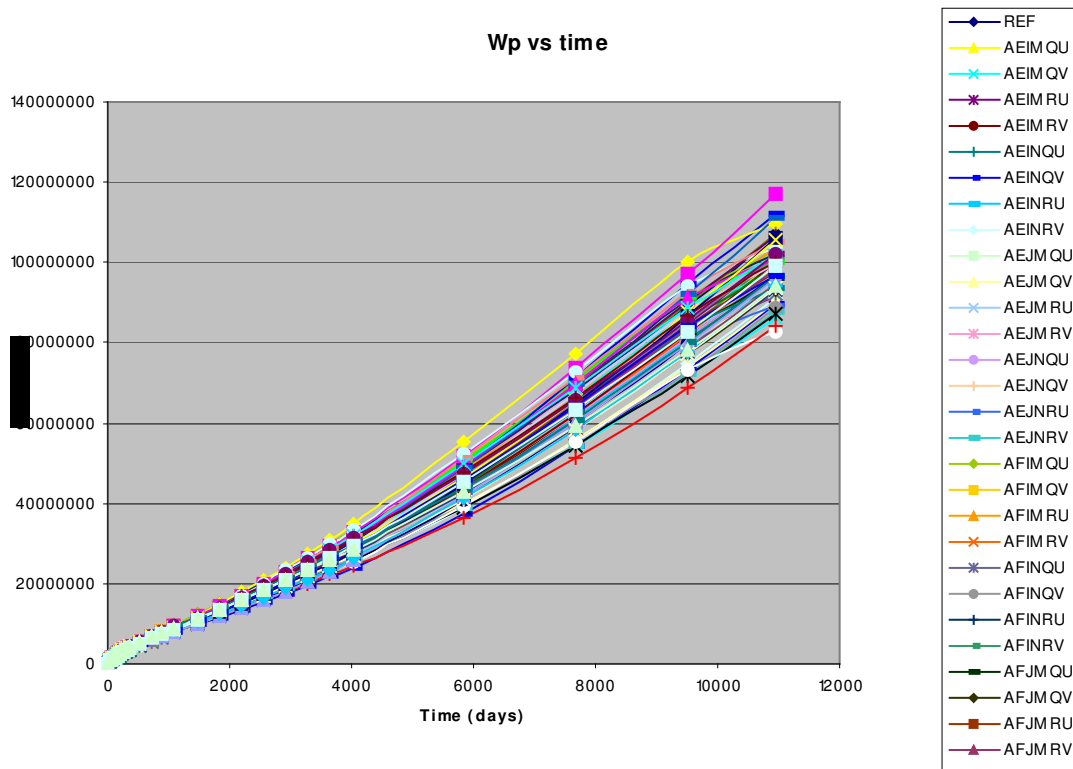


Figure 15: Wp range vs time (from 66 models)

The Figure 10 to Figure 15 illustrate the following reservoir characteristics:

- 1) OOIP ranges from 914.5 MMSTB (AFJNQU model) to 1,345 MMSTB (AEIMQV model). As presented in Figure 16, the OOIP data are divided in two groups depending on the value of erosion factor
- 2) N_p ranges from 203 (AFJNQU model) to 306 MMSTB (BEIMRV model). The models are also divided in two groups based on the erosion factor.
- 3) G_p ranges from 296 MMscf (AFJNQU model) to 474 MMscf (BFINQV model). The models are also separated in two groups, depending on the value of the erosion factor attributed.
- 4) Water produced range extends from 83 MMSTB (AFJNRU model) to 117 MMSTB (BEIMRV model). In this case, the set of data is homogeneous.
- 5) Gas Oil Ratio minimum value is 1.064 Mscf/STB (BFINRU model) and the maximum is equal to 1.44 Mscf/STB (AEIMQV model). The range of dataset is small.
- 6) Water cut: the dataset is divided in two groups, depending on the erosion factor value also: 0.331 (AFJNRU model) to 0.537 (BEJMQU model)
- 7) Recovery factor goes from 21% (AEIMQV model) to 24% (BEIMRU model). The dataset is grouped.

In summary, the influence of the erosion parameter is clear from the appearance of these plots. However, it does not have a major impact on the W_p and the recovery factor. The reference case, which is the model within which geological parameters have a average value, is located in the center of the dataset, as is the coarse model (model designed to test the sensitivity to upscaling).

5.3 Analysis of the Response Variables

5.3.1 Run Order Influence

To analyze the entire dataset one must first examine the response variables as compared with the order in which simulations were run. The choice of a certain run order could introduce a bias or a periodicity which could negatively affect the statistical analysis. Figure 16 to Figure 20 present those plots. The X axis is the run number, from runs 1 to 66. On the Y axis shows the values of the response variables.

The plots do not indicate that a certain periodicity exists because of run order. However, in all the plots except the one showing the recovery, data points are divided in two groups: one with OOIP=1,325 MMSTB, $N_p=290$ MMSTB, $W_p/N_p=0.42$, G_p/N_p between 1.48 and 1.50 and a second one with OOIP=925 MMSTB, $N_p=210$ MMSTB, $W_p/N_p=0.35$, G_p/N_p between 1.42 and 1.44.

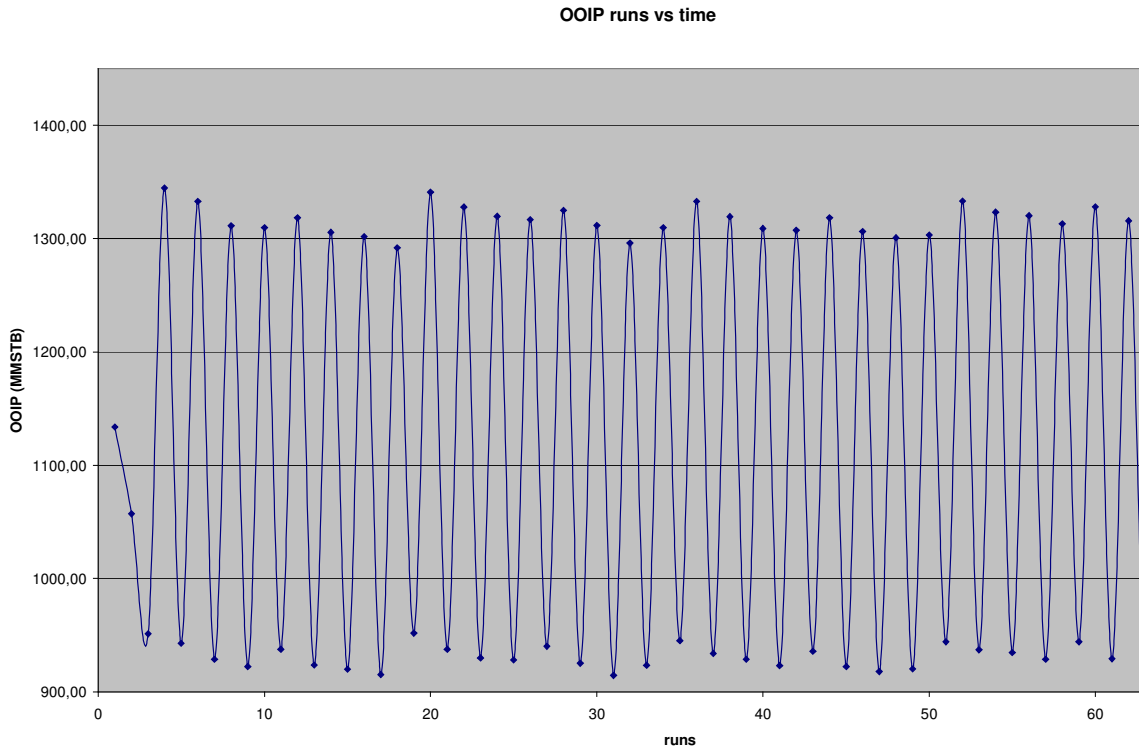


Figure 16: OOIP plot vs run order

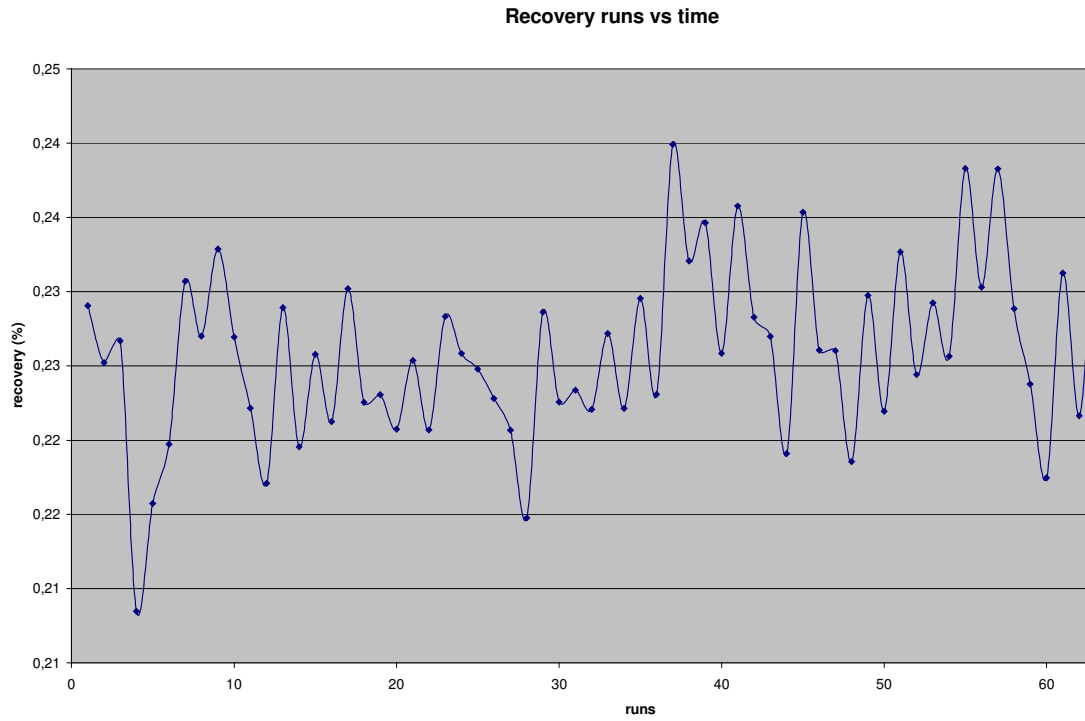


Figure 17: Recovery factor vs run time

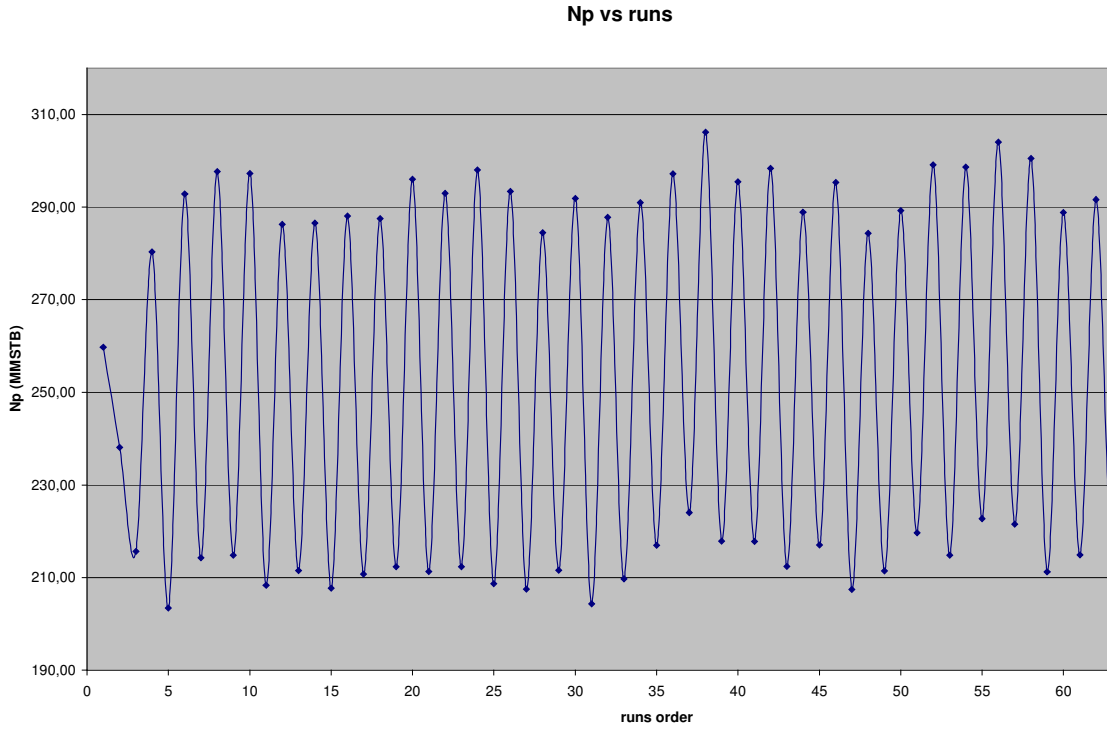


Figure 18: Cumulative oil produced vs run order

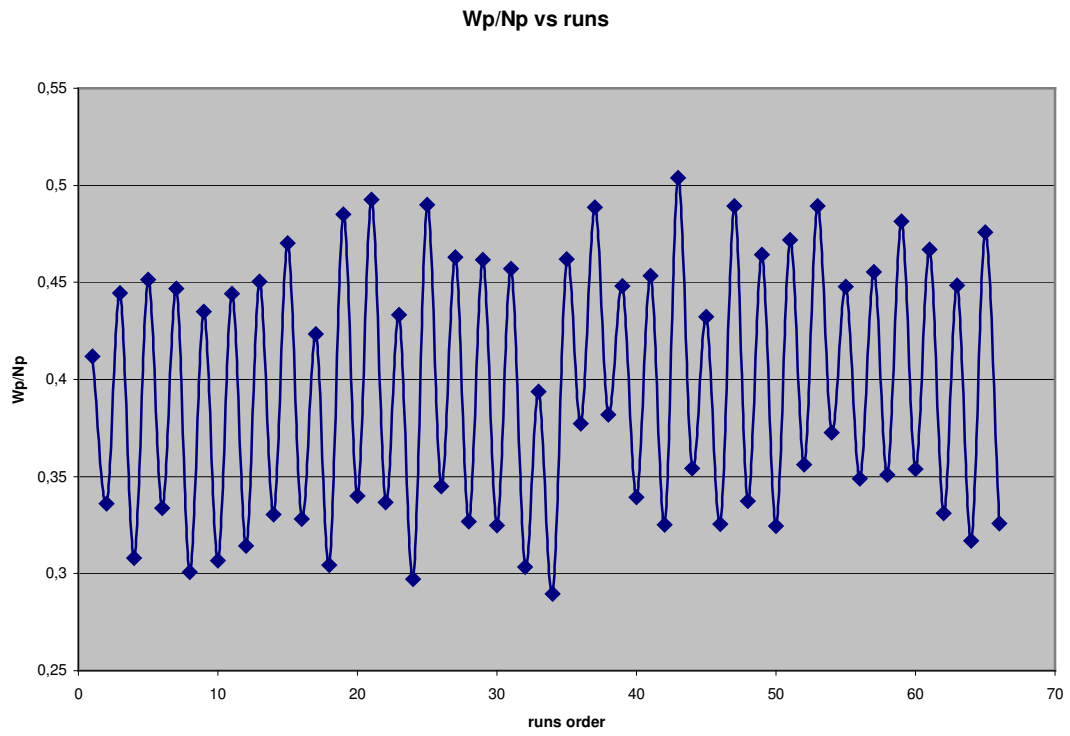


Figure 19: Wp/Np ratio versus run order

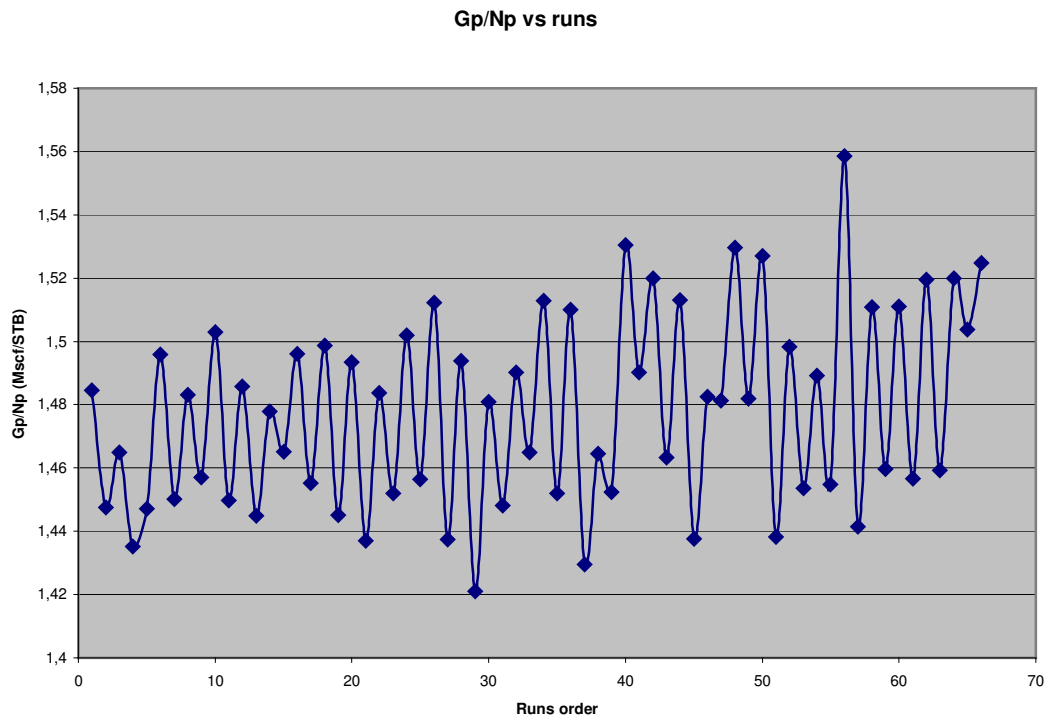


Figure 20: Gp/Np ratio versus run order

These two groups illustrate to the influence of the erosion parameter. The first group is linked to an erosion surface at +5m, the second to an erosion surface at -5m depth (plus or minus 5m compared to the average value). As this parameter is changing, so does the pore volume of the reservoir along with OOIP, N_p , W_p and the G_p .

The runs 1 and 2 represent the reference case and the coarse models. They are located in the middle of the two groups, which is logical due to their average values attributed to the parameters. From these plots, the top reservoir map has obviously a very strong influence on our response variables, except for the recovery.

5.3.2 Response Variable Distribution

The second analysis performed on the entire set of data is aimed at determining which statistical distribution is characteristic of the response variables, for example. Frequency histograms and cumulative frequency curves were generated for each of the five response variables. Figure 21 to Figure 25 present these response variable distributions.

Figure 21 to Figure 25 illustrate that the response variables, except recovery, are bimodally distributed with the modes corresponding to values assigned to the erosion factor. The recovery is normally distributed and the most probable value for recovery is around 22.8%. The recovery factor of the reference case is 23%, indicating that the choice of the reference case average value is good. So far in the analysis, it is the erosion parameter that has the greatest influence on the reservoir performance.

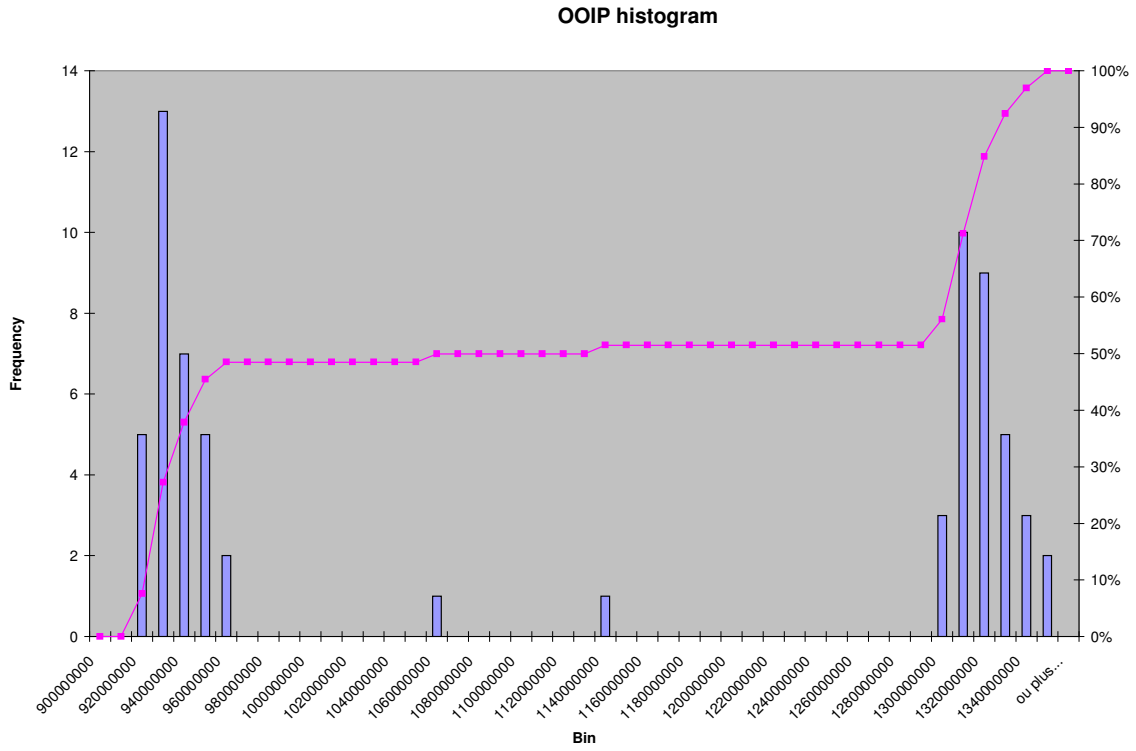


Figure 21: OOIP frequency histogram

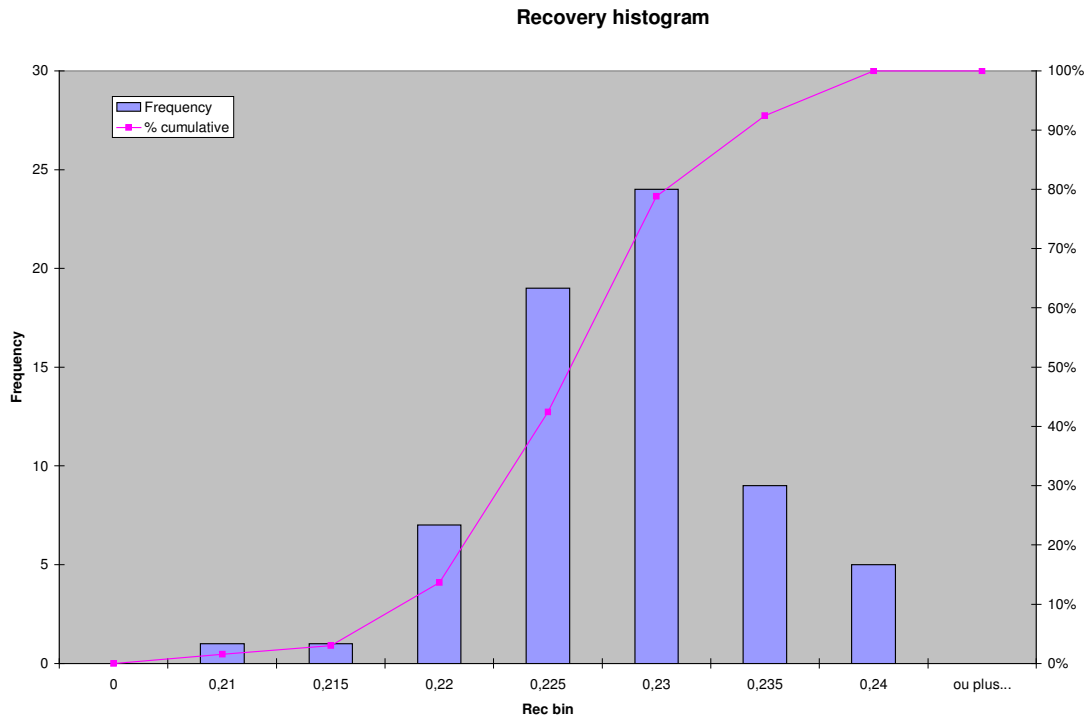


Figure 22: Recovery factor frequency histogram

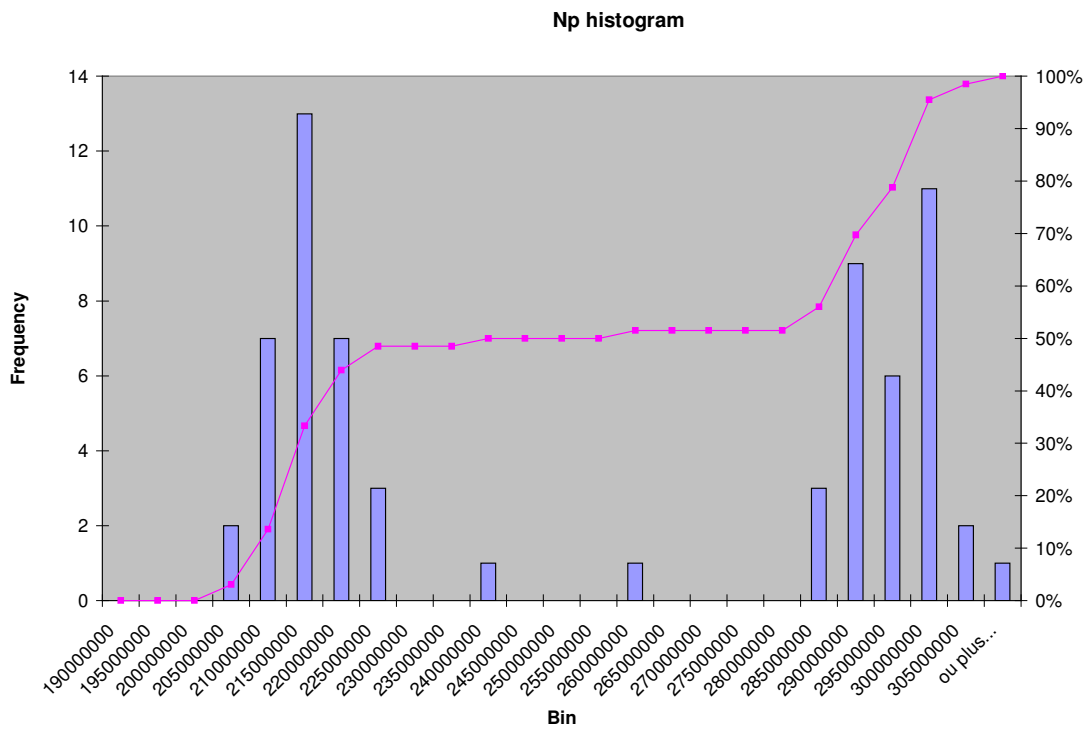


Figure 23: Cumulative oil production frequency histogram

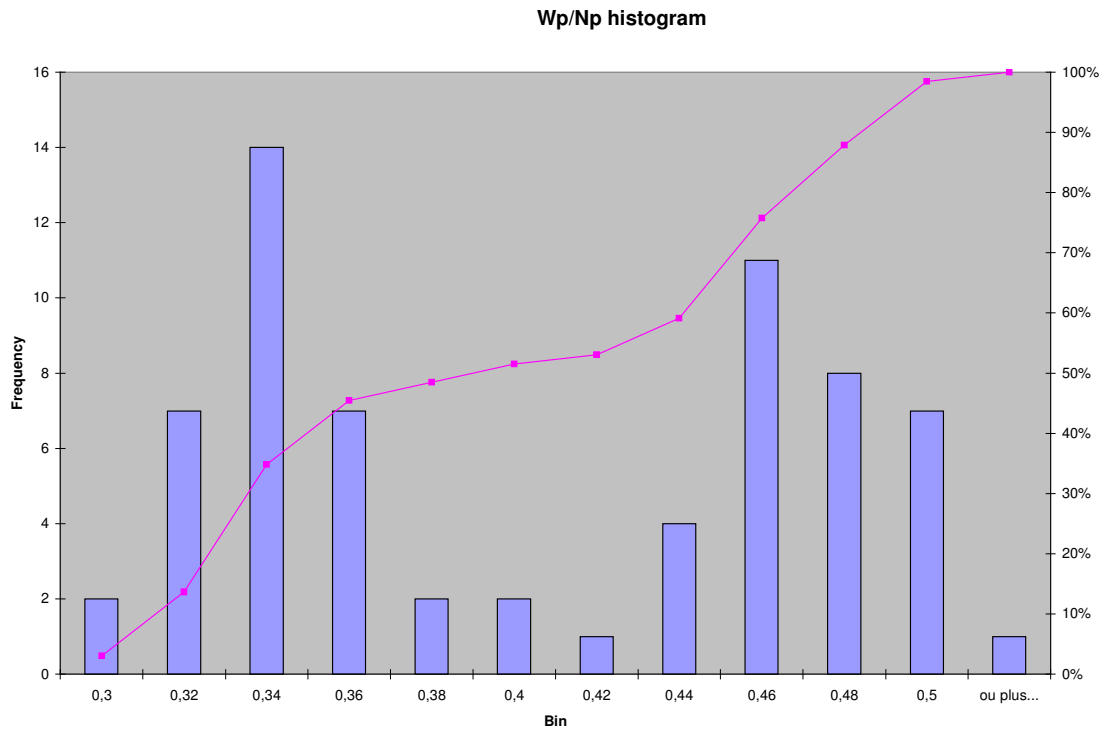


Figure 24: Wp/Np ratio frequency histogram

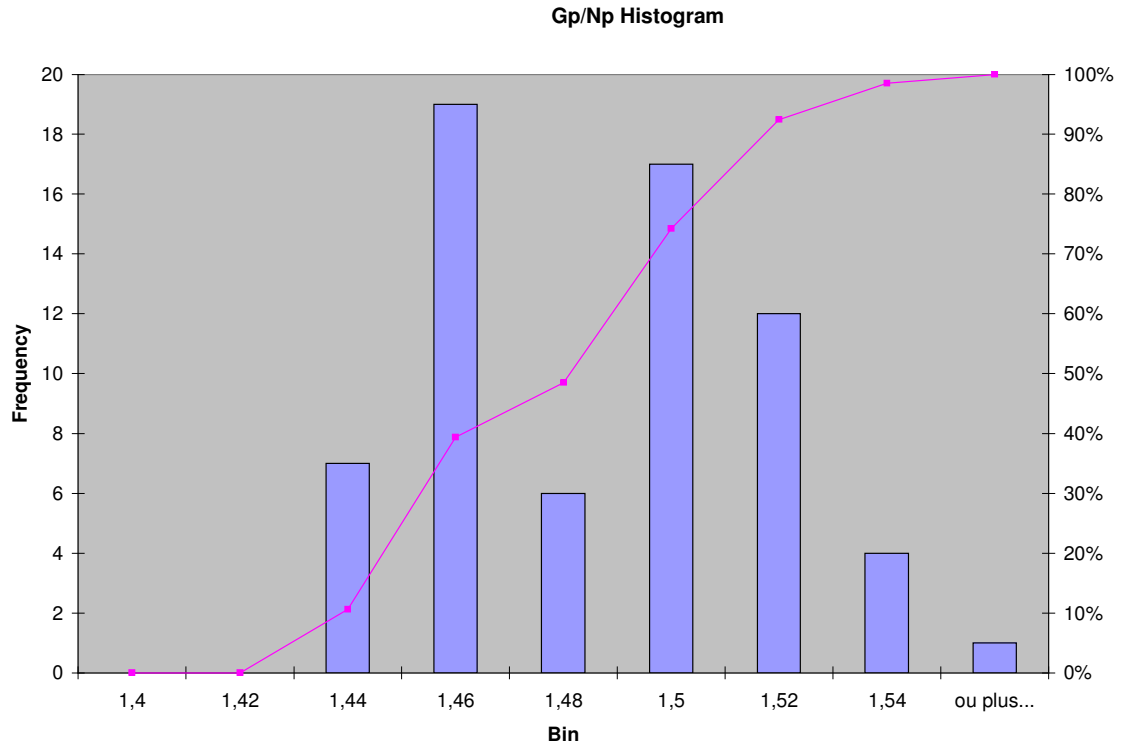


Figure 25: Gp/Np ratio frequency histogram

5.4 Influence of Individual Parameters

5.4.1 Classification of Models

Effect of any given factor is defined as the change in response produced by a change in the level (value) of that factor. This is called the *main effect* because it refers to the primary factors in the study. That is, changing factor A from level -1 to level $+1$ causes a change in the overall average response of the system. Because each model consists of a combination of the six parameters, the entire set of data for one response variable had to be renamed for the quantification. The designating letter for each geological configuration are given in table 1:

- 1) the letter A represents the negative 1 value of parameter 1 (the thickness variogram), B represents $+1$ value of the factor.
- 2) letter E represents -1 of the second parameter (bathymetric high or low, termed gulf or hump in this thesis), F, $+1$.
- 3) Shelf edge orientation is represented by the letter I equals -1 and J equals $+1$.
- 4) letters N and M represent -1 and $+1$ values of the “bathymetry range.
- 5) letters Q and R represent the -1 and $+1$ values of the “facies variogram”.
- 6) And finally U and V represent the -1 and $+1$ values of the “erosion factor”.

Geological configurations, or “models” are grouped in pairs in which only one parameter is changed at a time. That is, one “letter” as defined above, is changed at a time. If, for example, the thickness variogram factor is changed, the difference in the response variables between the two models in which factor level A and B vary will be singled out to determine the impact of that particular parameter. As an example, AEIMQU and BEIMQU is a valid couple, as AEINRV and BEINRV. Table 11 and Table 12 illustrate the organization of the geological models, in tests to determine factor impact on the recovery.

Table 11: First 32 models reorganized, example of the RF: -1 level models

Name	Param 1	Param 2	Param 3	Param 4	Param 5	Param 6	
	A/B	E/F	I/J	N/M	Q/R	U/V	
REF	0,23	REF	0,23	REF	0,23	REF	0,23
COARSE	0,23	COARSE	0,23	COARSE	0,23	COARSE	0,23
AEIMQU	0,23	AEIMQU	0,23	AEIMQU	0,23	AEIMQU	0,23
AEIMQV	0,21	AEIMQV	0,21	AEIMQV	0,21	AEINQU	0,23
AEIMRU	0,22	AEIMRU	0,22	AEIMRU	0,22	AEINRU	0,23
AEIMRV	0,22	AEIMRV	0,22	AEIMRV	0,22	AEINRV	0,23
AEINQU	0,23	AEINQU	0,23	AEINQU	0,23	AEJNQU	0,23
AEINQV	0,23	AEINQV	0,23	AEINQV	0,23	AEJNQV	0,22
AEINRU	0,23	AEINRU	0,23	AEINRU	0,23	AEJNRU	0,23
AEINRV	0,23	AEINRV	0,23	AEINRV	0,23	AEJNRV	0,22
AEJMQV	0,22	AEJMQV	0,22	AFIMQU	0,22	AFINQU	0,23
AEJMRU	0,23	AEJMRU	0,23	AFIMRU	0,23	AFINRU	0,22
AEJMRV	0,22	AEJMRV	0,22	AFIMRV	0,22	AFINRV	0,22
AEJNQU	0,23	AEJNQU	0,23	AFINQU	0,23	AFJNQU	0,22
AEJNQV	0,22	AEJNQV	0,22	AFINQV	0,23	AFJNQV	0,22
AEJNRU	0,23	AEJNRU	0,23	AFINRU	0,22	AFJNRU	0,23
AEJNRV	0,22	AEJNRV	0,22	AFINRV	0,22	AFJNRV	0,22
AFIMQU	0,22	BEIMQU	0,23	BEIMQU	0,23	BEINQU	0,23
AFIMQV	0,22	BEIMQV	0,22	BEIMQV	0,22	BEINQV	0,23
AFIMRU	0,23	BEIMRU	0,24	BEIMRU	0,24	BEINRU	0,24
AFIMRV	0,22	BEIMRV	0,23	BEIMRV	0,23	BEINRV	0,23
AFINQU	0,23	BEINQU	0,23	BEINQU	0,23	BEJNQU	0,23
AFINQV	0,23	BEINQV	0,23	BEINQV	0,23	BEJNQV	0,22
AFINRU	0,22	BEINRU	0,24	BEINRU	0,24	BEJNRU	0,23
AFINRV	0,22	BEINRV	0,23	BEINRV	0,23	BEJNRV	0,22
AFJMQV	0,22	BEJMQV	0,23	BFIMQU	0,23	BFINQU	0,24
AFJMRU	0,23	BEJMRU	0,24	BFIMRU	0,23	BFINRU	0,24
AFJMRV	0,22	BEJMRV	0,23	BFIMRV	0,23	BFINRV	0,23
AFJNQU	0,22	BEJNQU	0,23	BFINQU	0,24	BFJNQU	0,24
AFJNQV	0,22	BEJNQV	0,22	BFINQV	0,23	BFJNQV	0,23
AFJNRU	0,23	BEJNRU	0,23	BFINRU	0,24	BFJNRU	0,24
AFJNRV	0,22	BEJNRV	0,22	BFINRV	0,23	BFJNRV	0,23

Table 12: Last 32 models organized, for OOIP: level +1models for all factors

Name	Param 1 A/B	Param 2 E/F	Param 3 I/J	Param 4 N/M	Param 5 Q/R	Param 6 U/V					
BEIMQU	0,23	AFIMQU	0,22	AEJMQU	0,22	AEIMQU	0,23	AEIMRU	0,22	AEIMQV	0,21
BEIMQV	0,22	AFIMQV	0,22	AEJMQV	0,22	AEIMQV	0,21	AEIMRV	0,22	AEIMRV	0,22
BEIMRU	0,24	AFIMRU	0,23	AEJMRU	0,23	AEIMRU	0,22	AEINRU	0,23	AEINQV	0,23
BEIMRV	0,23	AFIMRV	0,22	AEJMRV	0,22	AEIMRV	0,22	AEINRV	0,23	AEINRV	0,23
BEINQU	0,23	AFINQU	0,23	AEJNQU	0,23	AEJMQU	0,22	AEJMRU	0,23	AEJMQV	0,22
BEINQV	0,23	AFINQV	0,23	AEJNQV	0,22	AEJMQV	0,22	AEJMRV	0,22	AEJMRV	0,22
BEINRU	0,24	AFINRU	0,22	AEJNRU	0,23	AEJMRU	0,23	AEJNRU	0,23	AEJNQV	0,22
BEINRV	0,23	AFINRV	0,22	AEJNRV	0,22	AEJMRV	0,22	AEJNRV	0,22	AEJNRV	0,22
BEJMQU	0,23	AFJMQU	0,22	AFJMQU	0,22	AFIMQU	0,22	AFIMRU	0,23	AFIMQV	0,22
BEJMQV	0,22	AFJMQV	0,21	AFJMQV	0,21	AFIMQV	0,22	AFIMRV	0,22	AFIMRV	0,22
BEJMRU	0,24	AFJMRU	0,23	AFJMRU	0,23	AFIMRU	0,23	AFINRU	0,22	AFINQV	0,23
BEJMRV	0,23	AFJMRV	0,22	AFJMRV	0,22	AFIMRV	0,22	AFINRV	0,22	AFINRV	0,22
BEJNQU	0,23	AFJNQU	0,22	AFJNQU	0,22	AFJMQU	0,22	AFJMRU	0,23	AFJMQV	0,21
BEJNQV	0,22	AFJNQV	0,22	AFJNQV	0,22	AFJMQV	0,21	AFJMRV	0,22	AFJMRV	0,22
BEJNRU	0,23	AFJNRU	0,23	AFJNRU	0,23	AFJMRU	0,23	AFJNRU	0,23	AFJNQV	0,22
BEJNRV	0,22	AFJNRV	0,22	AFJNRV	0,22	AFJMRV	0,22	AFJNRV	0,22	AFJNRV	0,22
BFIMQU	0,23	BFIMQU	0,23	BEJMQU	0,23	BEIMQU	0,23	BEIMRU	0,24	BEIMQV	0,22
BFIMQV	0,22	BFIMQV	0,22	BEJMQV	0,22	BEIMQV	0,22	BEIMRV	0,23	BEIMRV	0,23
BFIMRU	0,23	BFIMRU	0,23	BEJMRU	0,24	BEIMRU	0,24	BEINRU	0,24	BEINQV	0,23
BFIMRV	0,23	BFIMRV	0,23	BEJMRV	0,23	BEIMRV	0,23	BEINRV	0,23	BEINRV	0,23
BFINQU	0,24	BFINQU	0,24	BEJNQU	0,23	BEJMQU	0,23	BEJMRU	0,24	BEJMQV	0,22
BFINQV	0,23	BFINQV	0,23	BEJNQV	0,22	BEJMQV	0,22	BEJMRV	0,23	BEJMRV	0,23
BFINRU	0,24	BFINRU	0,24	BEJNRU	0,23	BEJMRU	0,24	BEJNRU	0,23	BEJNQV	0,22
BFINRV	0,23	BFINRV	0,23	BEJNRV	0,22	BEJMRV	0,23	BEJNRV	0,22	BEJNRV	0,22
BFJMQU	0,22	BFJMQU	0,22	BFJMQU	0,22	BFIMQU	0,23	BFIMRU	0,23	BFIMQV	0,22
BFJMQV	0,22	BFJMQV	0,22	BFJMQV	0,22	BFIMQV	0,22	BFIMRV	0,23	BFIMRV	0,23
BFJMRU	0,23	BFJMRU	0,23	BFJMRU	0,23	BFIMRU	0,23	BFINRU	0,24	BFINQV	0,23
BFJMRV	0,22	BFJMRV	0,22	BFJMRV	0,22	BFIMRV	0,23	BFINRV	0,23	BFINRV	0,23
BFJNQU	0,24	BFJNQU	0,23	BFJNQU	0,23	BFJMQU	0,22	BFJMRU	0,23	BFJMQV	0,22
BFJNQV	0,23	BFJNQV	0,23	BFJNQV	0,23	BFJMQV	0,22	BFJMRV	0,22	BFJMRV	0,22
BFJNRU	0,24	BFJNRU	0,23	BFJNRU	0,23	BFJMRU	0,23	BFJNRU	0,23	BFJNQV	0,23
BFJNRV	0,23	BFJNRV	0,22	BFJNRV	0,22	BFJMRV	0,22	BFJNRV	0,22	BFJNRV	0,22

5.4.2 Influence of Individual Parameters

5.4.2.1 DEX Scatter Plots

Once the models have been organized, Design EXperiments scatter plots (called DEX scatter plots) are computed in order to single out the parameters that have the most influence on response variables. DEX scatter plot shows the response variables for each level of each factor. The scatter plots illustrate graphically how the location (the centered values) and deviation (the spread of range value) vary for both within a factor (at different levels) and between different factors. According to Heckert and Filliben, 2002, the scatter plot aid by providing a ranked list of important factors.

For factor 1, response variables values are plotted with abscissa values between 0 and 1; the models with a level of -1 are plotted on the abscissa value $X=0.2$ in this example, whereas the $+1$ models are plotted on abscise $X=0.8$. Factor 2 will be plotted at 1.2 and 1.8, and so on. The point of this technique is to determine if a significant difference exists in response variable values between -1 and $+1$ for each geological model, and for each factor. Graphically, groups of points for level -1 of factor 1 should be shifted compared to level $+1$ values, if the factor has an impact on the response variable. The DEX scatter plots are presented Figure 26 to Figure 30.

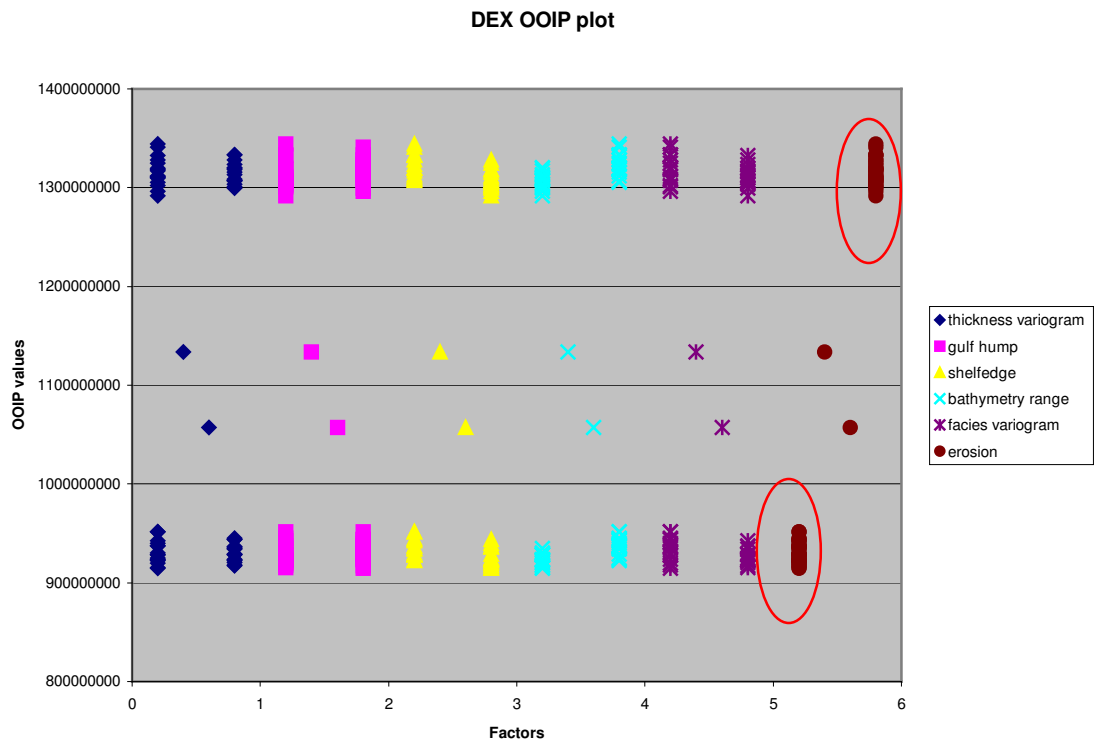


Figure 26: OOIP DEX scatter plot

From Figure 26, several interpretations can be made :

- 1) The most influential factor is the erosion factor, because it is the only factor for which -1 values are shifted compared to $+1$ values (maroon color);
- 2) For the other factors, data points from level -1 and $+1$ are to the same level, suggesting that the influence of these factors on OOIP is low compared to the erosion factor. Furthermore, groups with the same level (-1 or $+1$) fall into two groups, owing to the influence of the erosion factor.
- 3) The center points represent the reference case value and the coarse model value. The coarse model is the lower point (abscissa values equals to 0.6, 1.6, 2.6, etc). Their values are always the same and have been plotted for each factor to facilitate reading and comparison. These two models are just represented by one measure each.

Figure 27 proves that erosion, bathymetry and the thickness variogram have great influence on outcomes, but no single factor stands out as most influential. The influence of these factors on the recovery cannot be determined from this plot probably because of interaction between factors

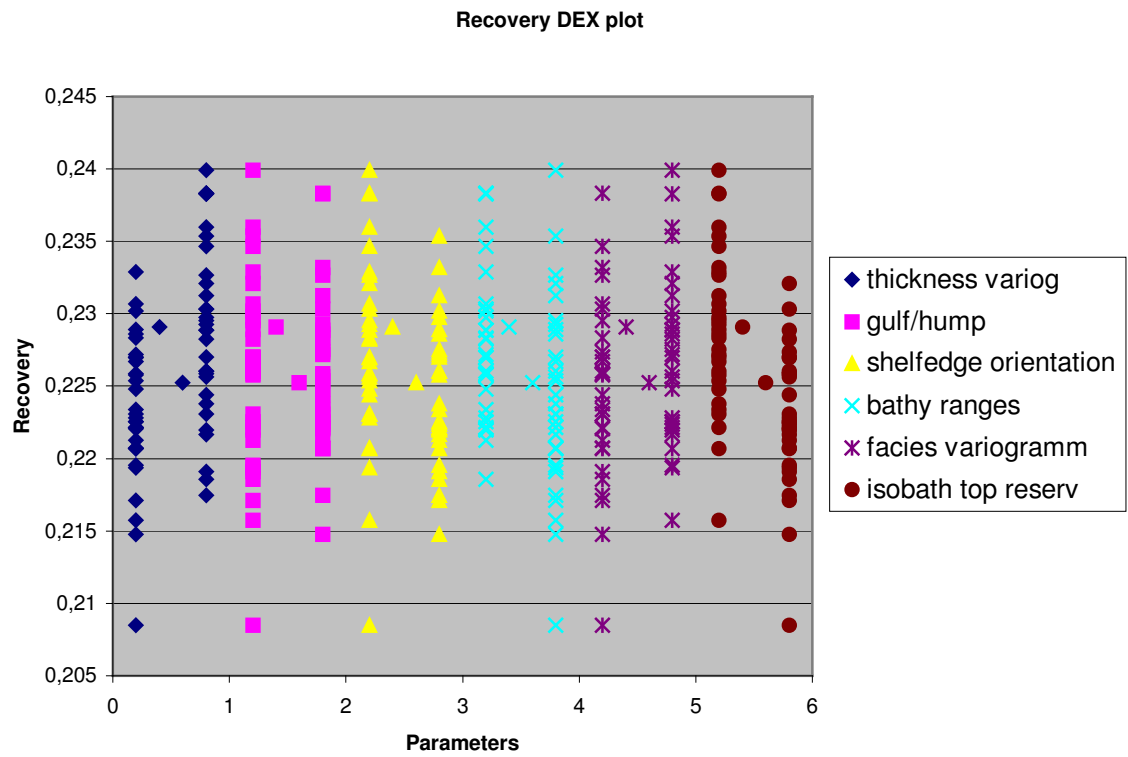


Figure 27: Recovery factor DEX scatter plot

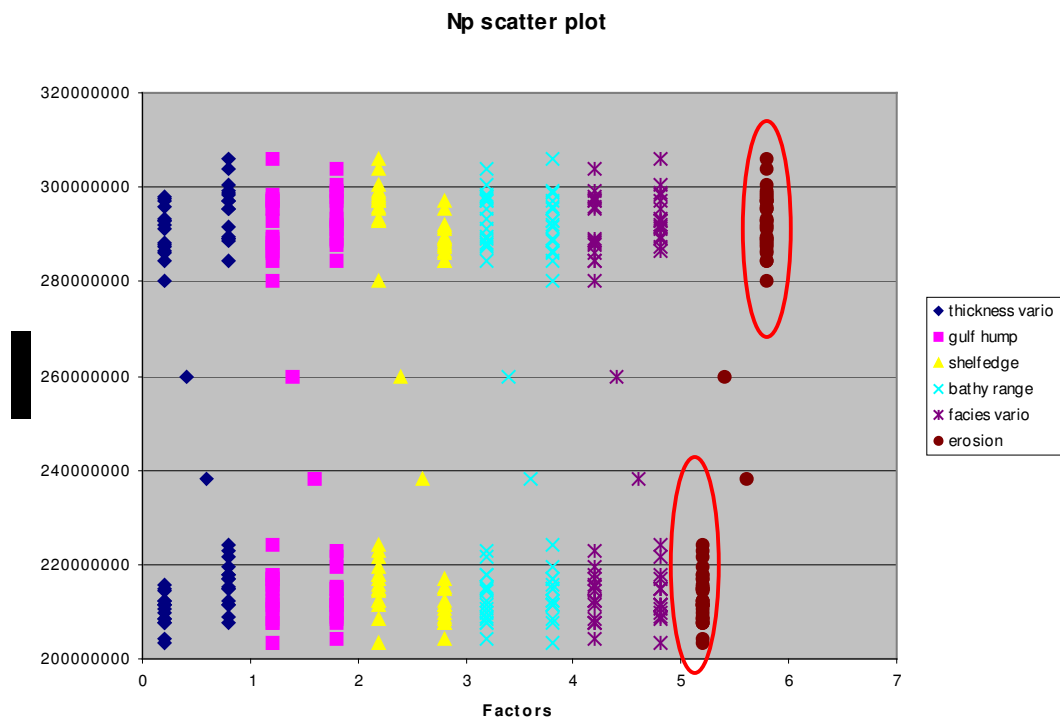


Figure 28: Cumulative oil produced DEX scatter plot

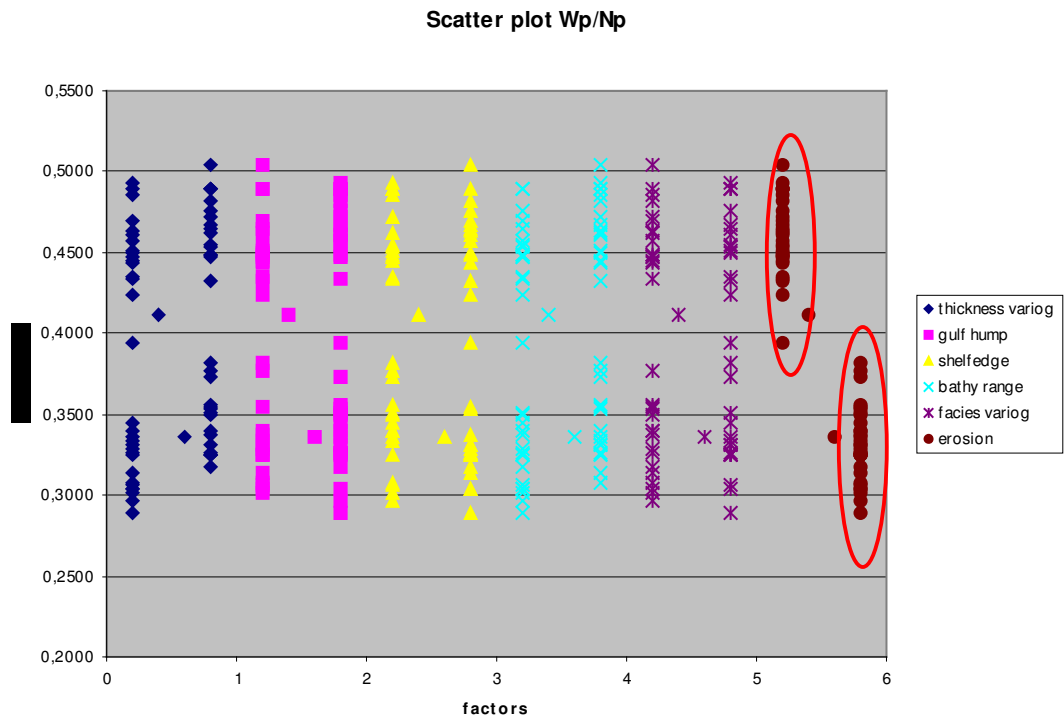


Figure 29: Wp/Np ratio DEX scatter plot

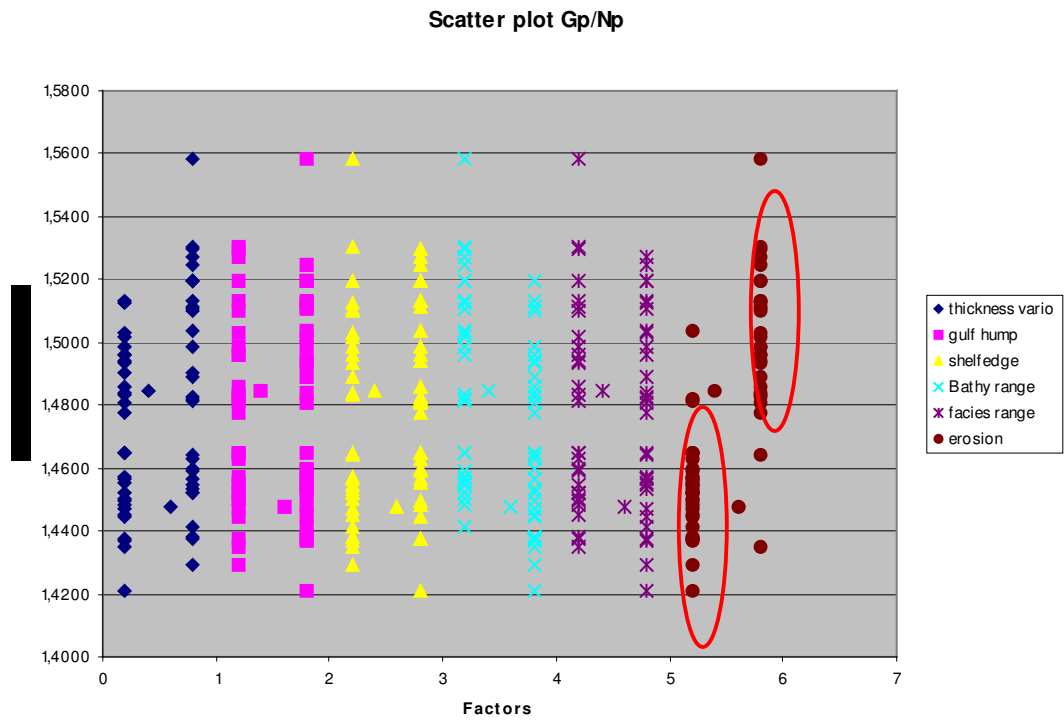


Figure 30: Gp/Np ratio DEX scatter plot

The Figure 28 to Figure 30 show the same situation. Erosion has such a great impact that it obscures the impact of the other factors. Note that no outliers are present (points isolated from the majority of points) and that reservoir recovery seems to behave differently than the other variables. This can be explained by the fact that recovery is also linked to transmissibility, itself depending on the thickness and the permeability. Finally, permeability is directly related to facies in this model. That is probably all these interactions that smooth an eventual individual parameter impact. So, other statistical methods are needed to conclude.

5.4.2.2 DEX Mean Plots

DEX mean plots help to assess the importance of factors other than erosion. These plots focus on the mean values or means of each level of each factor. The DEX mean plot shows mean values for the two levels of each factor plotted by factor. The means for a single factor are connected by a straight line (ESH, 2001). For each factor, the mean of the level -1 and the mean of the level $+1$ are computed, and plotted on a single horizontal axis. The slope and the length of the straight line connecting the two means of a same factor enable one to determine the influence of the factor on the response variable. Dex mean plots are presented Figure 31 to Figure 36.

Figure 31 and Figure 32 present the relative influence of each parameter on the OOIP. Obviously, from the Figure 31, erosion is still the most important parameter: it has the longest and steepest line. It means that the difference of mean is important, so, that changing factor levels has a strong influence on the response variable. If we just plot factors without the erosion map one, their individual influence is highlighted, relatively to the change of scale. The bathymetry ranges is the second influent parameter. Then, the shelf edge and the facies variogram act on the OOIP.

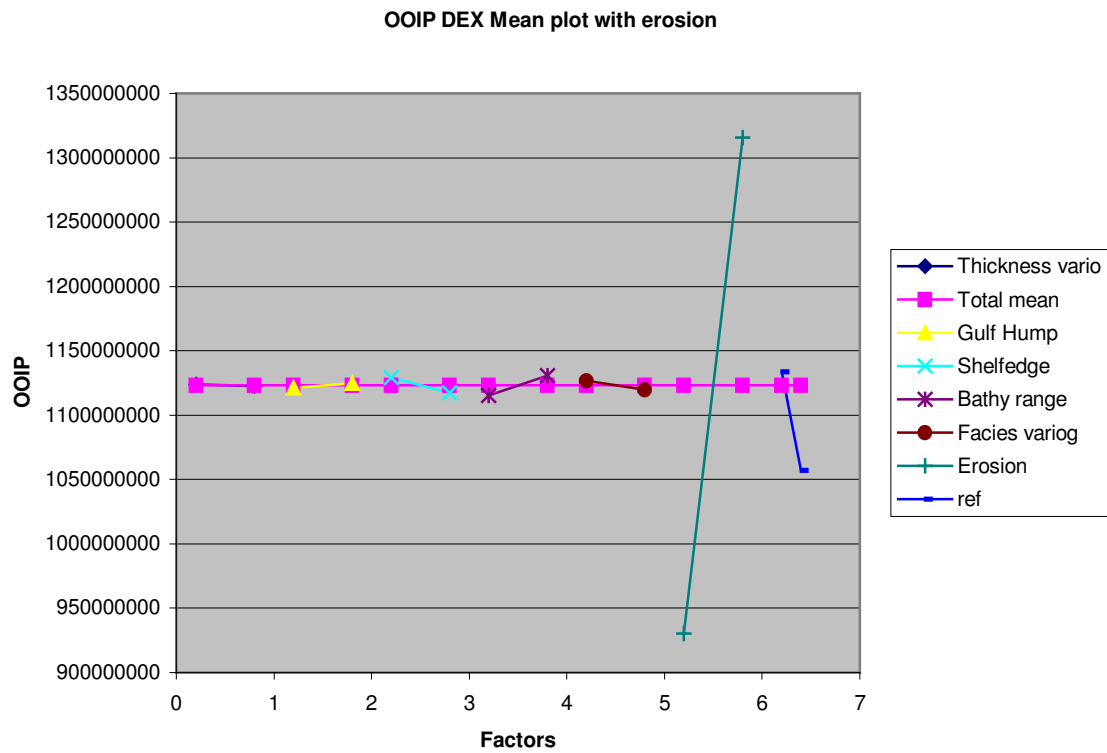


Figure 31: OOIP DEX mean plot

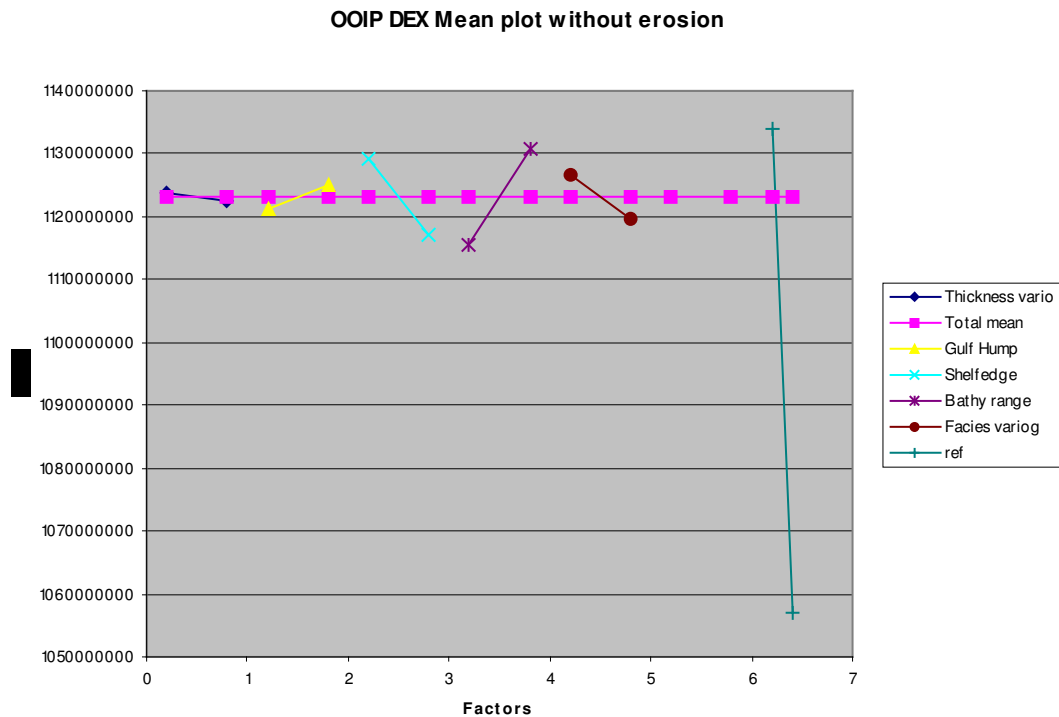


Figure 32: OOIP DEX mean plot without erosion factor plotted

Enlarging the bathymetry range induces a larger spatial extension of the good reservoir facies. So, we increase the size of the reservoir facies, with high oil saturation. This way, it clearly acts on the OOIP. The shelf edge and the facies variogram guide also the repartition of the good facies. The shelf edge and facies variogram's mean lines have negative slopes: the +1 value represents an E-W orientation. The more E-W is the platform, the lower is the OOIP. The larger the range of the facies variogram, the lower the OOIP. The reason why an E-W orientation and large range of facies variogram tend to decrease the OOIP doesn't seem to be straight forward to justify. Because the influence of these parameters is negligible compared to the erosion, and lower than the bathymetry ranges, it could be due to interaction between the four parameters.

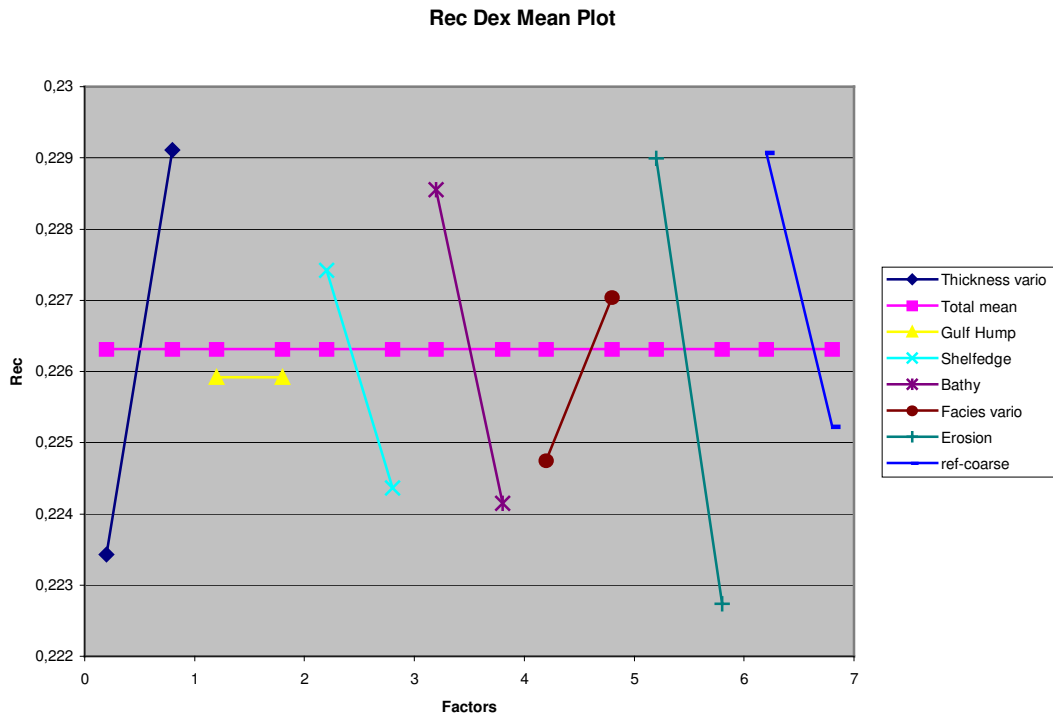


Figure 33: Recovery factor DEX mean plot

Finally, the last factor to be plotted is the reference case and the coarse model. It indicates the influence of the upscaling compared to other parameter impacts. For the OOIP, it is obvious that the upscaling is a critical step, which can change drastically the oil pool volume. As a warning, the reference case and the coarse case are represented by ONE measurement each, and not by a mean.

The preceding plots illustrate the relative influence of each parameter on OOIP. From Figure 32, erosion can be seen to remain the single most parameter because it has the longest and steepest line. This indicates that difference between mean values is important, and that changing assigned values for factors greatly influences the response variables. If factors are plotted without the erosion factor, the influence of each is highlighted. The second most influential factor on OOIP is the bathymetric range factor, followed by the orientation of the shelf edge and the facies variogram values. Increasing the bathymetric range causes a wider geographic spread of “good reservoir facies”. When the size of the reservoir facies is increased, it impacts on the OOIP.

The shelf edge and the facies variogram values have influence on the spatial arrangement of the “good” (porous and permeable) facies. The straight lines representing shelf edge and facies variogram mean values have negative slopes. The +1 value represents an E-W orientation and the more the platform tends to be oriented E-W, the lower the OOIP.

For the facies variogram, the larger the range of the variogram, the lower the OOIP. The reason an E-W orientation and large range of facies variogram tend to decrease the OOIP is not easy to explain. The influence of these parameters is negligible compared to erosion, and has less influence in general than the bathymetry factor. It appears that this result is again due to factor interaction in the computer algorithm.

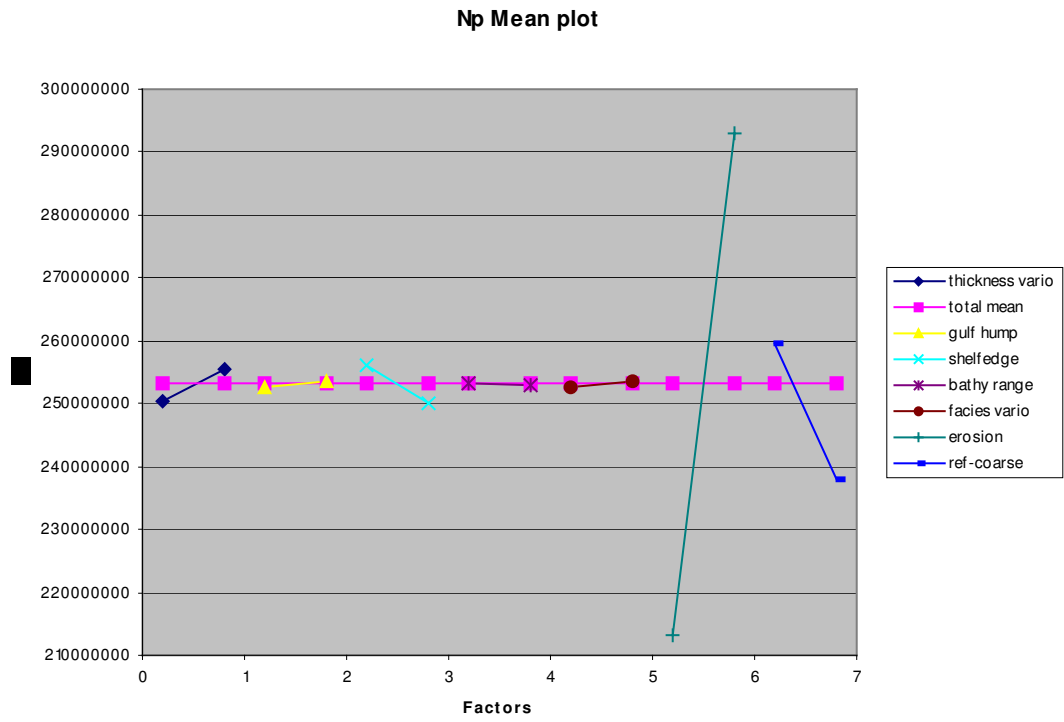


Figure 34: Cumulative oil produced DEX mean plot

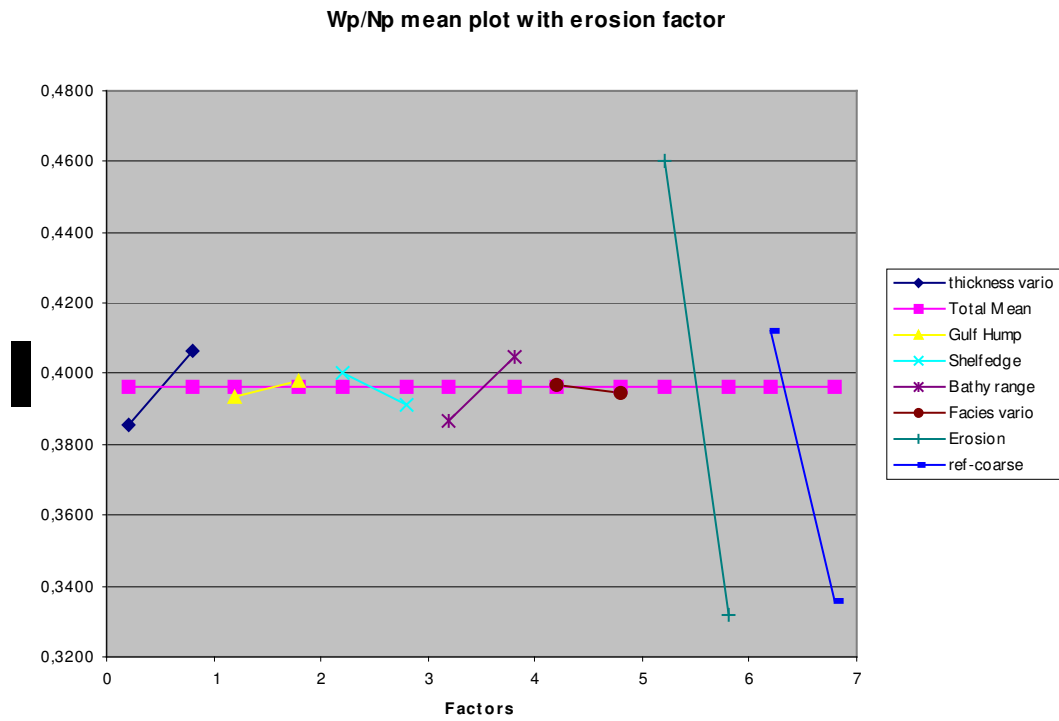


Figure 35: Wp/Np ratio DEX mean plot

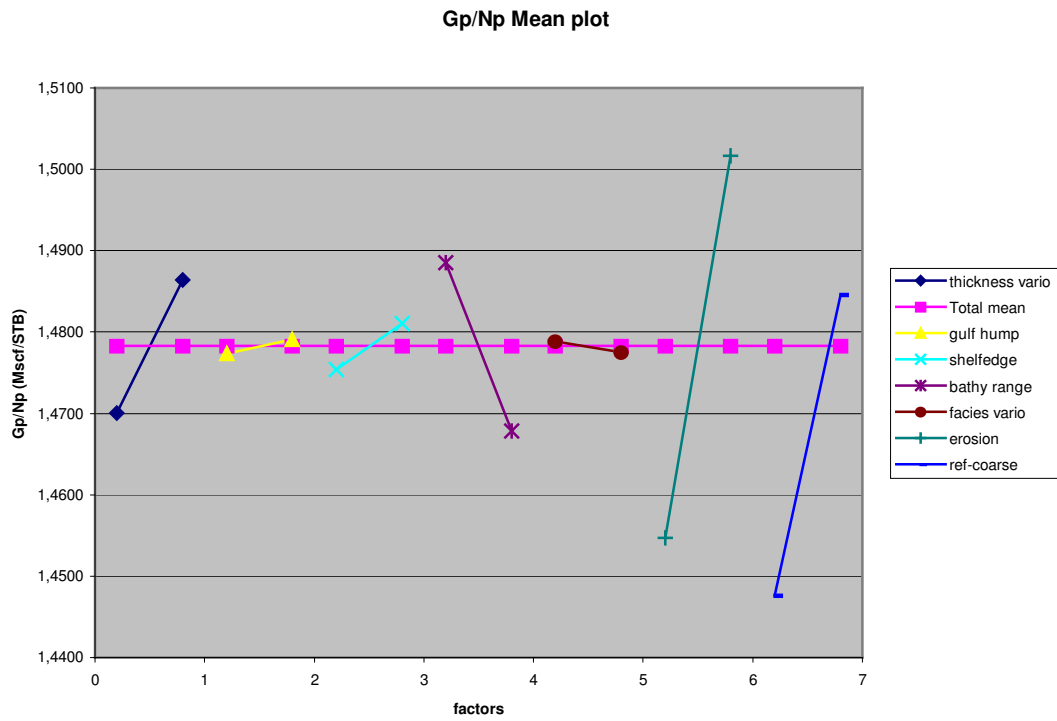


Figure 36: Gp/Np ratio DEX mean plot

For those three plots, the most influent factors are the erosion, then the bathymetry ranges and the thickness variogram finally. It is coherent to what was seen for the OOIP, because these factors are also strongly related to OOIP. If we consider the upscaling, the consequence of this step is one more time critical, in a sense that it changes drastically the original volumes in place, so the fluid volumes produced after.

To conclude, these graphical methods are pretty straight forward to draw and interpret. But it just allows us to make a relative hierarchy of the factor impacts. No percentage of effect is available at this stage of the study. This analysis is called a screening design, because we just define the impact of each factor relatively to the other parameters. In the next paragraph, we will present two methods which will bring us to a real quantification of uncertainty, a quantitative characterization of the effect of each geological and geostatistical factors.

5.5 Quantification of Uncertainty

5.5.1 DEX Mean Slope Method

This method is based on the analysis of the DEX mean plot slopes, presented in the previous paragraph. For each factor, the slope of the line joining the two means (one for level -1 and one for level $+1$) is calculated. Then, the entire slopes are summed, and this total is normalized, equals to 1. Finally, the percentage of the total slope that each factor slope represents, gives an idea of the effect of each parameter. This way, the impact of each parameter is quantified (a percentage of the total influence is given for each factor). Using the previous DEX mean plots, slopes and percentages were calculated. The results are presented in Table 13 to Table 17.

Table 13: Effect of each factor on the OOIP

OOIP	D (MMSTB)	% effect
Erosion	385.16	58.80
Bathymetry	-73.39	-11.2
Shelf-bathy	59.39	9.07
Gulf-Bathy	-57.14	-8.72
Thick-Bathy	-56.06	-8.56
Shelf edge	-11.85	-1.81
Facies	-7.19	-1.09
Gulf Hump	3.622	0.55
Thickness	-1.02	-0.15

Table 14: Effect of each factor on the recovery

REC	D (%)	% effect
Bathy-Facies	-0.017	-21.78
Thick-Bathy	-0.0164	-21.06
Gulf-shelf-Bathy	0.016	20.51
Bathymetry	-0.0114	-14.62
Erosion	-0.0063	-8.03
Thickness	0.0049	6.28
Shelf edge	-0.0031	-4.03
Facies	0.0024	3.06
Gulf Hump	-0.0001	-0.17

Table 15: Effect of each factor on the Np

Np	D (MMSTB)	% effect
erosion	79.95	65.59
Thick-Bathy	-15.27	-12.52
Bathymetry	-13.39	-10.98
Shelf edge	-6.19	-5.08
Thickness	5.06	4.16
Facies	1.09	0.89
Gulf hump	0.9	0.74

Table 16: Effect of each factor on the Wp/Np

Wp/Np	D (STB/STB)	% effect
Erosion	-0.13	-51.38
Bathymetry	0.047	18.8
Thick-Bathy	-0.029	-11.56
Thickness	-0.021	-8.36
Shelf edge	-0.009	-3.74
Thickn-Gulf-Shelf	0.006	2.38
Gulf hump	0.004	1.66
Facies	-0.002	-0.84

Table 17: Effect of each factor on the GP/Np

Gp/Np	D (Mscf/STB)	% effect
Shelf-Bathy-Ero	-0.097	-22.56
Thick-Gulf-Bathy	-0.095	-22.09
Shelf-Bathy-Facies	0.0941	21.88
Bathymetry	-0.07	-16.09
erosion	0.047	10.92
Thickness	0.017	3.81
Shelf edge	0.0057	1.33
Gulf hump	0.0019	0.44
facies	-0.001	-0.31

The most influent factor, whatever the response variable, is the erosion extension (the top reservoir isobath map location). It is almost the only parameter to influence the OOIP, the Np and the Wp/Np, whereas its impact is not so significant for the recovery factor compared to the impact of other parameters.

But, it is obvious from this analysis that the three main influent factors are the erosion, then the bathymetry range or the thickness variogram. As mentioned previously, the bathymetry range controls the lateral extension of the good reservoir facies, whereas the thickness variogram controls the transmissibility of the layers.

This analysis is very easy to compute and allows us to obtain results very quickly. However, based on this method, interactions between parameters are totally neglected. It is all the more false considering the relationship existing between our geological and geostatistical factors: Bathymetry ranges are directly linked to facies repartition, so to the facies variogram. This last factor is also linked to the shelf edge orientation. In a

second time, pore volume depends on the erosion map location as much as the thickness of the layers, (thickness variogram factor). Those two parameters interact also. To quantify the impact of each parameter and their interaction, a second method was used: the ANalysis Of the Variance method, called *ANOVA tables*.

5.5.2 Analysis of Variance Method: Effects and Interactions

5.5.2.1 Methodology

The goal of this method is to determine quantitatively the impact of each factor on the response variables and also evaluate the interactions between the factors. It comes directly from statistics. To explain how effects of factors will be characterized, let's take a simple example. The simplest type of 2^k design is a 2^2 , that is two factors A and B, each at two levels. These two levels are frequently called *high* and *low* levels. Figure 37 shows a graphical representation of this 2^2 design.

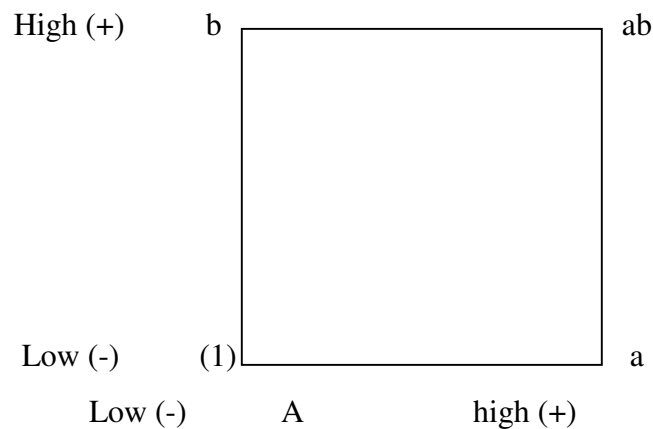


Figure 37: 2^2 factorial design

The design can be represented by a square with the $2^2=4$ runs forming the corners of the square. A special notation is used to represent the treatment combinations (a, ab, etc, here). If a letter is present, then the corresponding factor is run at its high level in that treatment combination; if it is absent, the factor is run at its low level. For example, treatment a indicates that factor A is at its high level, and factor B at its low level. The treatment combination with all the factors at their low levels is noted (1). The effects under interest in the 2^2 design are the main effects A and B, and the two-factor interaction effect AB. Say that (1), a, b and ab represent the entire combinations of our trial.

To estimate the main effect of A, we would average the observations on the right side of the square, where A is at its high level, and subtract from this average of the observations on the left side of the square (A at its low level). It can be written as:

$$A = ((a+ab)/2n) - ((b+(1))/2n)$$

$$A = (1/2n) [a+ab-b-(1)]$$

Following the same procedure:

$$B = ((b+ab)/2n) - ((a+(1))/2n)$$

$$B = (1/2n) [b+ab-a-(1)]$$

Finally, the AB interaction is estimated by taking the difference in the diagonal averages of the square:

$$AB = (1/2n) [ab+(1) - a-b]$$

The quantities in brackets in the previous equations are called *contrasts*. In these equations, the contrasts coefficients are always either -1 or $+1$.

A table of plus and minus signs, such as Table 18 below, can be used to determine the sign of each treatment combination for a particular contrasts. The column headings are the main effects A, B, AB interaction, and I, which represents the total. The row headings are the treatment combinations. Note that the sign in AB column are products of the signs of A and B.

Table 18: Constant contrasts table

Treatment combinations	Factorial effects			
	I	A	B	AB
(-1)	+	-	-	+
a	+	+	-	-
b	+	-	+	-
ab	+	+	+	+

So, calculating A, B and AB is equivalent to quantifying the effect of each parameter, and their interactions. We can summarize that with a formula:

$$\text{Effect} = \text{Contrasts} / (n2^{k-1})$$

N is the number of trial, or replicate, here 1.

K is the number of level, here, 2.

All these examples were taken from the book “Probability and statistics in engineering”, (Hines et al., 2003).

Residuals Analysis

Once these effects have been calculated, it is possible to determine a regression model, fitting the data set of response variables. It means an equation where all the influent parameters appear with their coefficient effect. If factors 1 and 2 have been determined as influent by the ANOVA effect computation, the regression model is:

$$Y = \beta_0 + \beta_1 x_1 + \beta_2 x_2 + \beta_3 x_1 x_2 + \varepsilon$$

x_1 represents factor 1, β_1 its half-coefficient effect, β_0 , the *grand mean* (the arithmetic average of the response variable for the entire set of data), and ε , the errors between the mathematical model here above and the data set, the response variables. This error term is also called *residuals*.

The low and high levels of factor 1 are assigned to the values -1 and $+1$. So, for example, if we consider the mean model where A and B are at -1 , x_1 coefficient effect was equal to 2, B coefficient=4, and AB coefficient=0.6, the grand mean=96, the response variable for one model = 100, then:

$$100 = 96 + (2/2)*(-1) + (4/2)(-1) + 0.6*(-1*-1) + \varepsilon$$

$$\varepsilon = 2.6$$

So, the regression model for this model will be :

$$Y = \beta_0 + x_1 \ 2x_2 + 0.6x_1x_2 + 2.6$$

The reason why the regression coefficient is one-half the effect estimate is because regression coefficients measure the effect of a unit change in x_1 on the mean of Y , and the effect estimate is based on a two-unit change (from -1 to $+1$) (Hides et al., 2003).

This model can be used to obtain the predicted values at all the points in the design. If the response variables are normally distributed, we can also plot a normal probability plot of the response variables, and of the residuals, to determine the outliers, a data point that falls far from most other points (Voelker and al, 2001). This is not the case in our study. As seen before, our distributions are bimodal. That's why we won't present these kinds of plots here.

5.5.2.2 Case Study

In this study, just one trial is available (1×64 runs). So, 1 mean, 6 main effects, 15 two-factor interactions, 20 three-factor interactions, 15 four-factor interactions, 6 five-factor interactions and 1 six-factor interactions are present and need to have their impacts quantified.

Effect Coefficients

The ANOVA method was applied to our results, and the impact of each parameter A, B, C, D, E, F and their interaction computed. As an example, the results obtained for the OOIP are presented Table 19 and Table 20. Some operations were done on the coefficient to ease the reading (ex: OOIP in MMSTB rather than STB, so coefficient/ 10^6).

Table 19: OOIP factor coefficient effect, part 1

Factors	Response variable: OOIP	
	COEFF (STB)	COEFF(MMSTB)
A	-1018240	-1,02
B	3622093	3,622
AB	1063514	1,064
C	-11851788	-11,852
AC	2910033	2,910
BC	839403	0,839
ABC	-511733	-0,512
D	-73397907	-73,398
AD	-56061806	-56,062
BD	-57134640	-57,135
CD	59399517	59,400
ABD	-59280202	-59,280
ACD	56373858	56,374
BCD	55258743	55,259
ABCD	57652535	57,653
E	-7192744	-7,193
AE	-508838	-0,509
BE	467146	0,467
CE	405831	0,406
DE	-52925457	-52,925
ABE	-1564676	-1,565
ACE	-381947	-0,382
ADE	-59072770	-59,073
BCE	515342	0,515
BDE	-57506981	-57,507
CDE	59642542	59,643
ABCE	-1935823	-1,936
ABDE	-60527002	-60,527
ACDE	57855051	57,855
BCDE	58818816	58,819
ABCDE	57084541	57,085

Table 20: OOIP factor coefficient effect, part 2

Response variable: OOIP		
Factors	COEFF (STB)	COEFF(MMSTB)
F	385161259	385,161
AF	-566159	-0,566
BF	1069266	1,069
CF	-2018533	-2,019
DF	56777382	56,777
EF	140583	0,141
ABF	-330870	-0,331
ACF	1167456	1,167
ADF	58096258	58,096
AEF	-74903	-0,075
BCF	300893	0,301
BDF	58414651	58,415
BEF	143234	0,143
CDF	-57537055	-57,537
DEF	58190914	58,191
CEF	171259	0,171
ABCF	-533042	-0,533
ABDF	57641365	57,641
ABEF	-484429	-0,484
ACDF	-57993663	-57,994
ACEF	123725	0,124
ADEF	57978567	57,979
BCDF	-58599808	-58,600
BCEF	544701	0,545
BDEF	57810722	57,811
CDEF	-58735207	-58,735
ABCDF	-57939114	-57,939
ABCEF	-220398	-0,220
ABDEF	57814398	57,814
ACDEF	-58161637	-58,162
BCDEF	-57361027	-57,361
ABCDEF	-58567612	-58,568

Predicted Models

So, from these matrices, the following regression models are:

X_1 = thickness variogram

X_2 = gulf or hump

X_3 = shelf edge orientation

X_4 = bathy range

X_5 = facies variogram

X_6 = top reservoir map

$$Y_{\text{OOIP}} = 1123.13 - 0.51x_1 + 1.811x_2 - 5.93x_3 - 36.7x_4 - 3.6x_5 + 192.6x_6 - 28.03x_1x_4 - 28.06x_2x_4 + 29.7x_3x_4$$

$$Y_{\text{Recovery Factor}} = 0.2259 + 0.00245x_1 - 0.00005x_2 - 0.0012x_3 - 0.0057x_4 + 0.0012x_5 - 0.00315x_6 + 0.008x_2x_3x_4 - 0.0082x_1x_4$$

$$Y_{\text{Np}} = 253.04 + 2.534x_1 + 0.45x_2 - 3.095x_3 - 6.695x_4 + 0.544x_5 + 40x_6 - 7.635x_1x_4$$

$$Y_{\text{Wp/Np}} = 0.3958 - 0.0105x_1 + 0.00205x_2 + 0.0047x_3 - 0.0235x_4 - 0.0012x_5 - 0.065x_6 - 0.0155x_1x_4 + 1.165x_1x_2x_3$$

$$Y_{\text{Gp/Np}} = 1.4782 + 0.0082x_1 + 0.000095x_2 + 0.00285x_3 - 0.0345x_4 - 0.00065x_5 + 0.0235x_6 - 0.0475x_1x_2x_4 + 0.047x_3x_4x_5 - 0.0485x_3x_4x_6$$

After normalization, a percentage of effect for each parameter and its interactions is presented in Table 21.

Table 21: Quantification of uncertainty for each factor and its interactions

OOIP	D (MMSTB)	% effect
Erosion	385,16	58,8
Bathymetry	-73,39	-11,2
Shelf-bathy	59,39	9,07
Gulf-Bathy	-57,14	-8,72
Thick-Bathy	-56,06	-8,56
Shelf edge	-11,85	-1,81
Facies	-7,19	-1,09
Gulf Hump	3,622	0,55
Thickness	-1,02	-0,15

REC	D (%)	% effect
Bathy-Facies	-0,017	-21,78
Thick-Bathy	-0,0164	-21,06
Gulf-shelf-Bathy	0,016	20,51
Bathymetry	-0,0114	-14,62
Erosion	-0,0063	-8,03
Thickness	0,0049	6,28
Shelf edge	-0,0031	-4,03
Facies	0,0024	3,06
Gulf Hump	-0,0001	-0,17

Np	D (MMSTB)	% effect
erosion	79,95	65,59
Thick-Bathy	-15,27	-12,52
Bathymetry	-13,39	-10,98
Shelf edge	-6,19	-5,08
Thickness	5,06	4,16
Facies	1,09	0,89
Gulf hump	0,9	0,74

Wp/Np	D (STB/STB)	% effect
Erosion	-0,13	-51,38
Bathymetry	0,047	18,8
Thick-Bathy	-0,029	-11,56
Thickness	-0,021	-8,36
Shelf edge	-0,009	-3,74
Thickn-Gulf-Shelf	0,006	2,38
Gulf hump	0,004	1,66
Facies	-0,002	-0,84

Gp/Np	D (Mscf/STB)	% effect
Shelf-Bathy-Ero	-0,097	-22,56
Thick-Gulf-Bathy	-0,095	-22,09
Shelf-Bathy-Facies	0,0941	21,88
Bathymetry	-0,07	-16,09
erosion	0,047	10,92
Thickness	0,017	3,81
Shelf edge	0,0057	1,33
Gulf hump	0,0019	0,44
facies	-0,001	-0,31

The second column of each table, called D (units), represents the change of value of the response variable, when factors are varying from level -1 to level +1. For example, for the OOIP response variable, when the thickness variogram varied from level -1 to +1, the OOIP decreases of 1.02 MMSTB. This variation of 1.02 MMSTB represents a variation of 0.16% of the total variation of the OOIP.

Residuals Analysis

The residuals were calculated for all the models, for all the response variables. These equations are presented in Appendix 69 and Appendix 70.

CHAPTER VI

RESULTS AND DISCUSSION

6.1 Quantification of Uncertainty

6.1.1 Impact of Each Geological Factor on the Reservoir Performances

Table 22 summarizes results obtained with ANOVA method. The most influent factors for each response variable are:

For the OOIP (influence decreasing downward):

- 1) top reservoir map : 59%
- 2) bathymetry range: 11%
- 3) interaction between bathymetry and shelf edge: 9%

The 4-order interaction terms and higher were neglected

For the recovery factor variable (influence decreasing downward):

- 1) interaction between bathymetry and facies variogram: 22%
- 2) bathymetry range: 21%
- 3) interaction between gulf, bathymetry and facies: 21%

The 4-order interaction terms and higher were neglected.

Table 22: ANOVA coefficient effects

OOIP	D (MMSTB)	% effect
Erosion	385,16	58,8
Bathymetry	-73,39	-11,2
Shelf-bathy	59,39	9,07
Gulf-Bathy	-57,14	-8,72
Thick-Bathy	-56,06	-8,56
Shelf edge	-11,85	-1,81
Facies	-7,19	-1,09
Gulf Hump	3,622	0,55
Thickness	-1,02	-0,15

REC	D (%)	% effect
Bathy-Facies	-0,017	-21,78
Thick-Bathy	-0,0164	-21,06
Gulf-shelf-Bathy	0,016	20,51
Bathymetry	-0,0114	-14,62
Erosion	-0,0063	-8,03
Thickness	0,0049	6,28
Shelf edge	-0,0031	-4,03
Facies	0,0024	3,06
Gulf Hump	-0,0001	-0,17

Np	D (MMSTB)	% effect
erosion	79,95	65,59
Thick-Bathy	-15,27	-12,52
Bathymetry	-13,39	-10,98
Shelf edge	-6,19	-5,08
Thickness	5,06	4,16
Facies	1,09	0,89
Gulf hump	0,9	0,74

Wp/Np	D (STB/STB)	% effect
Erosion	-0,13	-51,38
Bathymetry	0,047	18,8
Thick-Bathy	-0,029	-11,56
Thickness	-0,021	-8,36
Shelf edge	-0,009	-3,74
Thickn-Gulf-Shelf	0,006	2,38
Gulf hump	0,004	1,66
Facies	-0,002	-0,84

Gp/Np	D (Mscf/STB)	% effect
Shelf-Bathy-Ero	-0,097	-22,56
Thick-Gulf-Bathy	-0,095	-22,09
Shelf-Bathy-Facies	0,0941	21,88
Bathymetry	-0,07	-16,09
erosion	0,047	10,92
Thickness	0,017	3,81
Shelf edge	0,0057	1,33
Gulf hump	0,0019	0,44
facies	-0,001	-0,31

For the Cumulative oil produced variable (influence decreasing downward):

- 1) top reservoir map: 66%
- 2) interaction bathymetry and thickness: 13%
- 3) bathymetry range: 11%

The 4-order interaction terms and higher were neglected.

For the produced water cut, W_p/N_p ratio, (influence decreasing downward):

- 1) top reservoir map: 51%
- 2) bathymetry: 19%
- 3) interaction thickness and bathymetry: 12%

The 4-order interaction terms and higher were neglected.

G_p/N_p ratio influent factors (influence decreasing downward):

- 1) interaction between shelf edge, bathymetry and erosion: 23%
- 2) interaction between thickness, gulf-hump and bathymetry: 22%
- 3) interaction shelf edge, bathymetry and facies: 22%

The 4-order interaction terms and higher were neglected.

As shown by the ANOVA analysis, the top reservoir map is the most influent factor for the OOIP, N_p , and W_p/N_p (range from 50 to 66% of influence). For the recovery and the G_p/N_p , the ranges of bathymetry attributed for each facies is the preponderant factor (around 20% of effect). But these two variables are more sensitive to the interaction between bathymetry and others factors, rather than by a single factor.

6.1.2 Discussion of the Impact of Each Factor

The objectives of this discussion are, first, to determine which reservoir parameters are affected when geological factors are changing. Second, to understand how response variable values will evolve when geological factor levels are varying from -1 to $+1$.

Three kind of information can be interpreted from response variable behavior:

- 1) the OOIP gives the size of the original pore volume or the size of the original oil pool of the reservoir
- 2) the Recovery factor indicates the efficiency of the oil production
- 3) the W_p/N_p and GP/N_p ratios give an idea of the water injection efficiency, so of the pressure maintenance inside the reservoir: an increase of gas and water produced indicate a less efficient water injection (more water produced for the same quantity of oil produced, so less oil displaced), whereas a decrease of those variables prove a better flooding of the reservoir (less gas produced indicates a higher reservoir pressure, so a better pressure maintenance).

Table 23 summarizes the effect of each factor for all the response variables. This table comes from ANOVA analysis. All the geological parameter levels changed from level -1 (minimum) to $+1$ (maximum value). The signs of the coefficient indicate if the response variable will increase (positive sign) or decrease (negative sign) when levels of geological factors go from -1 to $+1$.

Table 23: Effect of each factor on all response variables

Thickness variogram			Gulf or hump			Shelf edge		
Variable	Delta	%	Variable	Delta	%	Variable	Delta	%
OOIP	-1,020	0,70	OOIP	3,622	0,21	OOIP	-11,852	0,56
recovery	0,0049	6,28	recovery	-0,0001	0,17	recovery	-0,0031	4,03
Np	5,0675	4,16	Np	0,9000	0,74	Np	-6,1900	5,08
Wp/Np	0,0209	8,36	Wp/Np	0,00414	1,66	Wp/Np	-0,00936	-3,74
Gp/Np	0,0164	3,81	Gp/Np	0,00189	0,44	Gp/Np	0,0057	1,33

Bathymetry range			Facies variogram			Erosion		
Variable	Delta	%	Variable	Delta	%	Variable	Delta	%
OOIP	-73,390	-10,98	OOIP	-7,193	-1,39	OOIP	385,161	58,80
recovery	-0,0114	14,62	recovery	0,0024	3,06	recovery	-0,0063	8,03
Np	-13,3900	10,98	Np	1,0875	0,89	Np	79,9511	65,59
Wp/Np	0,047	18,80	Wp/Np	-0,002089	-0,84	Wp/Np	-0,12845	-51,38
Gp/Np	-0,0692	-16,09	Gp/Np	-0,001327	-0,31	Gp/Np	0,04695	10,92

RV	Units
OOIP	MMSTB
Np	MMSTB
RF	%
Wp/Np	STB/STB
Gp/Np	Mscf/STB

Delta: variation of the response variable values due to the change of factor level.

6.1.2.1 OOIP

Thickness Variogram Range Factor

When thickness variogram factor evolves from -1 to $+1$, variogram becomes larger. So the correlation distance between two data points is larger, thickness changes are smoother. The hard data located at the well are emphasized and thickness changes are harder. A decrease of the thickness layer is induced by this smoothing, reservoir height is lower, creating a decrease of the pore volume so the OOIP. When variogram range is larger, OOIP decreases.

Gulf-Hump

The level -1 of this factor represent morphology of gulf around well 14. The level $+1$ illustrates a hump morphology around well 14. So, when this factor varies from level -1 to $+1$, gulf is replaced by a hump around the well 14. It induces more height of the reservoir around the well, so, a larger pore volume. When the morphology is changing for a hump, OOIP increases.

Shelf Edge Orientation

The studied reservoir is a carbonate one, with shoal barriers. These shoals are located parallel to the shelf edge of the platform. Thus, the orientation of the shelf edge acts directly on the shoal (reservoir) orientation. At model scale, the shelf edge orientation determines the polarity of the platform: where is the basin located, where is the coast. Going from level -1 to $+1$ indicates a shelf edge orientation change from N-S to E-W. The hard data located at the wells remain unchanged. When the shelf edge is N-S oriented, it seems that more poor reservoir quality facies are simulated, decreasing the total porosity of the reservoir, so the OOIP. This is illustrated by Figure 38.

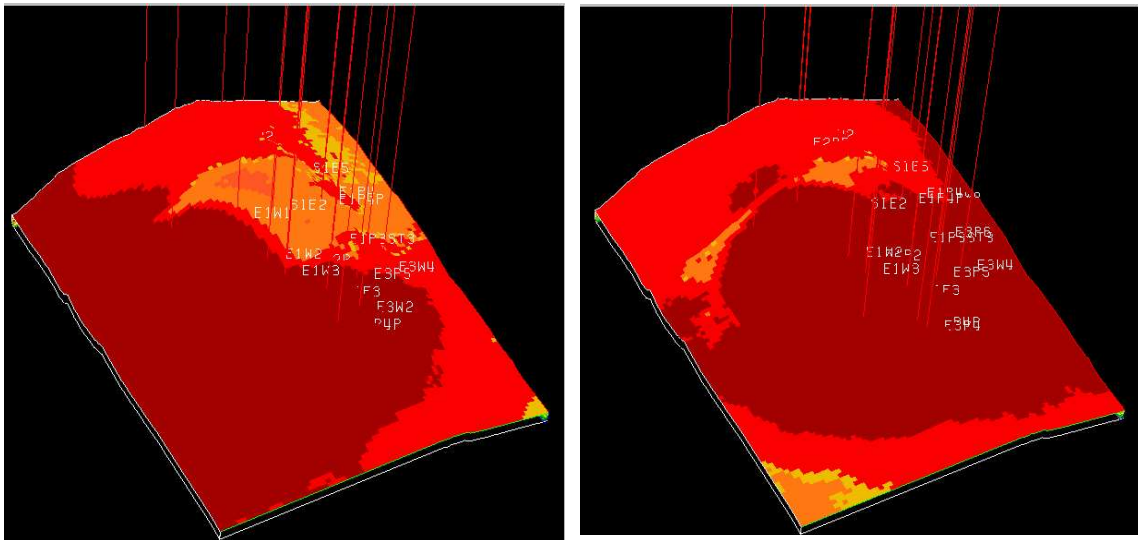
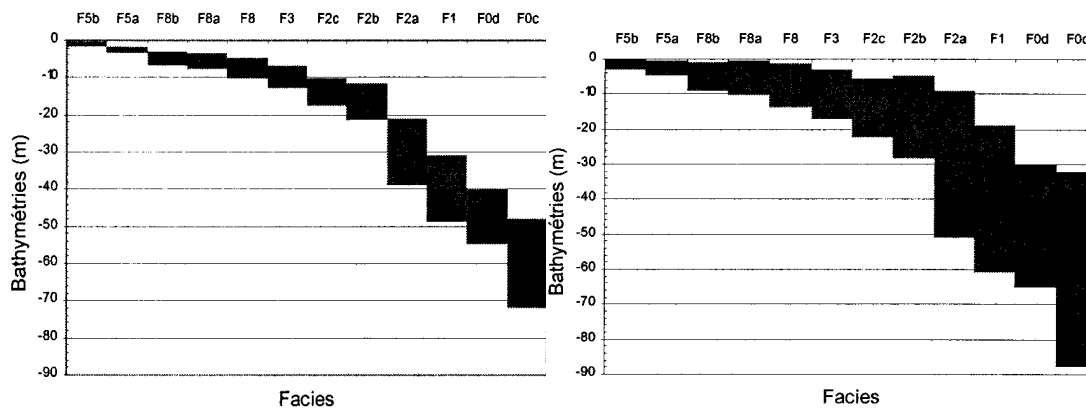


Figure 38: Gocad models: shelf edge orientation and facies repartition

Bathymetry Range

Going from level -1 to level $+1$ induces larger bathymetry ranges attributed per facies.

Figure 39 illustrates this principle.



Tight bathymetry ranges per facies

large bathymetry ranges

Facies names (shallow facies on the left, basin facies on the right of each picture)

Figure 39: Bathymetry range for levels -1 and $+1$ (after Lodola, 2002b)

If you draw a line at bathymetry = -20m on the two plots, you will see that in the second case (larger ranges), you have a very high probability to simulate bad facies. So, the bathymetry ranges overlap more on each other. On a reservoir point of view, bad quality reservoir facies are more represented, so low porosity facies appear more inside the reservoir. The reservoir pore volume decreases, as the OOIP, when bathymetry ranges are larger.

Facies Variogram Range

Going from level -1 to +1 of this factor induces a larger value attributed to the variogram range. As for the bathymetry ranges, it favors the presence of poor reservoir quality facies inside geological model, decreasing the total porosity so the pore volume of the reservoir. When facies variogram range is larger, OOIP decreases.

Erosion

When this factor goes from level -1 to +1, the depth of the top reservoir map of the reservoir goes shallower. Thus, the erosion is less intense at the top of the reservoir. Less good reservoir diagenetic facies are eroded. It means that more facies with high porosity are present. This creates a bigger pore volume, so more OOIP: the OOIP increases when the erosion intensity decreases.

Interaction between Shelf Edge and Bathymetry

These two factors are strongly correlated. As explained previously, the shelf edge orientation influences the repartition of the facies inside the reservoir. The bathymetry ranges were attributed on a facies per facies basis. So, it is clear that changing the shelf edge orientation, facies repartition, so bathymetry ranges are modified in the same time. The change from level -1 to +1 of these two factors act in the same direction: OOIP decreases due to more frequent poor reservoir quality facies.

Interaction between Bathymetry and Gulf

This interaction is related to the morphology of the platform around the well 14. When a hump is present, it creates a positive morphology on the platform. The assumption is that sea level is not changing here. So, if sediments deposit on this hump, their bathymetry will be shallower than if a gulf was present. It induces a change of the bathymetry ranges attributed to facies around well 14. As seen in the bathymetry range paragraph, larger ranges induced more poor quality facies and so a decrease of the pore volume as of the OOIP.

6.1.2.2 Recovery Factor and Oil Produced

These variables will be analyzed together because they both illustrate reservoir production performances.

Thickness Variogram Range

When thickness variogram factor evolves from -1 to $+1$, the correlation distance between two data points is larger, thickness changes are smoother. It means that the transmissibility of the reservoir (permeability multiplied by thickness) per layer is more homogeneous. It results a better recovery factor. When thickness variogram range is larger, recovery is better.

Gulf-Hump

As seen before, the implantation of a hump around well 14 rather than a gulf increases the height of the reservoir in this area. However, well 14 is located in the aquifer. So, increasing the reservoir height around well 14 induces more water produced, so less recovery. Finally, this well closes after few months of production. So, these conclusions have to be taken with extreme precautions.

Shelf Edge Orientation

As mentioned previously, good reservoir bodies are located parallel to the shelf edge of the platform. Thus, the orientation of the shelf edge acts directly on the shoal (reservoir) orientation. At model scale, the shelf edge orientation determines the polarity of the platform: where is the basin located, where the coast is.

Going from level -1 to $+1$ indicates a shelf edge orientation change from N-S to E-W.

The hard data located at the wells remain unchanged. When the shelf edge is N-S oriented, it seems that more poor reservoir quality facies are simulated, decreasing the total permeability of the reservoir, so the transmissibility. Finally, when the shelf edge is oriented N-S, the recovery is lower.

Bathymetry

Going from level -1 to level +1 induces larger bathymetry ranges attributed per facies. It favors the presence of poor reservoir quality facies, so low permeability. The presence of these low K facies creates vertical flow barriers, which limit the recovery of oil.

Facies Variogram Range

Going from level -1 to +1, the facies variogram range is enlarged. It favors smoother change of facies, so more homogeneous permeability values. The reservoir transmissibility is thus increased, the recovery becomes better. When facies changes are smoother, recovery is higher.

Erosion

When this factor goes from level -1 to +1, the depth of the top reservoir map of the reservoir goes shallower. Thus, the erosion is less intense at the top of the reservoir. Less good reservoir diagenetic facies are eroded. It means that more facies with high porosity are present. This creates a bigger pore volume. In a same time, the water injection efficiency remains the same. So, it allows the formation of a larger gas cap. That's why, even if good permeability facies are present at the top of the reservoir, oil recovery. So, mainly gas is produced. (It is proven by Gp/Np variable evolution). When erosion is less intense, recovery factor decreases.

The interaction between gulf, shelf edge and bathymetry can be explained as done before. The change of the morphology (gulf or hump) and orientation of the platform influences the facies spatial distribution inside the reservoir, so the bathymetry ranges.

These three factors tend to decrease the recovery.

6.1.2.3 Production Water Cut and Gas Oil Ratio

Thickness Variogram Range

Going from level -1 to $+1$, the thickness changes are smoother. It induces a more homogeneous permeability field, so a better transmissibility and a higher water injection efficiency.

Gulf-Hump

The implantation of a hump around well 14 induces a higher water height (well located in the aquifer), so more water produced. Because this well closes very early in the production history of the field, this conclusion has to be taken with caution.

Shelf Edge Orientation

The shelf edge orientation has to be correlated with injector location over the field. Shelf edge orientation influences the polarity of the deposits (where is the basin, where is the land). In carbonate platforms, good reservoir quality facies are generally located at the shelf edge, parallel to it, where waves brake. So, when the shelf edge of the platform is changing, reservoir body's orientation and their lateral extension change also. In this field, injectors are located as illustrated in Figure 40.

In the E-W oriented shelf edge scenario, more wells are located in good reservoir quality facies area. Those facies having high permeability, water injection is thus more efficient. If the reservoir body is oriented E-W, the injected water invaded quickly the reservoir body. If the reservoir bodies are N-S oriented, reservoir body is not flushed efficiently. The higher recovery is obtained for E-W shelf edge orientation.

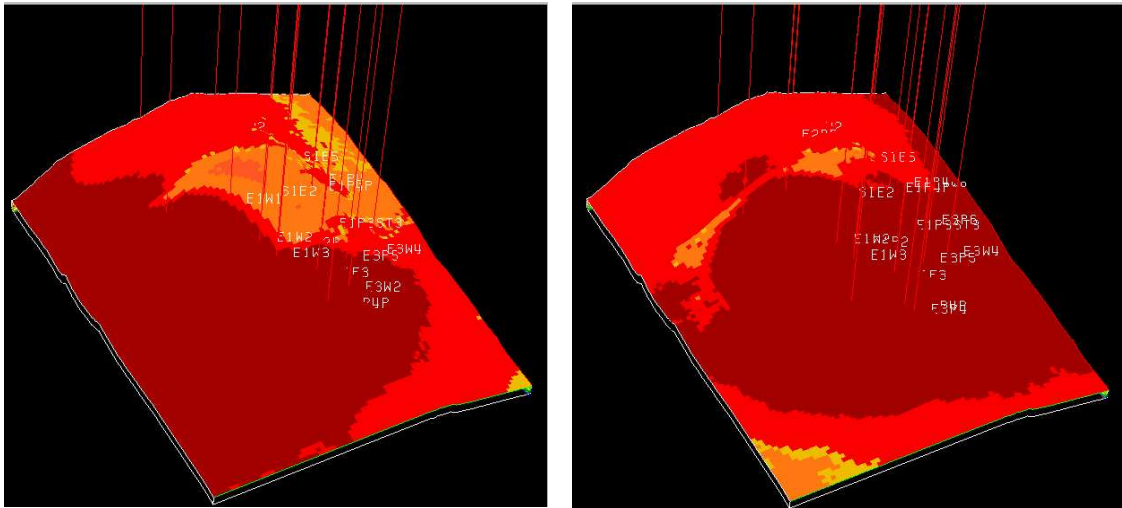


Figure 40: Injector locations compared to reservoir elongation

Rem: well names on the figure are deliberately unreadable because of confidentiality.

When shelf edge orientation is varying from N-S to E-W, water injection is more efficient. However, as seen in the previous paragraph, recovery is lower. So, it highlights that water injection is thus not the only mechanism to produce the reservoir, but solution gas drive is also very influential for the recovery. Because the water injection is not totally efficient, it is hard to determine which production mechanism is more influential (water injection or solution gas drive).

Bathymetry Ranges

From level -1 to level +1, bathymetry ranges are getting larger. It means that the poor reservoir quality facies are more represented. If extended, these facies act as permeability barrier, decreasing the water injection efficiency.

Facies Variogram Range

As explained previously, larger facies variogram range allows smoother change of facies. It induces smoother permeability changes, so a higher water injection efficiency.

Erosion

The limited extension of the top reservoir erosion favors the presence of very good reservoir quality facies. So, high permeability are present at the top of the reservoir. It induces a good transmissibility so a better water injection efficiency. However, it is reminded that most of these porous and permeable layers are filled by gas in the case study. That's why, even if the water injection is more efficient, the oil recovery factor is still lower.

Interaction Between Thickness, Gulf and Shelf Edge

The interaction between thickness and gulf is obvious: if, instead of a gulf, a hump is present around well 14, the layer thickness will be modified. Thus, it interacts with the variogram which simulate the thickness layer. The interaction between these two parameters and the shelf edge orientation is harder to justify: the positive relief created by the hump influences the platform geometry. Thus, it could act on the shelf edge orientation, in order to respect hard data located on wells.

6.2 Discussion on the Different Methods of Quantification

A comparative table is presented in Table 24 to Table 28. It summarizes the quantified effect percentage of each factor, calculated with the two different methods, Mean slope method and ANOVA table.

Table 24: Comparison mean slope and ANOVA methods for OOIP

OOIP	D (MMSTB)	% effect
Erosion	385.16	58.80
Bathymetry	-73.39	-11.2
Shelf-bathy	59.39	9.07
Gulf-Bathy	-57.14	-8.72
Thick-Bathy	-56.06	-8.56
Shelf edge	-11.85	-1.81
Facies	-7.19	-1.09
Gulf Hump	3.622	0.55
Thickness	-1.02	-0.15

Table 25: Comparison mean slope and ANOVA methods for recovery

REC	D (%)	% effect
Bathy-Facies	-0.017	-21.78
Thick-Bathy	-0.0164	-21.06
Gulf-shelf-Bathy	0.016	20.51
Bathymetry	-0.0114	-14.62
Erosion	-0.0063	-8.03
Thickness	0.0049	6.28
Shelf edge	-0.0031	-4.03
Facies	0.0024	3.06
Gulf Hump	-0.0001	-0.17

Table 26: Comparison mean slope and ANOVA methods for Np

Np	D (MMSTB)	% effect
erosion	79.95	65.59
Thick-Bathy	-15.27	-12.52
Bathymetry	-13.39	-10.98
Shelf edge	-6.19	-5.08
Thickness	5.06	4.16
Facies	1.09	0.89
Gulf hump	0.9	0.74

Table 27: Comparison mean slope and ANOVA methods for Wp/Np

Wp/Np	D (STB/STB)	% effect
Erosion	-0.13	-51.38
Bathymetry	0.047	18.8
Thick-Bathy	-0.029	-11.56
Thickness	-0.021	-8.36
Shelf edge	-0.009	-3.74
Thickn-Gulf-Shelf	0.006	2.38
Gulf hump	0.004	1.66
Facies	-0.002	-0.84

Table 28: Comparison mean slope and ANOVA methods for Gp/Np

Gp/Np	D (Mscf/STB)	% effect
Shelf-Bathy-Ero	-0.097	-22.56
Thick-Gulf-Bathy	-0.095	-22.09
Shelf-Bathy-Facies	0.0941	21.88
Bathymetry	-0.07	-16.09
erosion	0.047	10.92
Thickness	0.017	3.81
Shelf edge	0.0057	1.33
Gulf hump	0.0019	0.44
facies	-0.001	-0.31

Obviously, the deviation between the two methods goes from 0.05 to 40% of difference. The Mean slope method, as mentioned previously, doesn't take into account interaction effects. For this reason, interactions between coefficients are not taken into account. In this case of data set, within variables are strongly dependant (bathymetry, facies and shelf edge geometry are linked), errors reaching 40% can occur. It introduces first errors of percentage, but also errors in the hierarchy of most influent factors. So, the interpretation is erroneous.

The ANOVA table method, longer to compute, is however definitely more efficient, and allows to quantify the impact of each parameters, and also their interactions. For example, for the Gp/Np analysis, interactions control everything rather than one individual factor.

This analysis proves that to quantify geological parameters impacts, we **MUST** consider the interaction between factors, because it drastically influences your results, and, if not considered, can introduce such big bias that interpretation is wrong. It is so important that in some cases, these interactions are the main drivers of your response variable evolution. The importance of these interactions is directly related to the geological nature of the parameters. As shown before, changing the shelf edge orientation of the platform influences the facies distribution, so the bathymetry ranges. Another interaction is present between gulf and thickness factors, because both are related to thickness layers.

Finally, whatever the model studied, when impacts of geological parameters have to be quantified, interactions will have a strong influence. It is inherent to the interactions which already exist between geological parameters. Geological parameters are rarely independent from each other.

CHAPTER VII

CONCLUSIONS

A simplified black oil reservoir model was created within which updated 3D geological models were incorporated. The reservoir was modeled to produce for 30 years with the aid of water injection. Reservoir pressure was difficult to maintain in the model and as a result, the model produced below the bubble point pressure early in the history of the 30 year run. A consequence of poor pressure maintenance resulted in the formation of a secondary gas cap early in the production history, forcing a high gas-oil ratio to result. However, even if water injection had limited impact, reservoir heterogeneities were sufficiently highlighted.

Utilizing multiple versions of geological settings to define the geology in the simplified reservoir model allowed us to quantify the impact of each geological factor on reservoir performance, or “response variables”. The response variables were found to be bimodally distributed and greatly influenced by the erosion factor in the geological settings. Only the reservoir recovery results were found to be normally distributed.

The Analysis of Variance (ANOVA) method used to quantify uncertainty revealed that the erosion factor had the greatest impact on simulation outcomes as OOIP, N_p , and W_p/N_p . This resulted simply because the erosion factor dictated the vertical height, and consequently the total volume, of the reservoir. The results of this study indicate that additional work, especially 3D-seismic survey and dipmeter analysis, should be conducted to refine the three dimensional geometry of the reservoir.

In addition, the bathymetry factor in the geological setting exerted excessive influence on how the reservoir simulator processed information about facies distributions and facies characteristics such as porosity and permeability. Further work should include refinements to the bathymetry factor. For example, reservoir recovery was found to be greatly influenced by comparatively small variations in the bathymetry factor and resultant changes in the facies variograms. Because the bathymetry factor has such a great impact on simulation outcomes, it also generates the greatest uncertainty among the geological parameters, and it is very difficult to assign “correct” values to this factor. A possible solution to this problem that resulted from this study is to reduce the statistical “weight” of the bathymetry factor in the GOCAD® algorithm.

One of the most significant contributions of this study is that it illuminates the importance of interaction between the geological factors. The geological factor interactions were found to be so influential that the methods which don't take interaction between factor into account will give erroneous quantification of uncertainty. This fact was particularly well illustrated by the response of the G_p/N_p and the recovery factor response variables.

The great impact of the bathymetry factor on facies distributions, and subsequently on reservoir performance was probably emphasized because the model was not run with dynamic layering. That is, flow barriers and low transmissibility layers were not incorporated in the reservoir model. The only barriers to fluid flow were assumed to be low-Permeability facies such as shale.

Finally, predictive regression models were calculated for each response variable. Even with this simplified reservoir model and its accompanying development scheme, this study revealed how reservoir performance will proceed when the values of geological parameters values are known. The results of this work should provide a strong basis on which to develop future, more refined reservoir simulation models.

REFERENCES CITED

Alsharhan, A.S. and A. E. M. Nairn, 1993, Carbonate platform models of Arabian Cretaceous Reservoirs: Cretaceous Carbonate Platforms, *in* J.A.S. Toni Simo, Robert W., Masse J. P. (eds), Carbonate Platform Models of Arabian Cretaceous Reservoirs: Cretaceous Carbonate Platforms, AAPG Memoir 56, pp. 173-184.

Corre, B., P. Thore, V. de Feraudy and G. Vincent, 2000, Integrated uncertainty assessment for project evaluation and risk analysis: SPE European Petroleum Conference, Paris, France, Oct. 2000, SPE 65205.

Elf Aquitaine Company, 1975, Flow study on CaHu field samples: Elf Aquitaine Company report, Boussens, France.

Elf Company, 1997, CaHu-field, final reservoir development study: TEP/DEG/RES/MO, CSTJF, Pau, France.

Guy L., N. Lenoir and C. Begert, 2000, CaHu field geological model update: TFE report, Total CSTJF, Pau, France.

Heckert A. and J. Filliben, 2002, NIST/SEMATECH e-Handbook of Statistical Methods, <http://www.itl.nist.gov/div898/handbook>.

Hines W.W., D.C. Montgomery, D.M. Goldsman and C.M. Borror, 2003, Probability and statistics in engineering, John Wiley and Sons Inc., Phoenix.

Laroche, P., 2000, CaHu field- Full field reservoir simulation model, version 3: TFE report, Total CSTJF, Pau, France.

Leparmentier, F., 1981, Champs et accumulation de la region de CaHu field- District X : S.N.E.A.P., DOZN n° 1981/226, FL/GT, Total CSTJF, Pau, France.

Lodola D., 2002a, A Cenomanian carbonate platform example: The Maria of Colombia. Sequential analysis and stochastic facies modeling: DEA Lithosphere Cinetics, TFE report, Total CSTJF, Pau, France.

Lodola D., 2002b, The Maria Formation, CaHu field : Accumulation computation and uncertainty analysis on Neptune's models: TFE report, Total CSTJF, Pau, France.

Massonnat, G., 1999, Breaking of a paradigm: Geology can provide 3D complex probability fields for stochastic facies modeling: 1999 SPE Annual Technical Conference and Exhibition, Houston, Texas, SPE 56652.

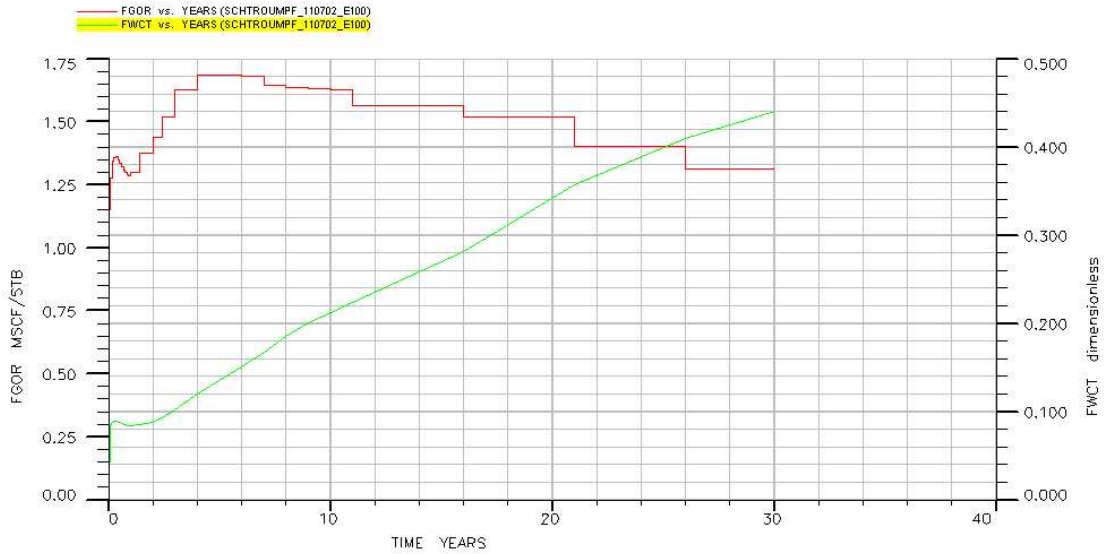
Total company, 1997, X-field, water core flood experiments at reservoir conditions-well-13: Total Scientific and Technical Center, Paris, France.

Voelker D.H., Z. Orton, and S.V. Adams, 2001, Cliff's quick review: statistics, John Wiley and Sons Inc, Boston.

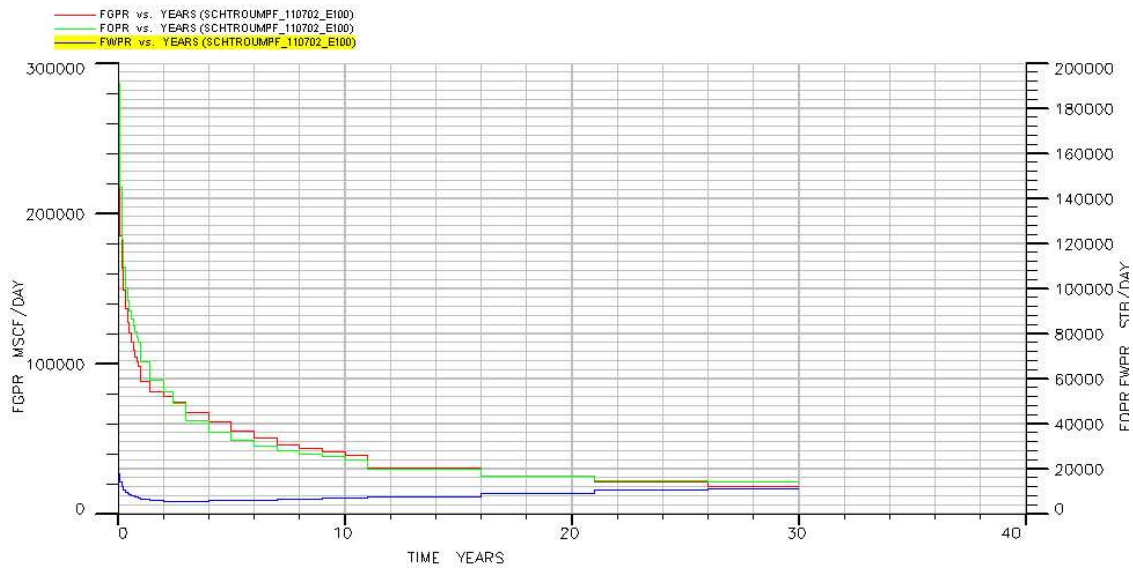
.

APPENDICES

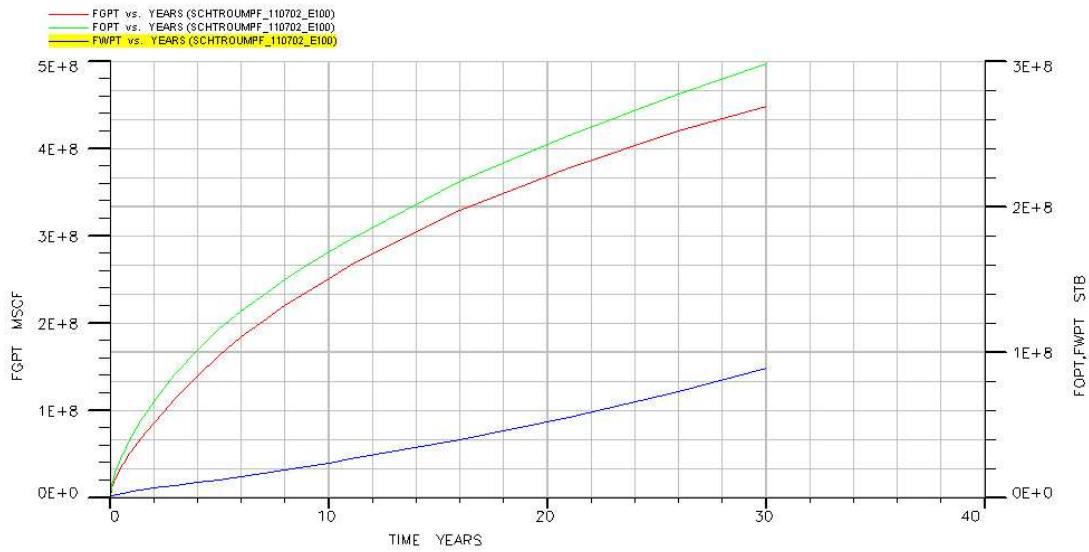
Appendix 1: Field production ratios, AFINQV model



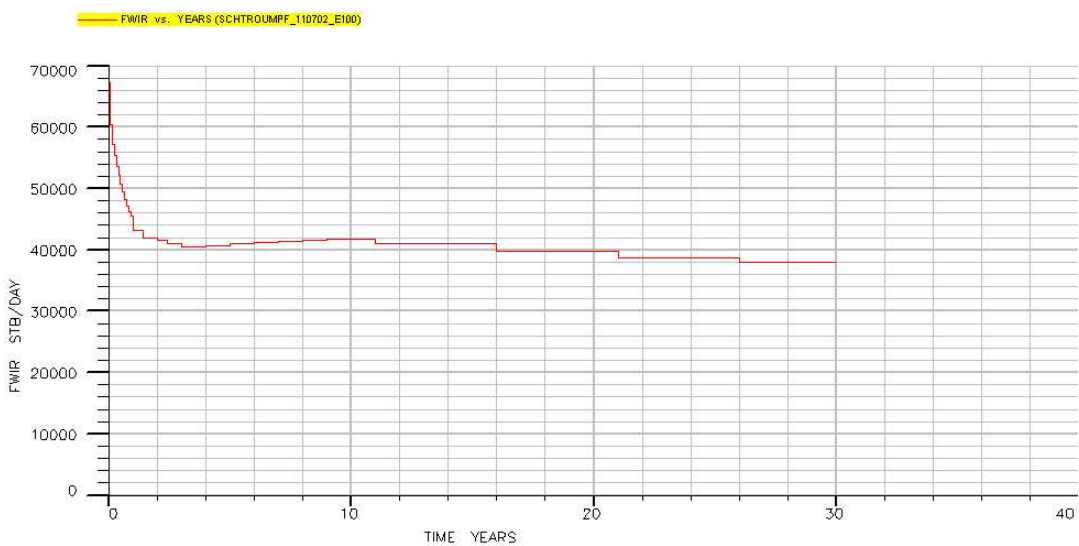
Appendix 2: Field production ratios, AFINQV model



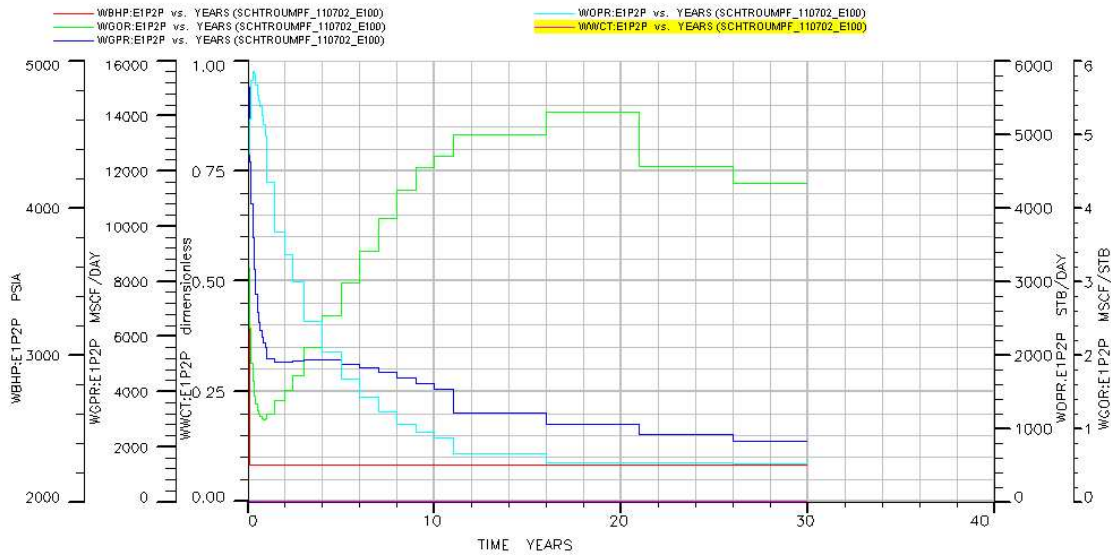
Appendix 3: Field fluid rates, AFINQV model



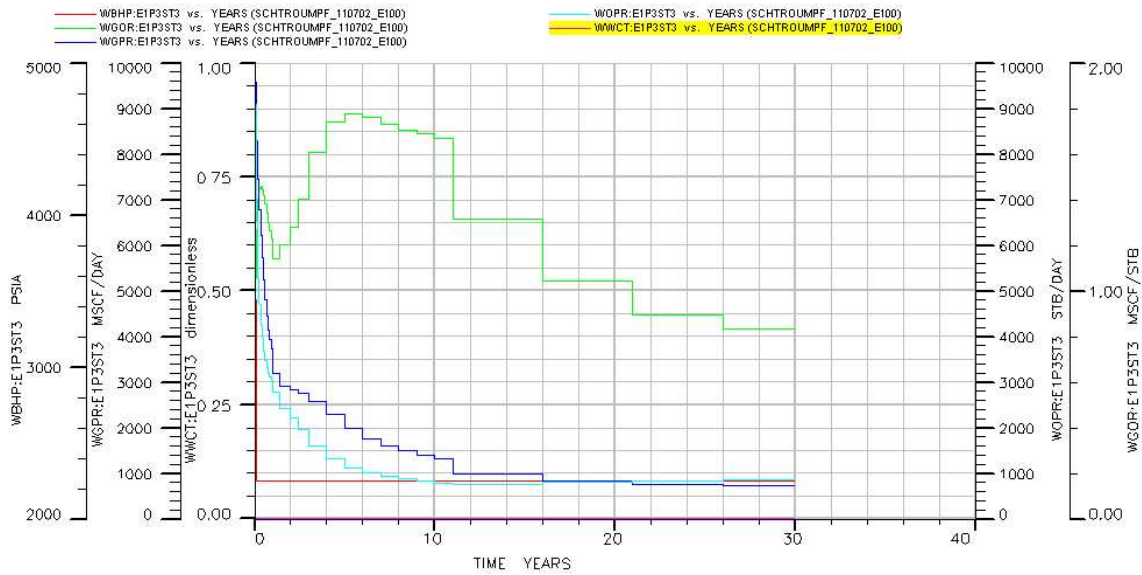
Appendix 4: Field water injection rate, AFINQV model



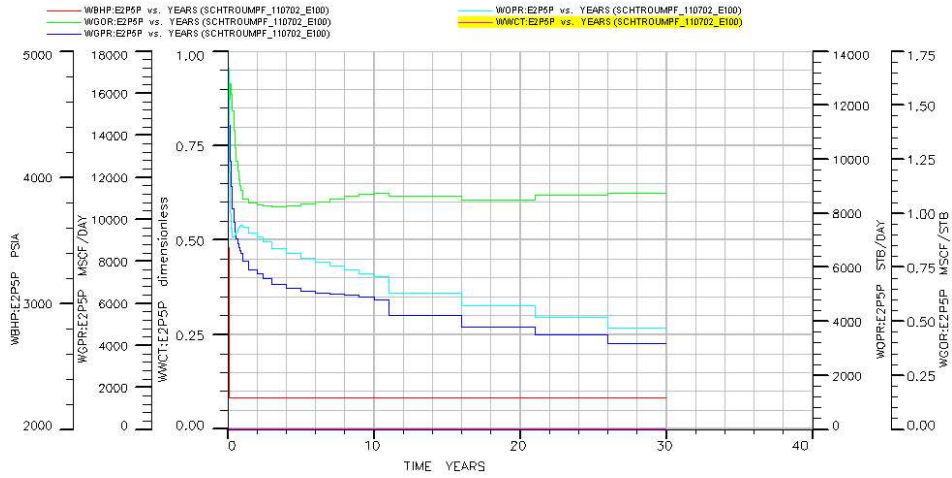
Appendix 5: WELL 1 well performance, AFINQV model



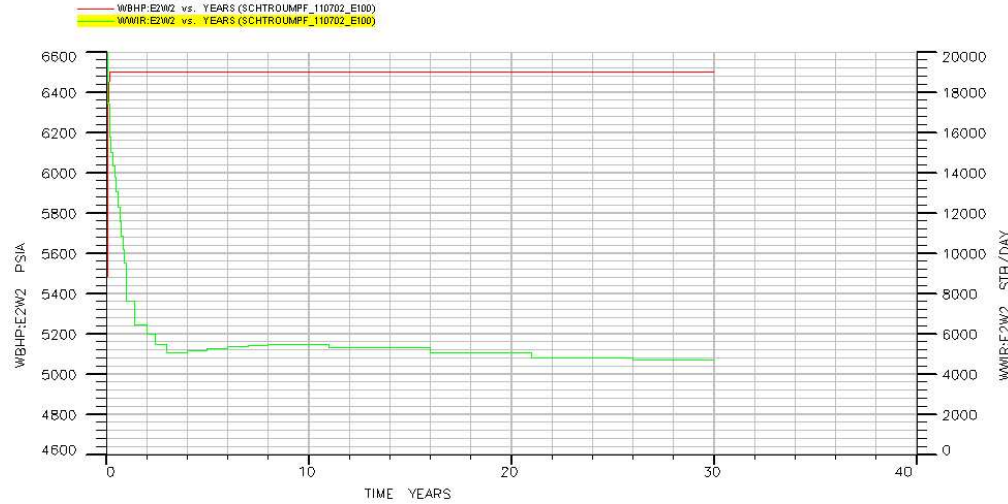
Appendix 6: WELL 2 well performances, AFINQV model



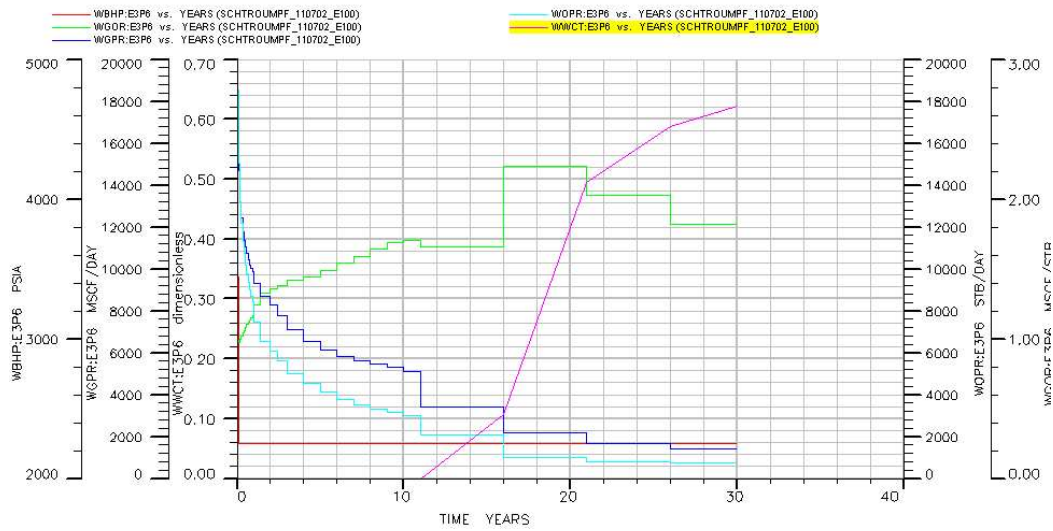
Appendix 7: WELL 6 well performances, AFINQV model



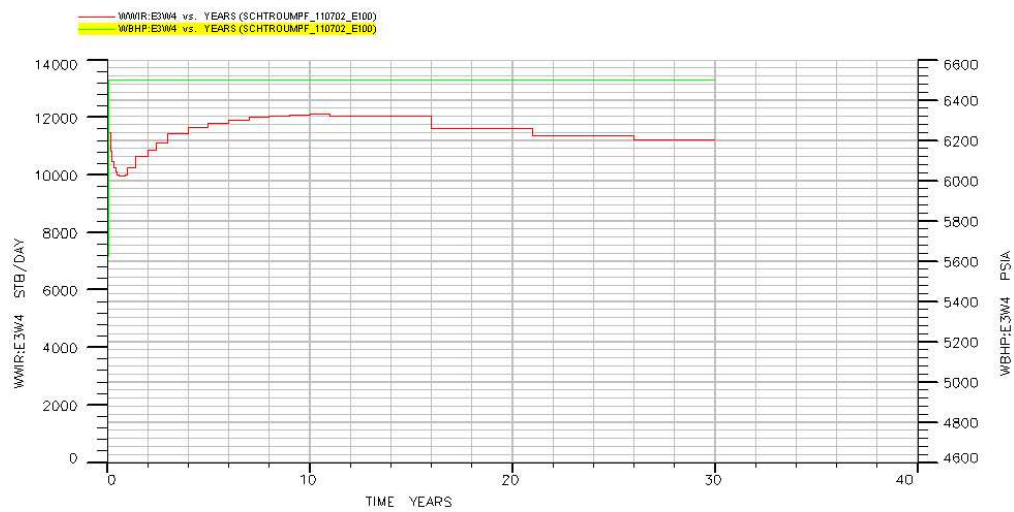
Appendix 8: WELL 16 well performances, AFINQV model



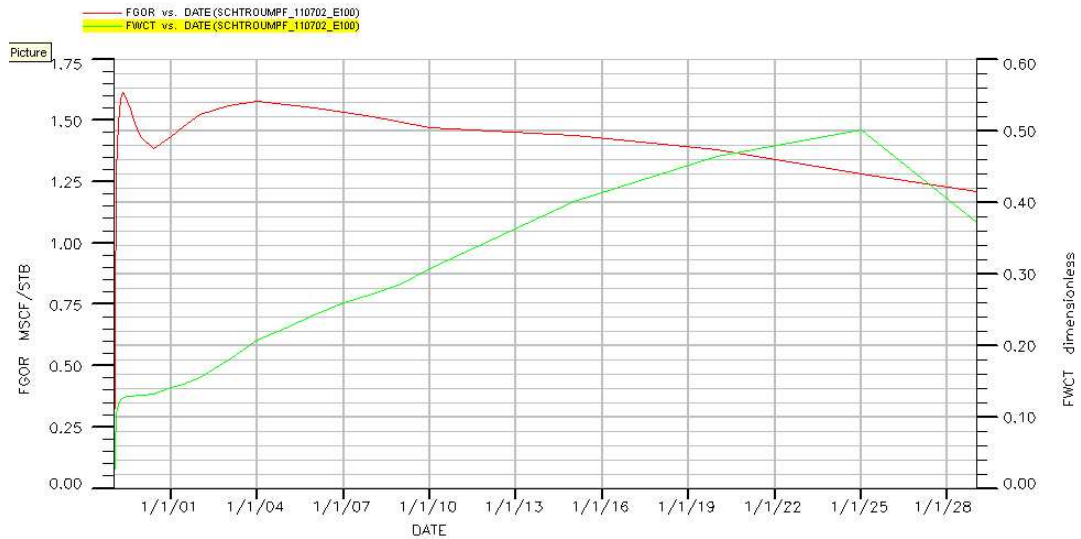
Appendix 9: WELL 9 well performances, AFINQV model



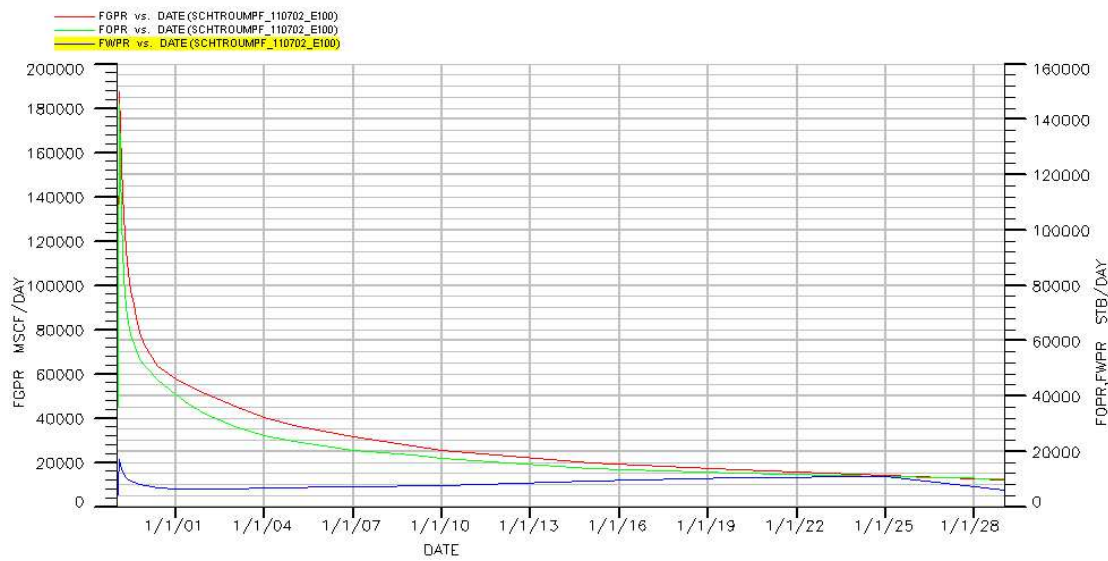
Appendix 10: WELL 18 well performances, AFINQV model



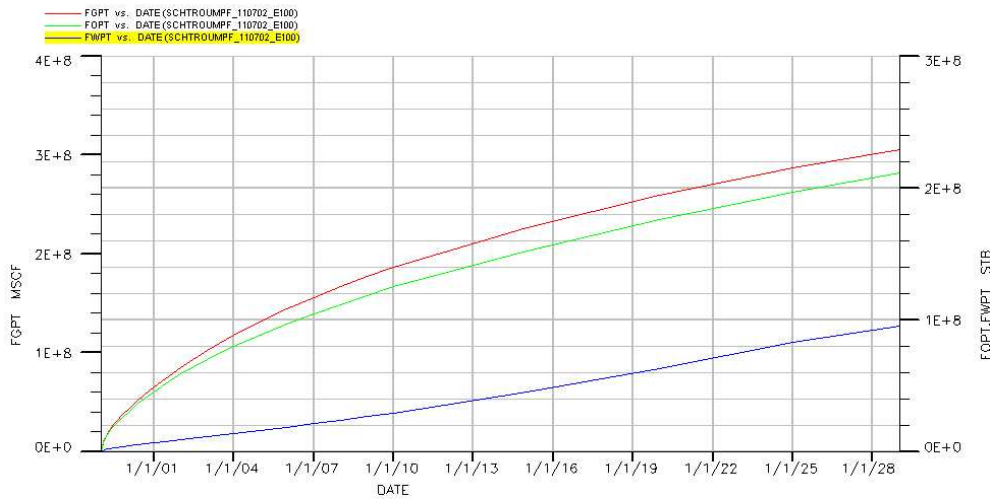
Appendix 11: Field production ratios, AEJMRU model



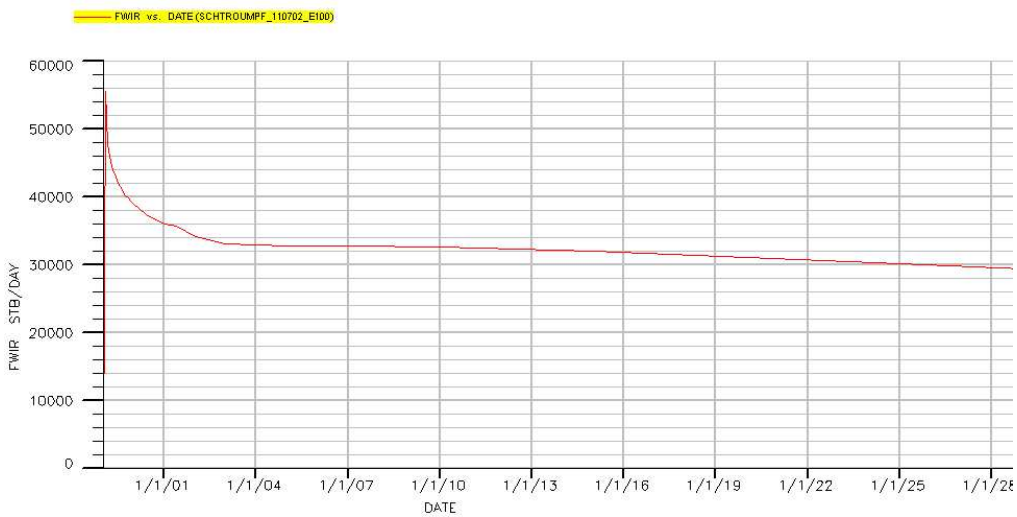
Appendix 12: Field fluid rates, AEJMRU model



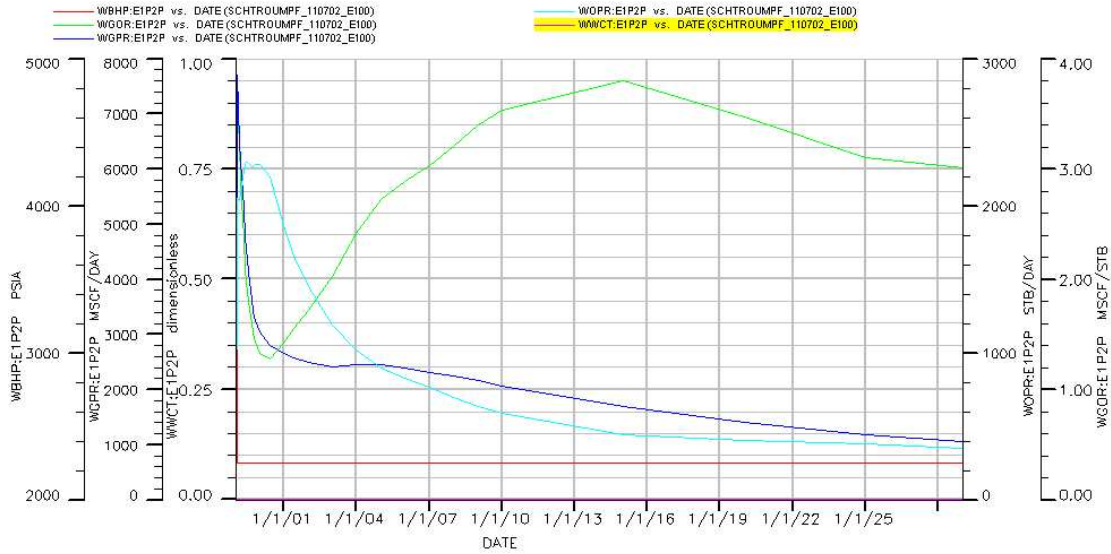
Appendix 13: Cumulative productions, AEJMRU model



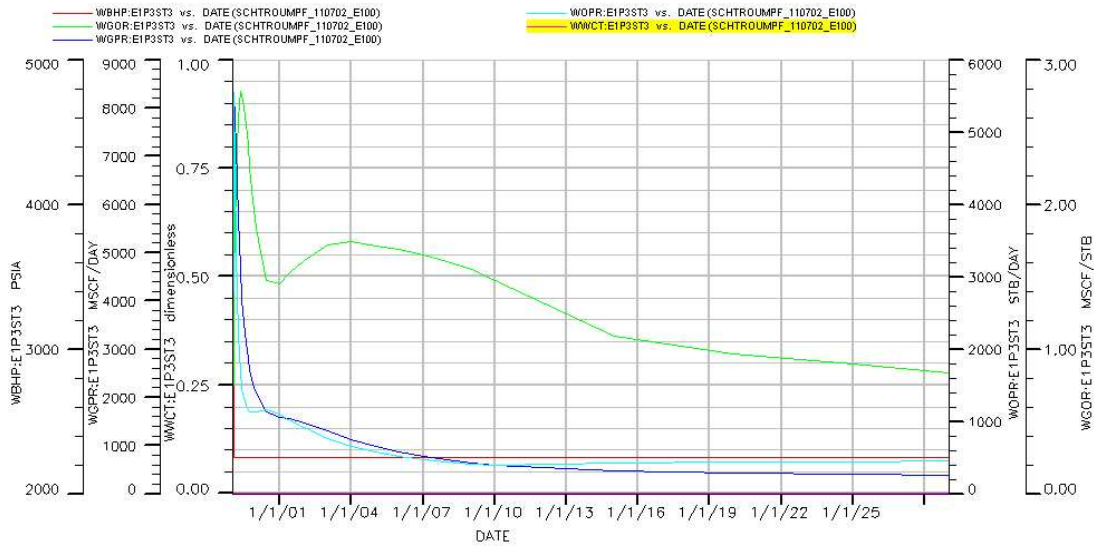
Appendix 14: Field water injection rate, AEJMRU model



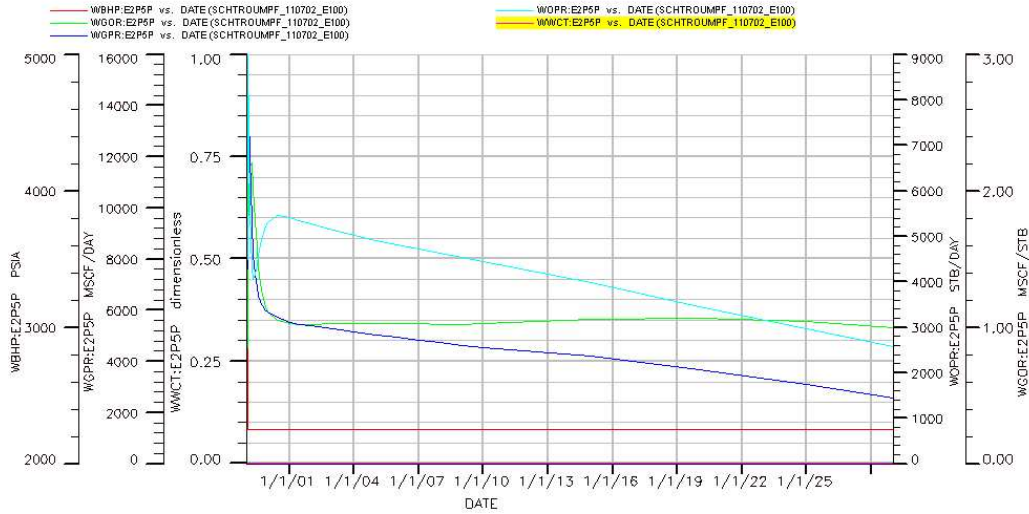
Appendix 15: WELL 1 well performances, AEJMRU model



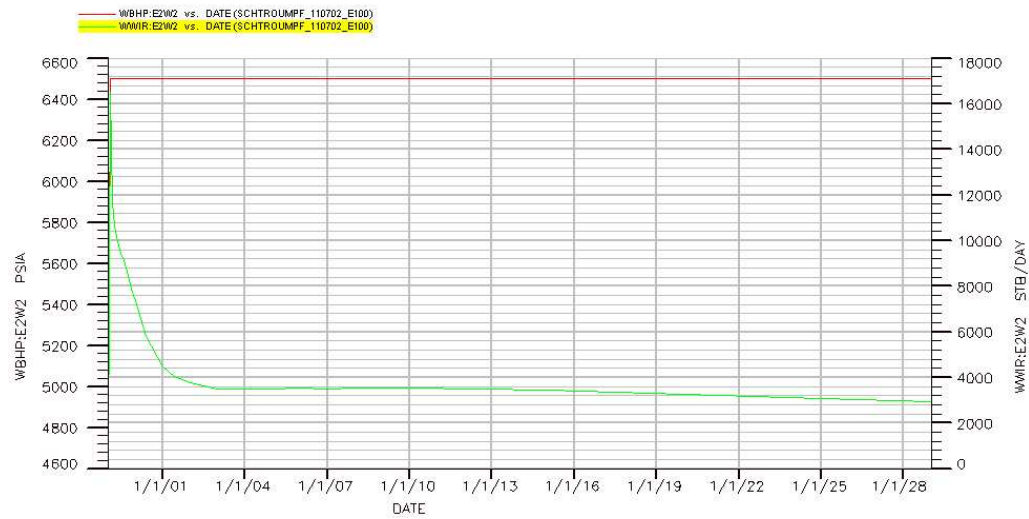
Appendix 16: WELL 2 well performances, AEJMRU model



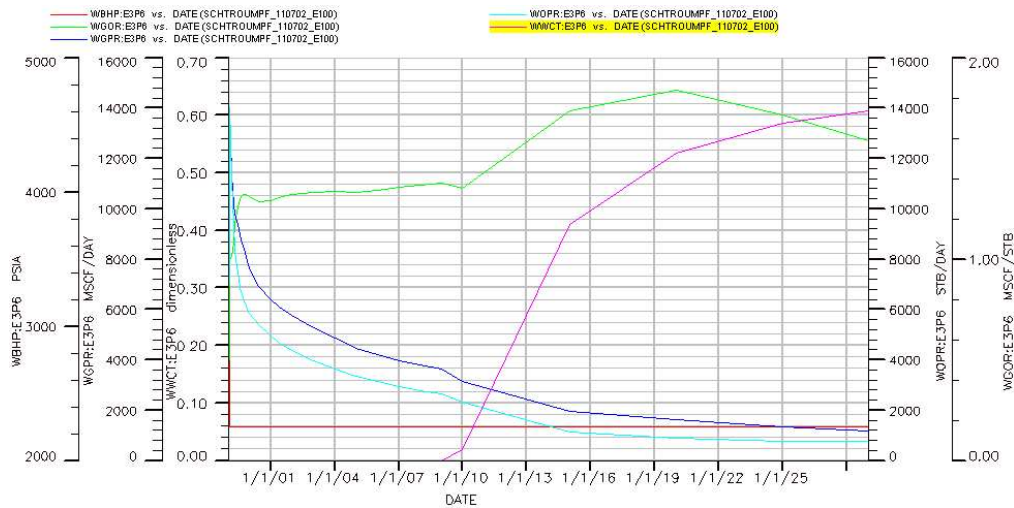
Appendix 17: WELL 6 well performances, AEJMRU model



Appendix 18: WELL 16 well injection performances, AEJMRU model



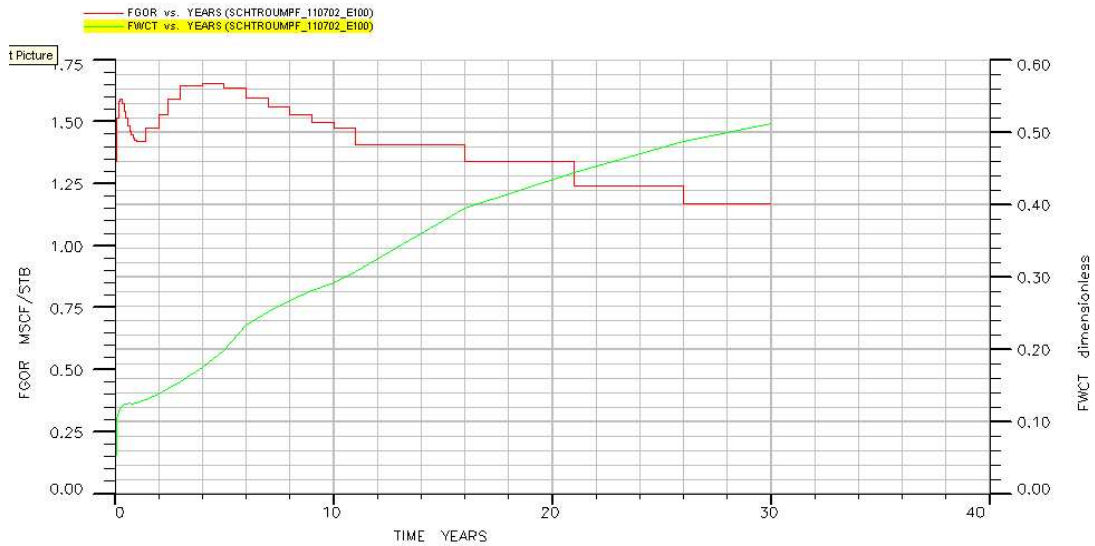
Appendix 19: WELL 9 well performances, AEJMRU model



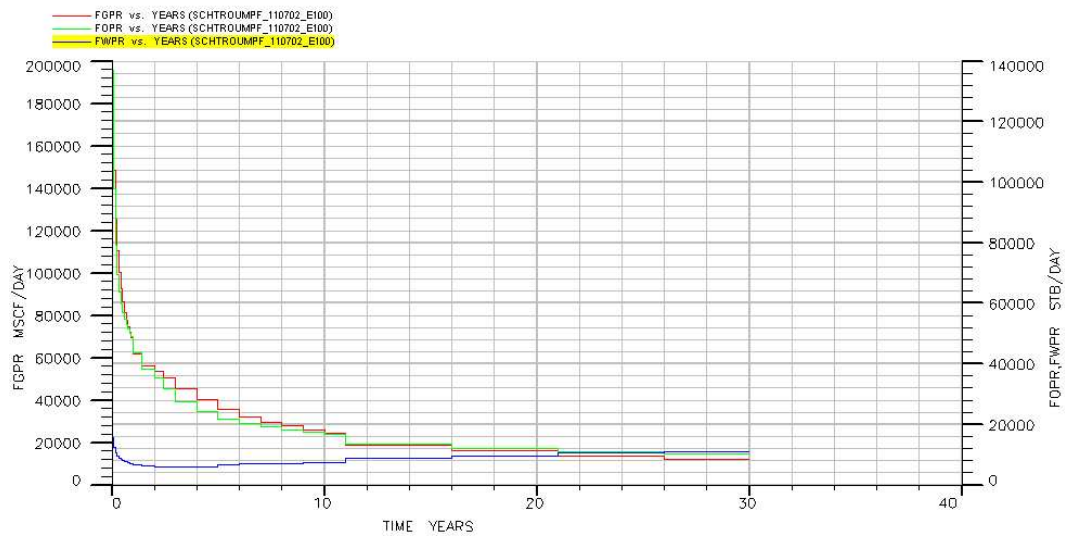
Appendix 20: WELL 18 well injection performances, AEJMRU Model



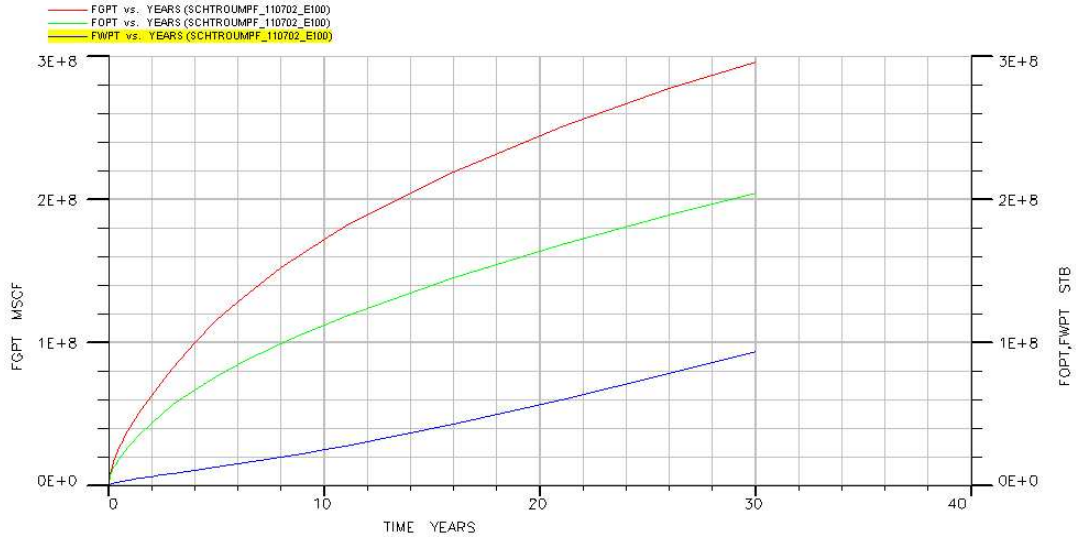
Appendix 21: Field production ratios, AFJNQU model



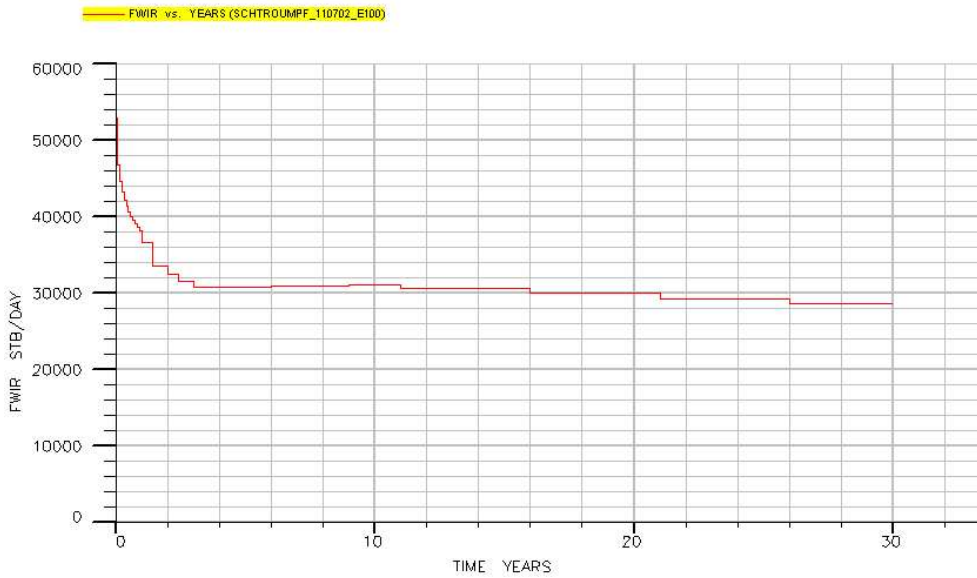
Appendix 22: Field production rates, AFJNQU model



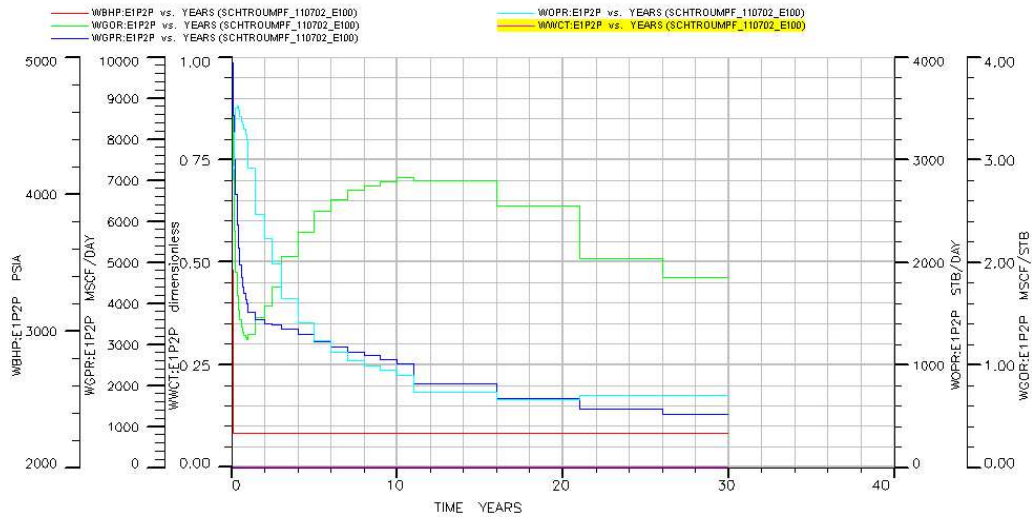
Appendix 23: Field cumulative fluid production, AFJNQU model



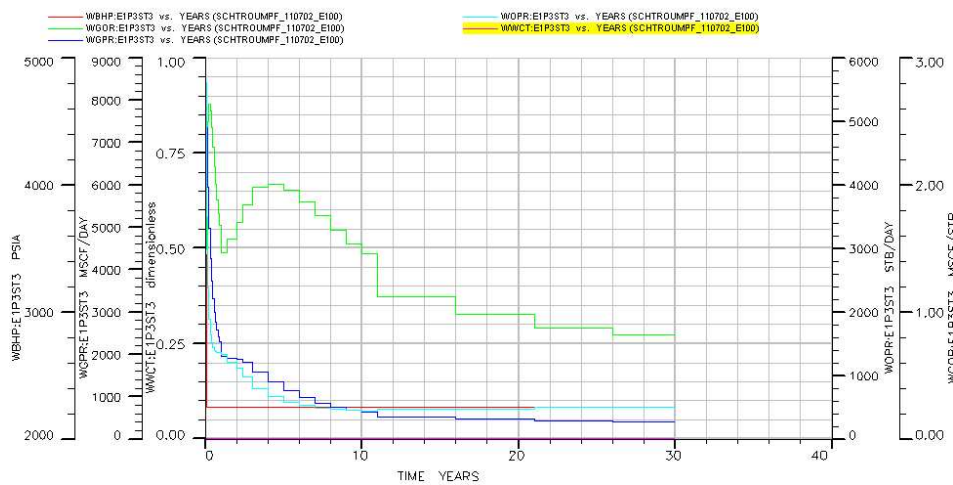
Appendix 24: Field water injection rate, AFJNQU model



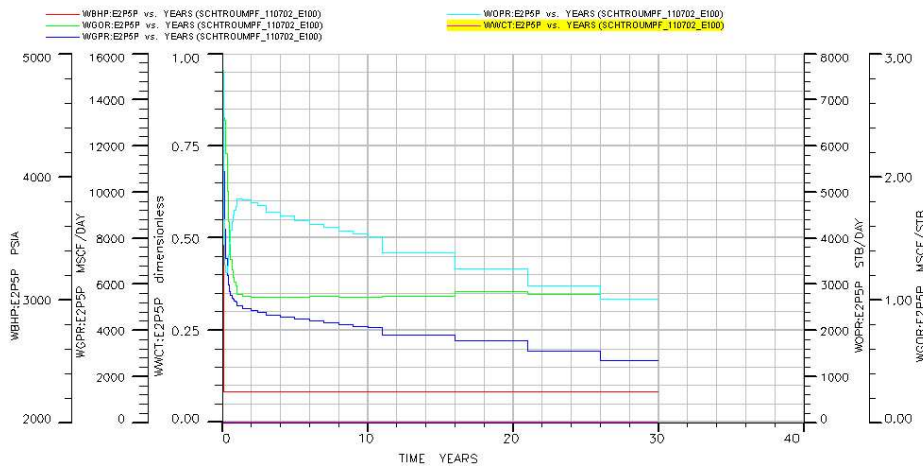
Appendix 25: WELL 1 well performances, AFJNQU model



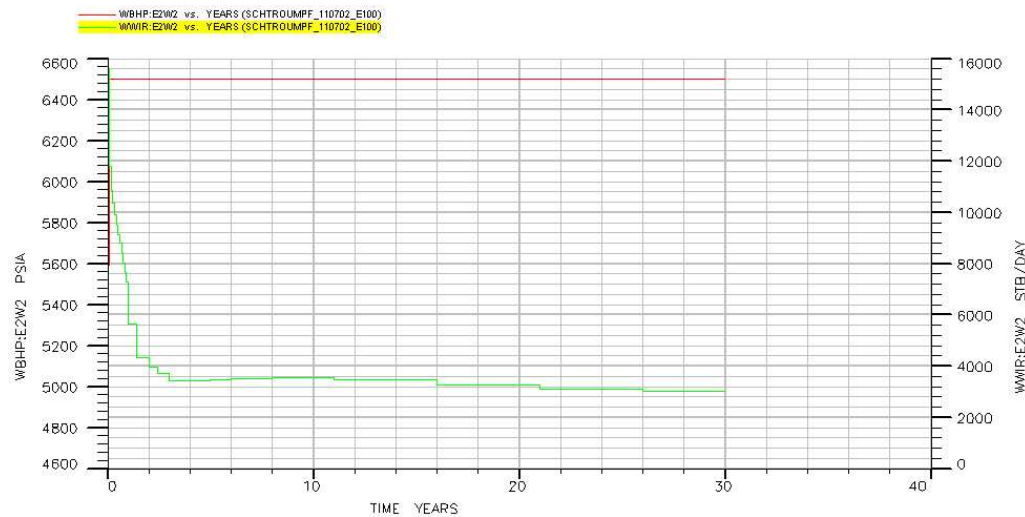
Appendix 26: WELL 2 well performances, AFJNQU model



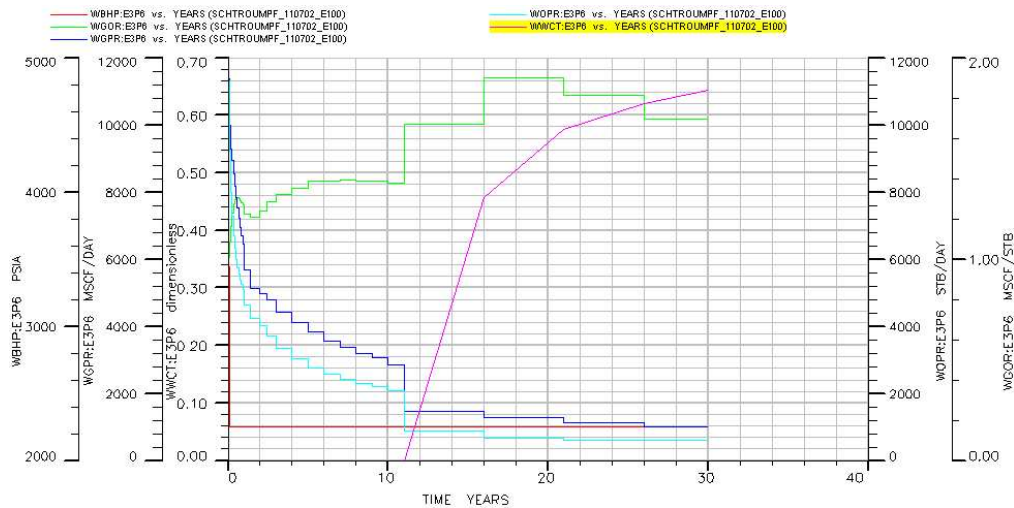
Appendix 27: WELL 6 well performances, AFJNQU model



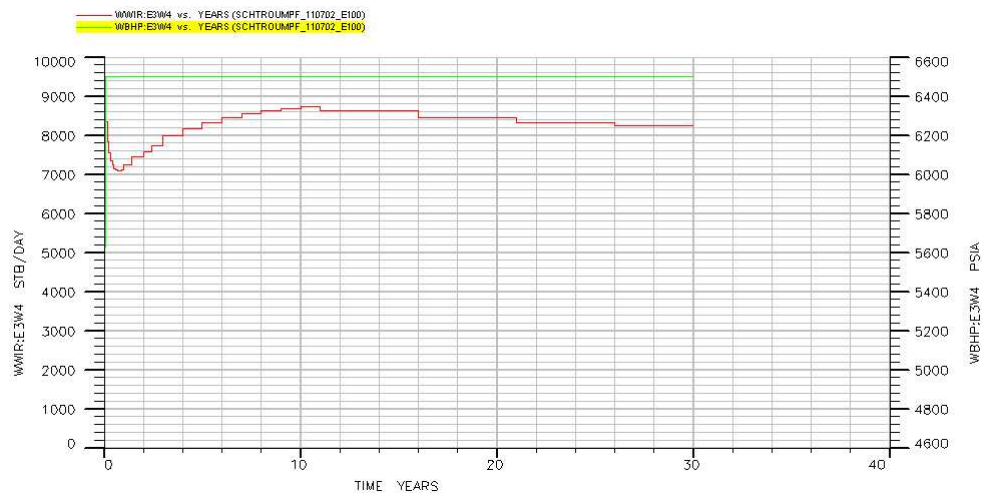
Appendix 28: WELL 16 well performances, AFJNQU model



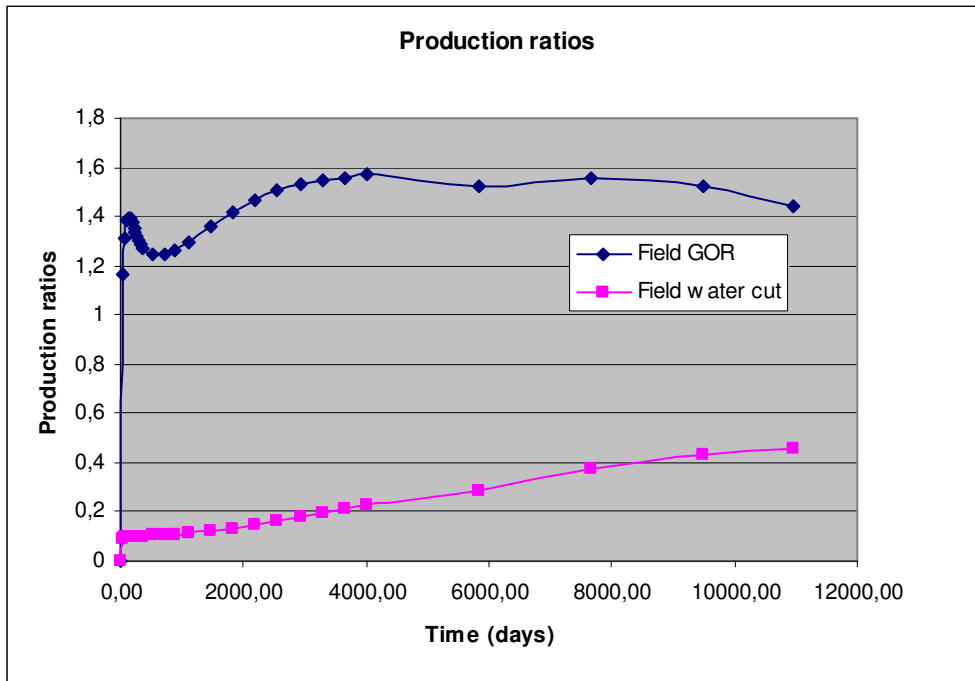
Appendix 29: WELL 9 well performances, AFJNQU model



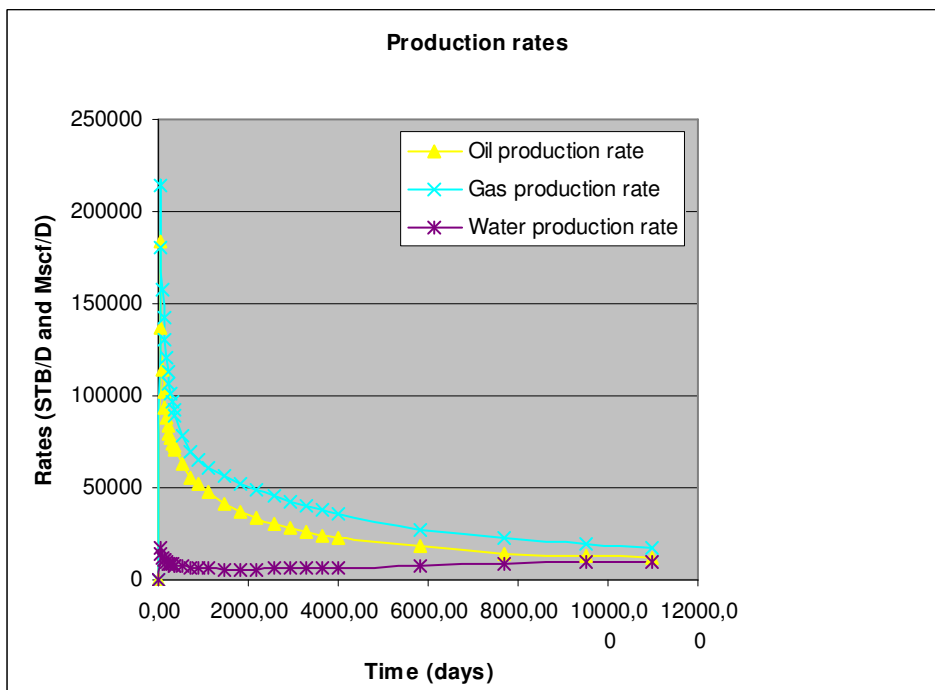
Appendix 30: WELL 18 well injection performances, AFJNQU model



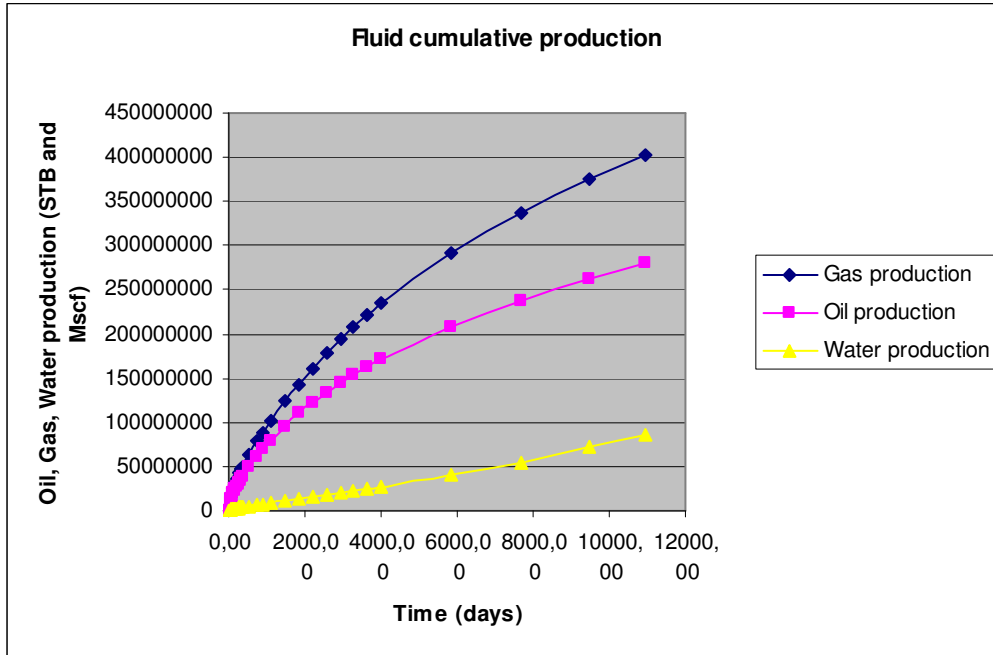
Appendix 31: Field production ratios, AEIMQV model



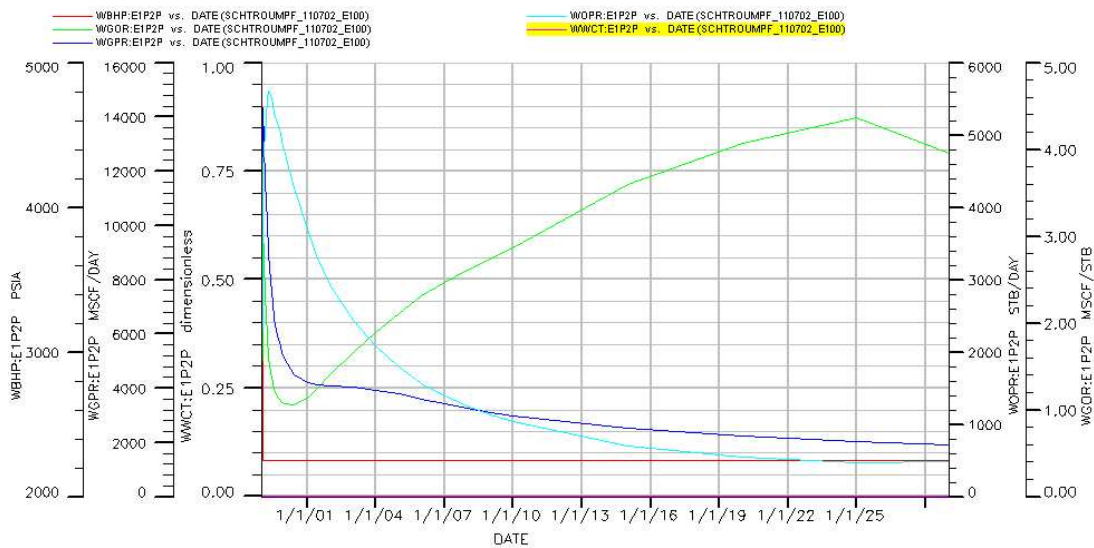
Appendix 32: Field production rates, AEIMQV model



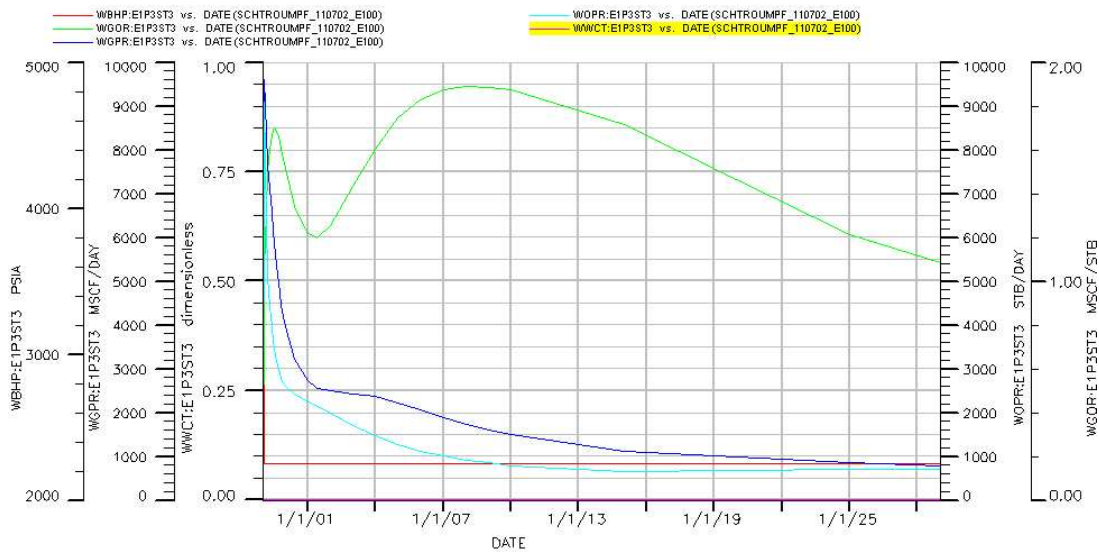
Appendix 33: Field cumulative fluid production, AEIMQV model



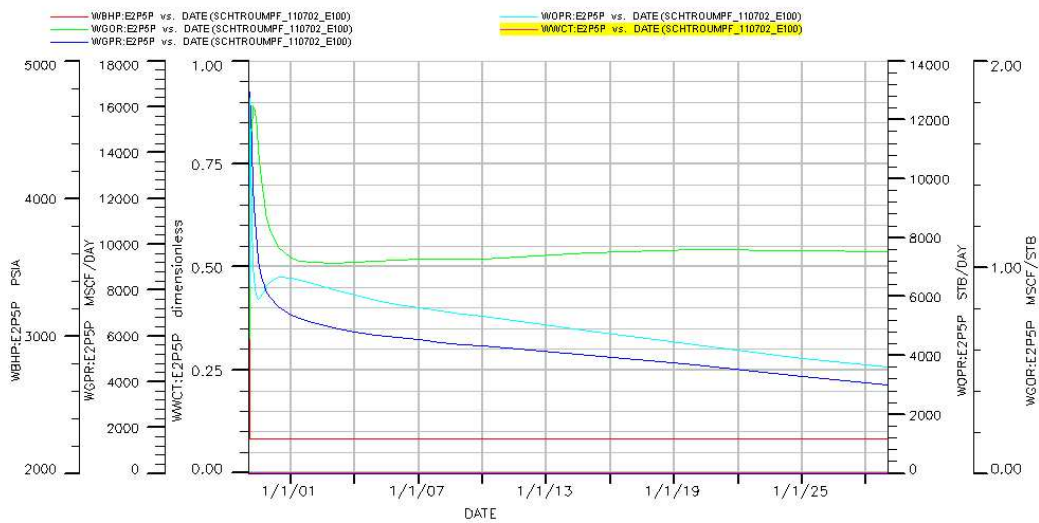
Appendix 34: WELL 1 well performances, AEIMQV model



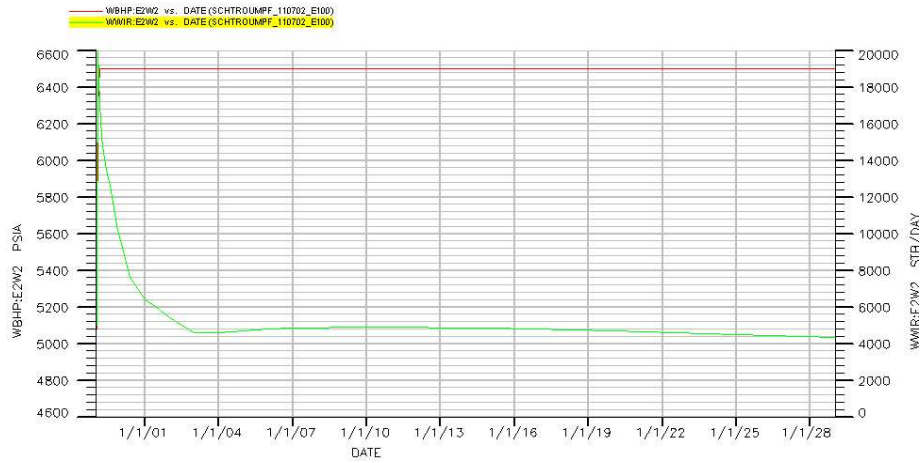
Appendix 35: WELL 2 well performances, AEIMQV model



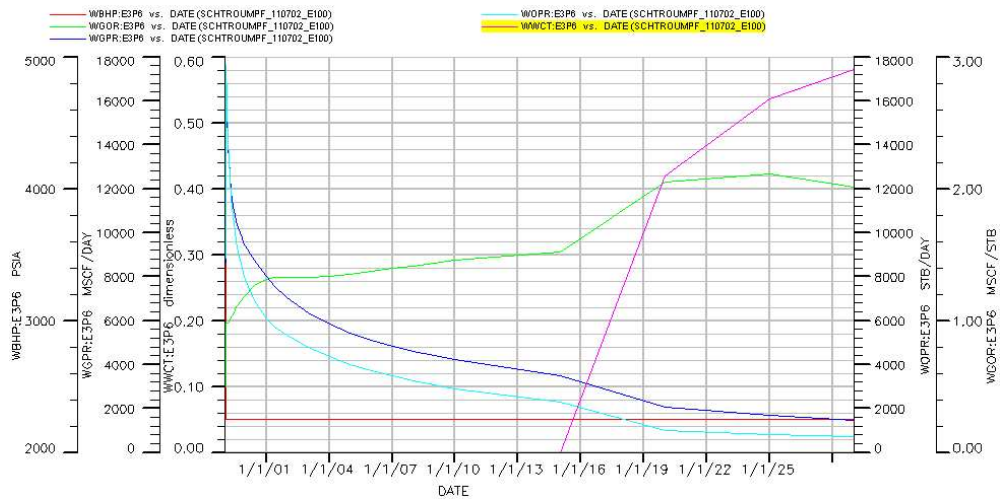
Appendix 36: WELL 6 well performances, AEIMQV model



Appendix 37: WELL 16 well injection performances, AEIMQV model



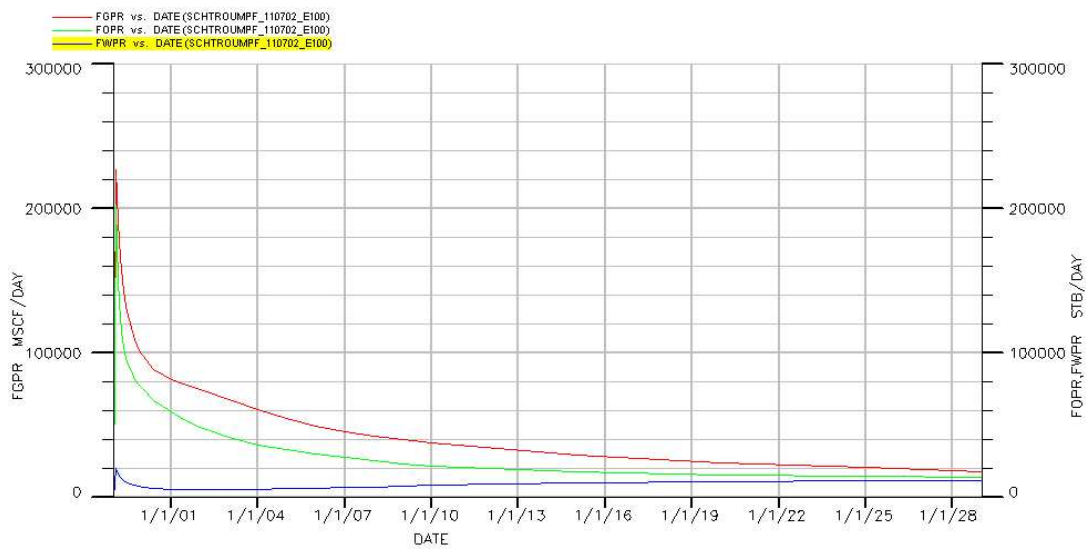
Appendix 38: WELL 9 well performances, AEIMQV model



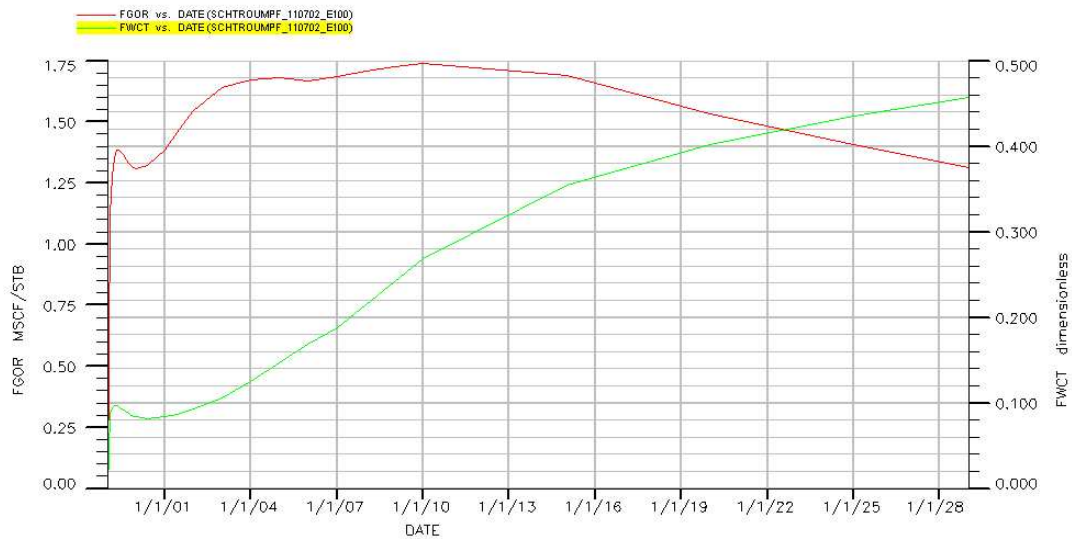
Appendix 39: WELL 18 well injection performances, AEIMQV model



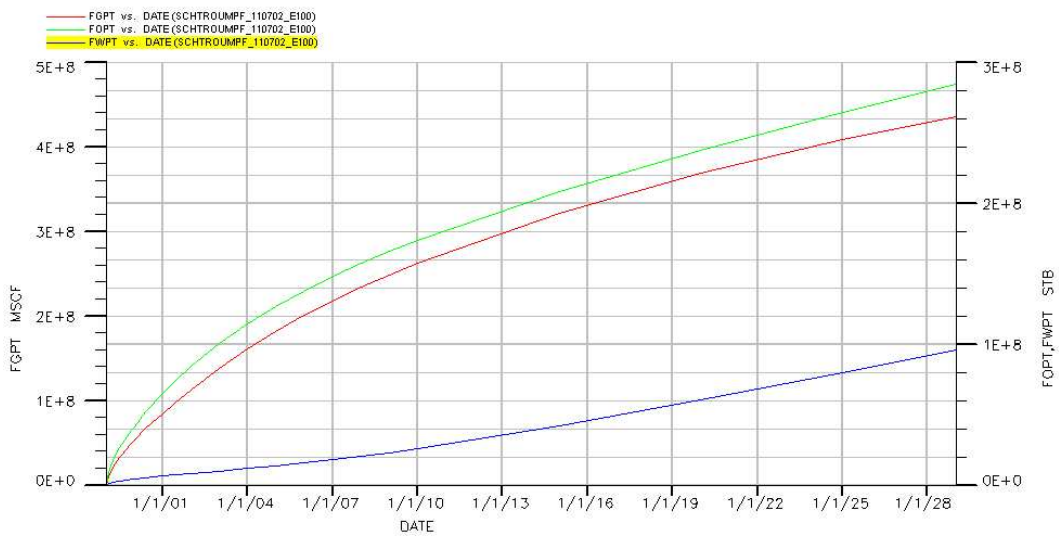
Appendix 40: Field production rates, BEJNQV model



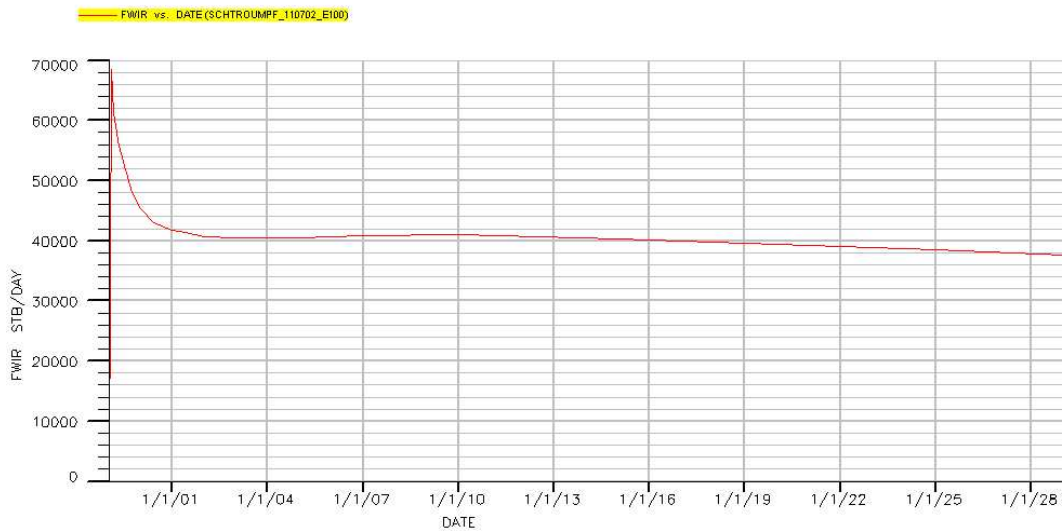
Appendix 41: Field production ratios, BEKNQV model



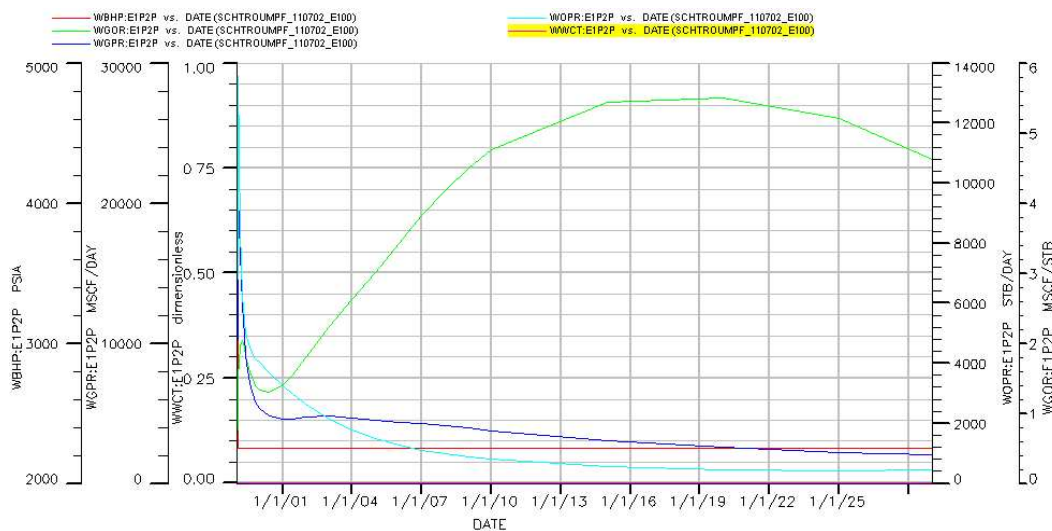
Appendix 42: Cumulative fluid productions, BEJNQV model



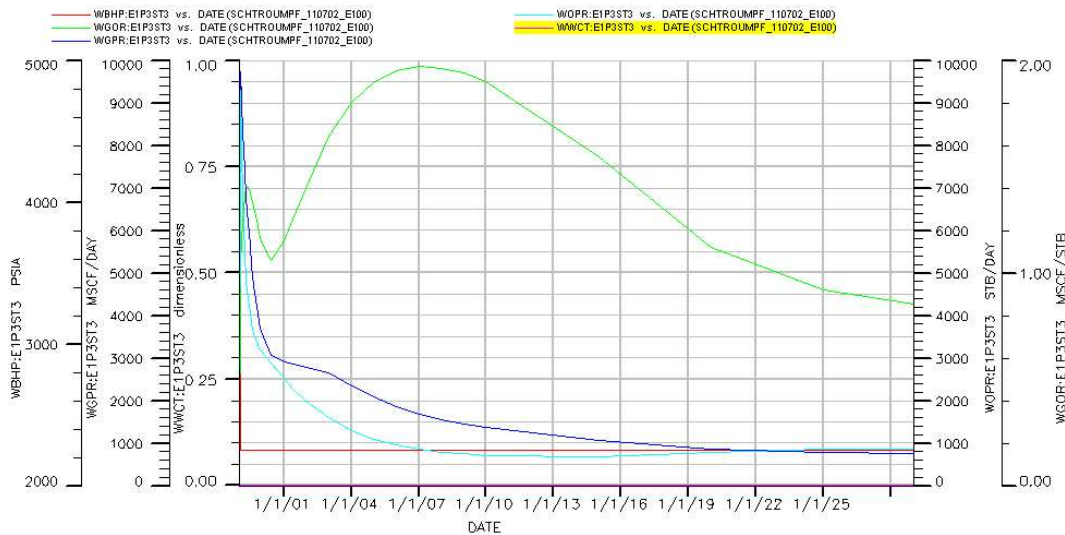
Appendix 43: Field water injection rate, BEJNQV model



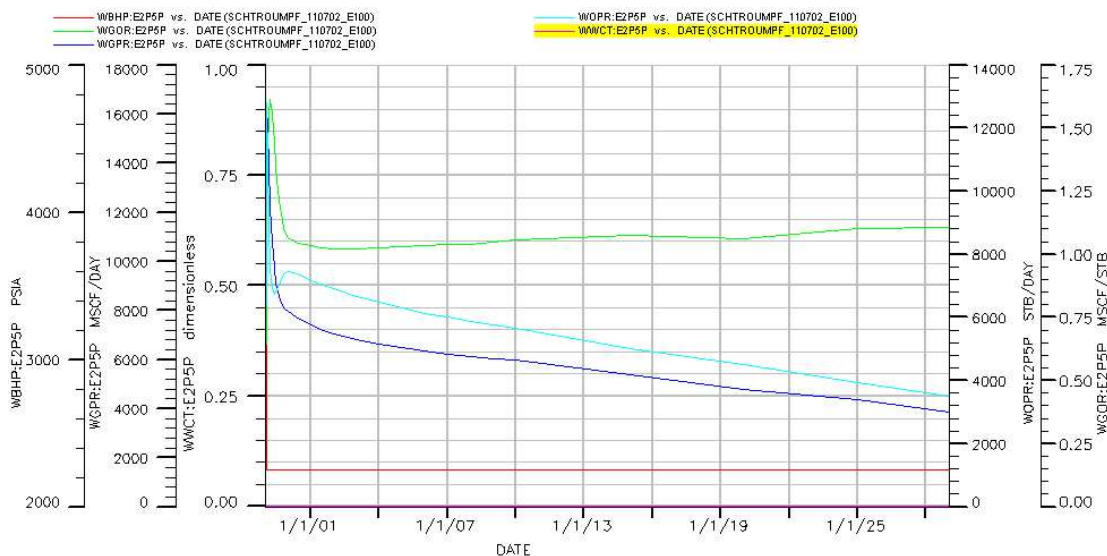
Appendix 44: WELL 1 well performances, BEJNQV model



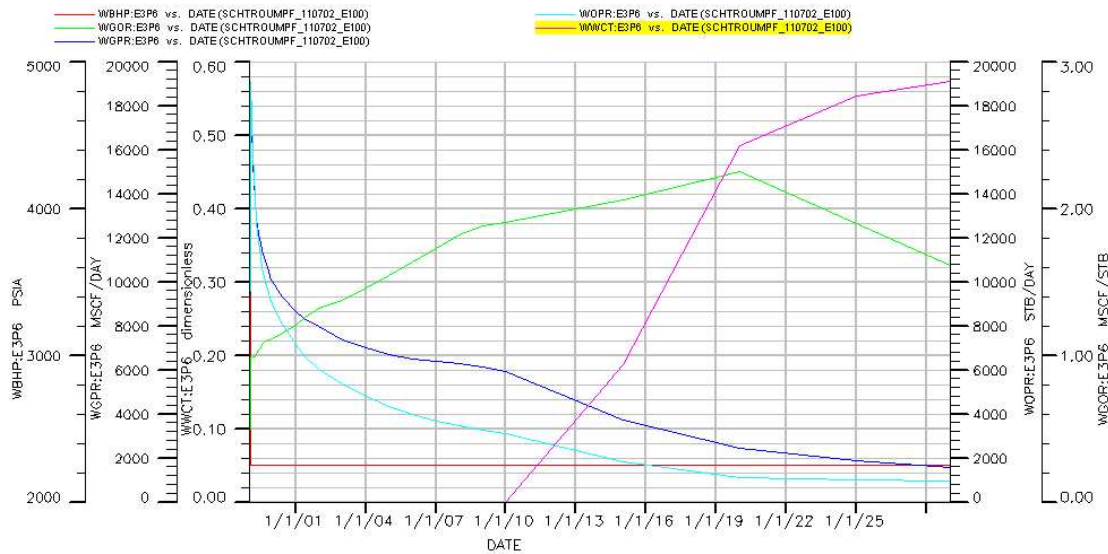
Appendix 45: WELL 2 well performances, BEJNQV model



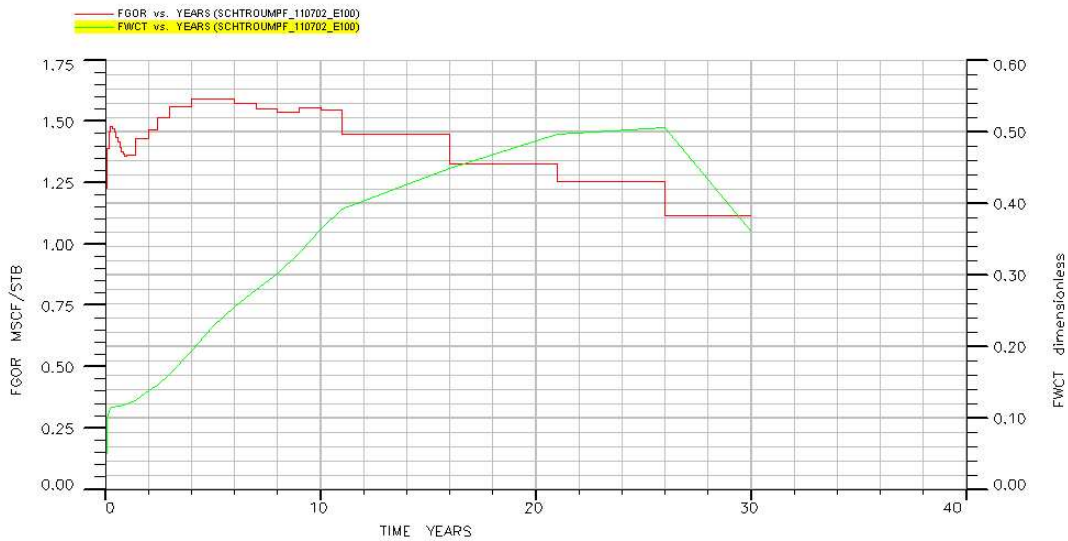
Appendix 46: WELL 6 well performances, BEJNQV model



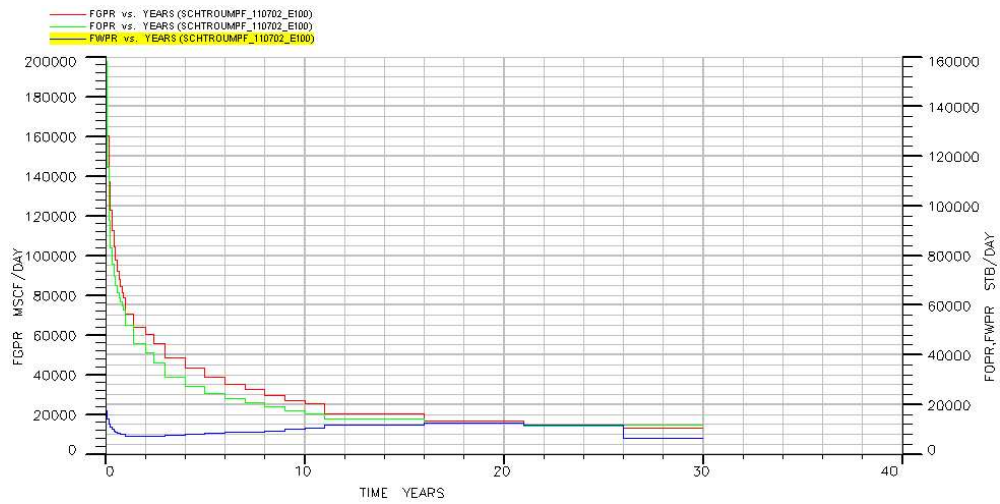
Appendix 47: WELL 9 well performances, BEJNV model



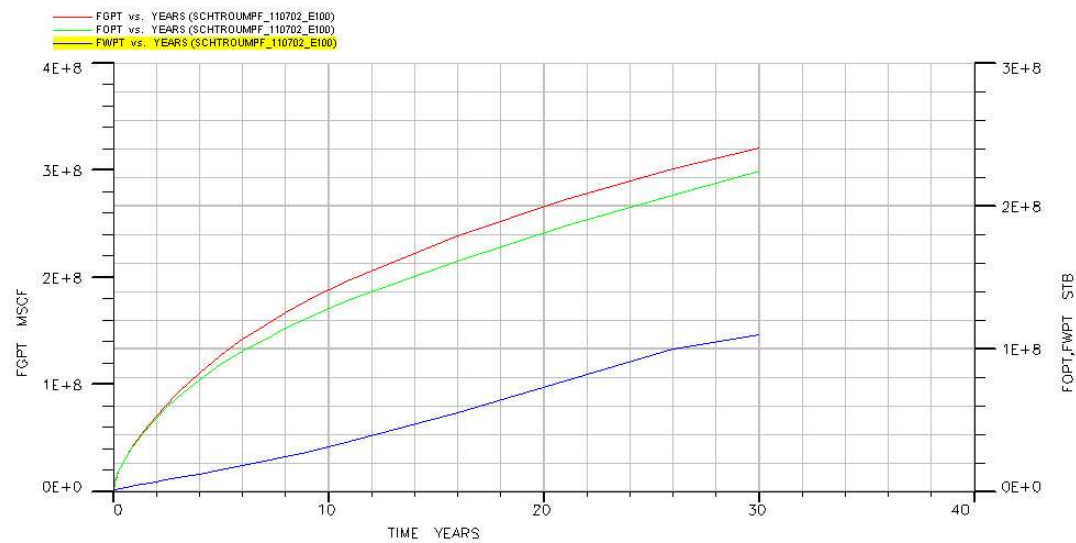
Appendix 48: Field production ratios, BEIMRU model



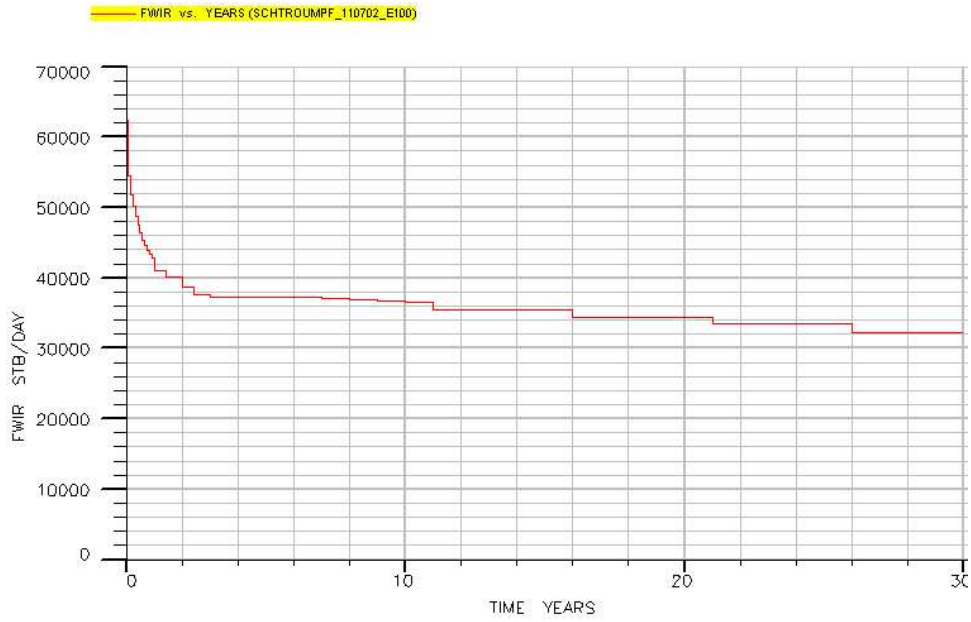
Appendix 49: Field production rates, BEIMRU model



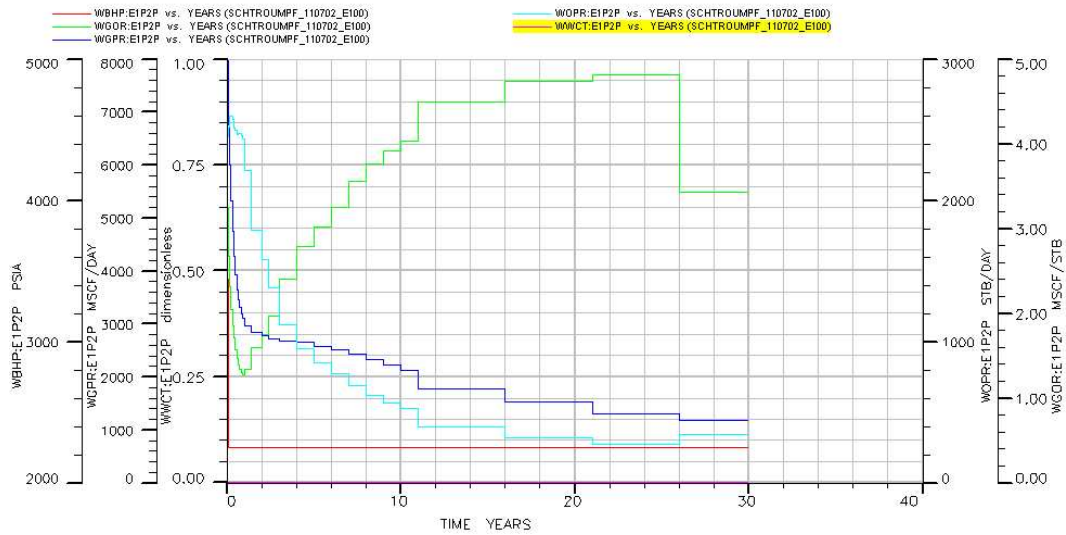
Appendix 50: Field cumulative fluid production, BEIMRU model



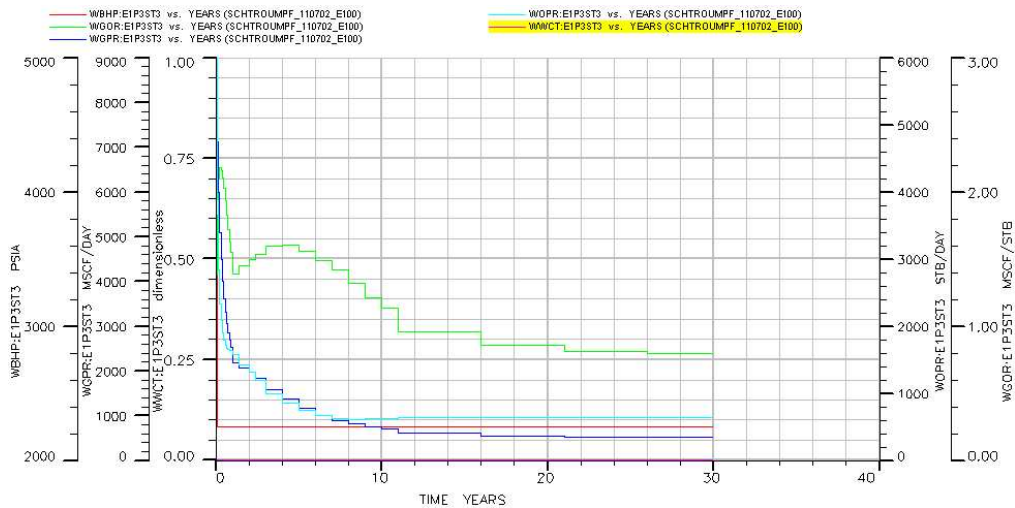
Appendix 51: Field water injection rate, BEIMRU model



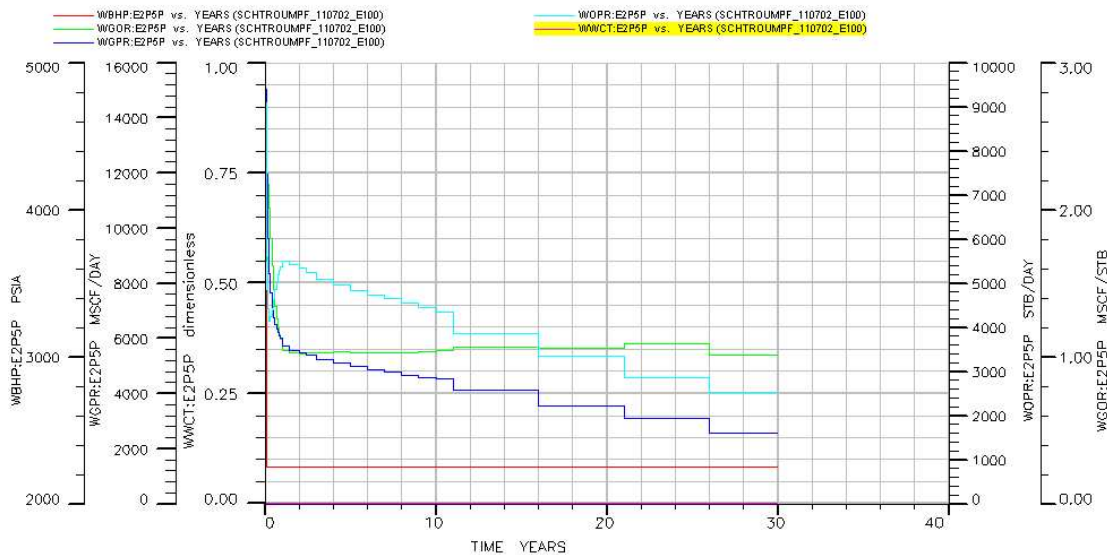
Appendix 52: WELL 1 well performances, BEIMRU model



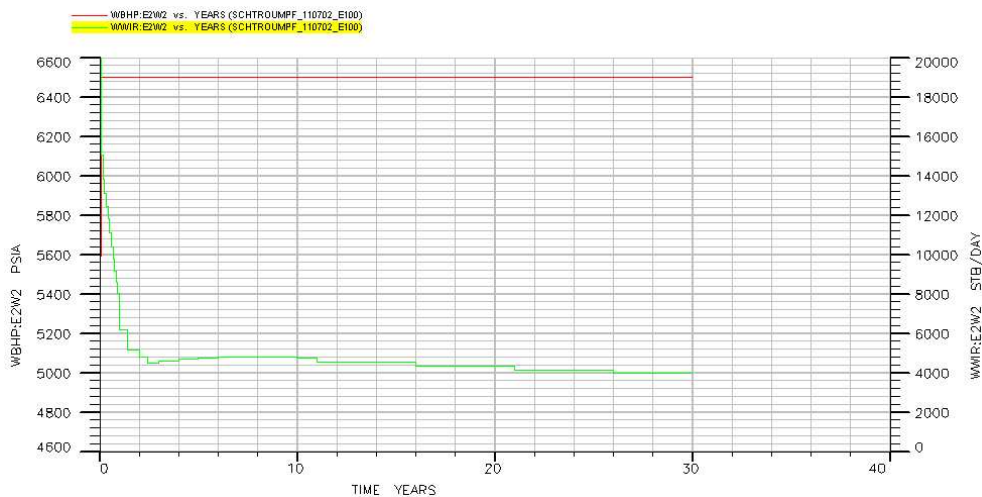
Appendix 53: WELL 2 well performances, BEIMRU model



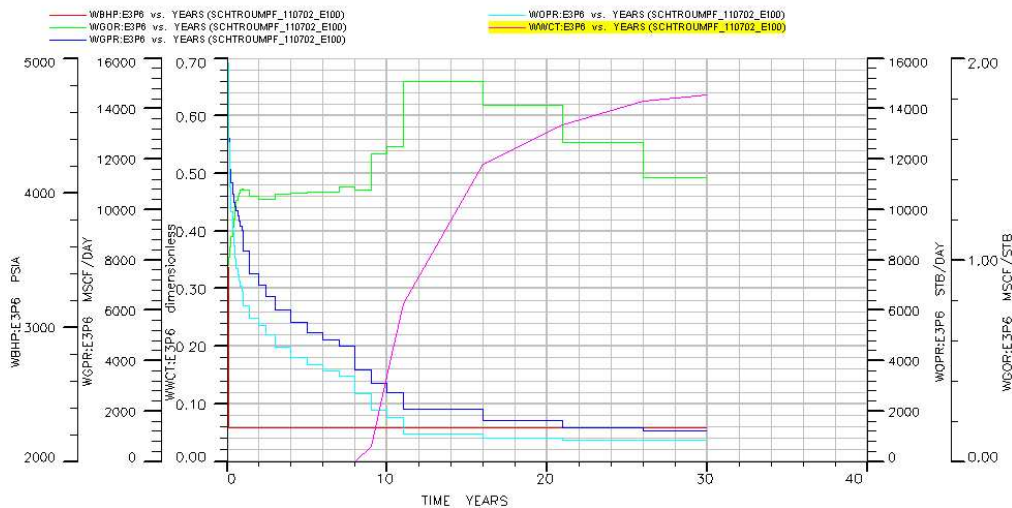
Appendix 54: WELL 6 well performances, BEIMRU model



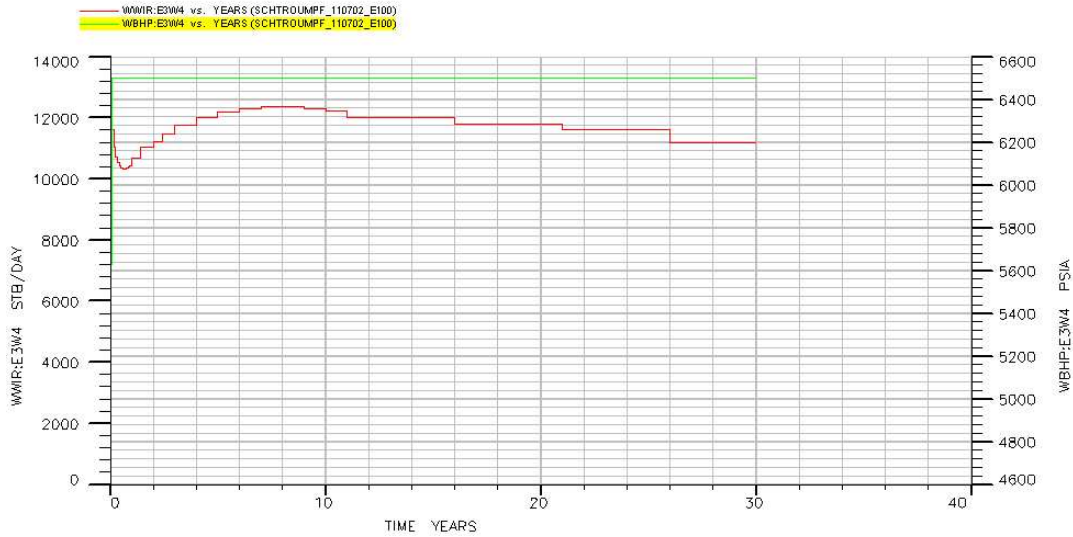
Appendix 55: WELL 16 well injection performances, BEIMRU model



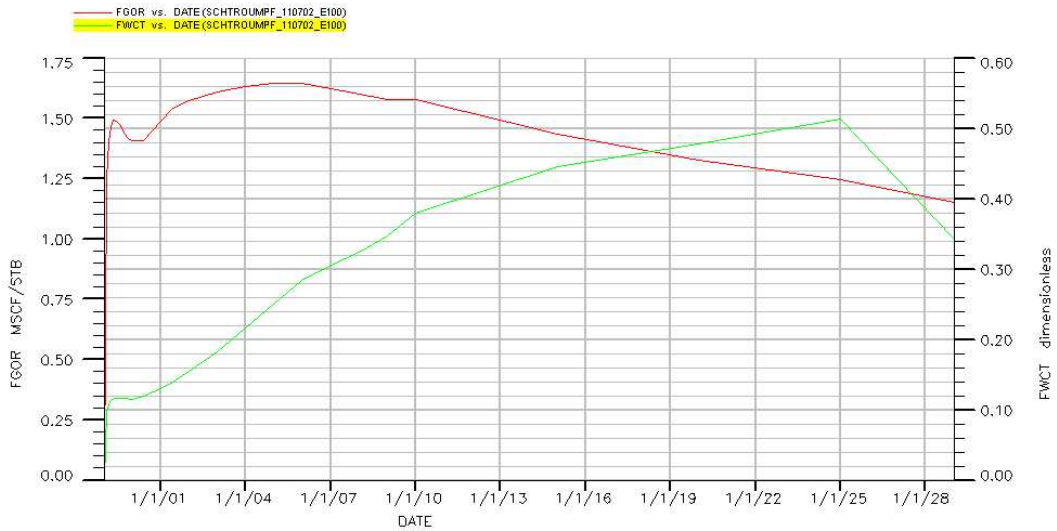
Appendix 56: WELL 9 well performances, BEIMRU model



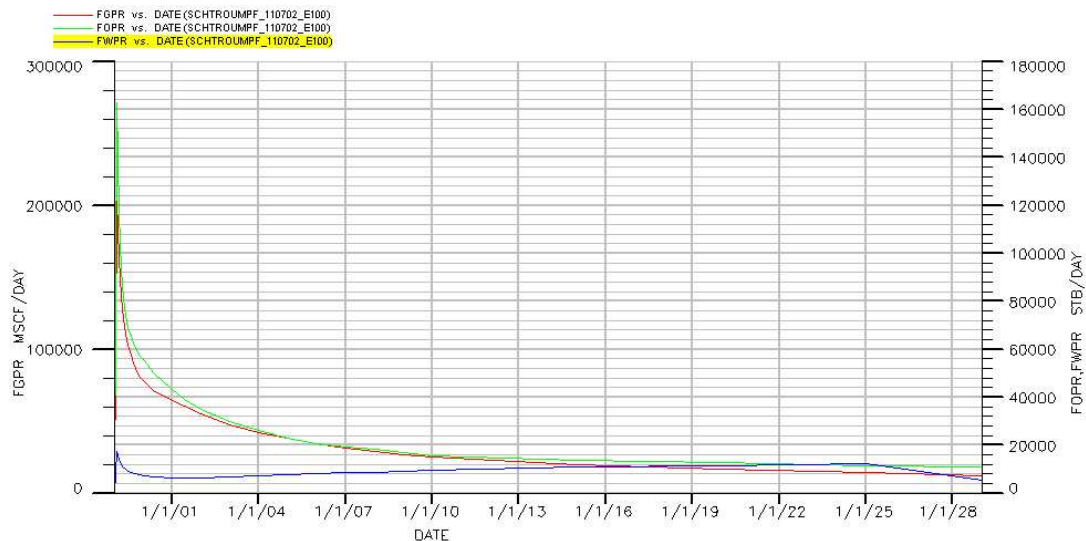
Appendix 57: WELL 18 well injection performances, BEIMRU model



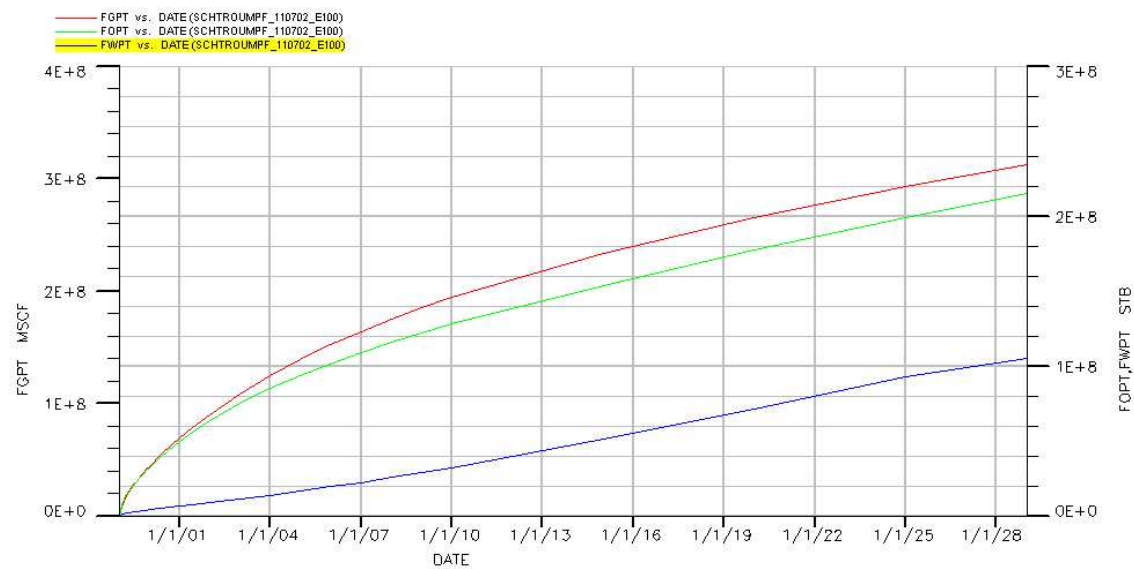
Appendix 58: Field production ratios, BFIMRU model



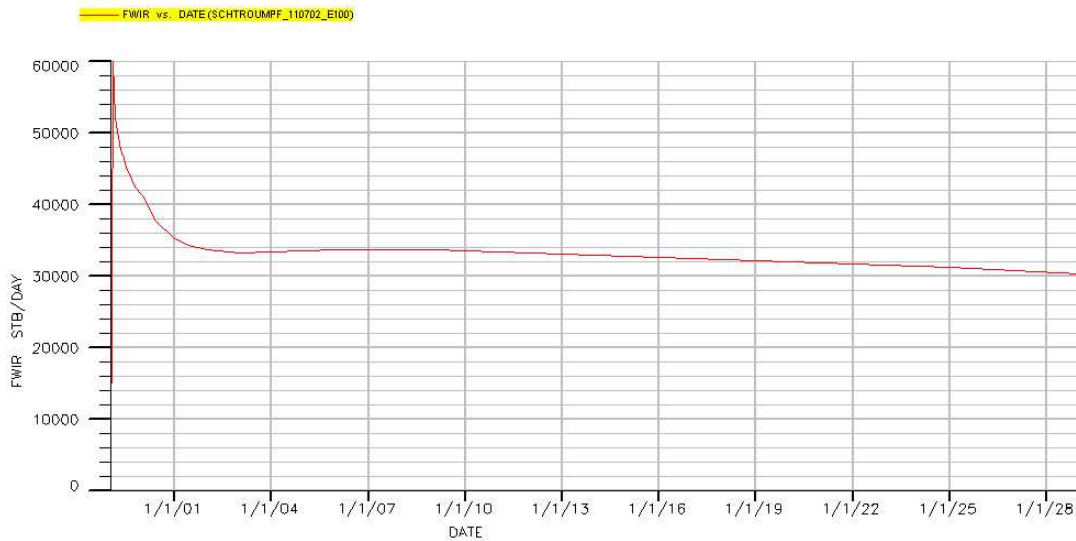
Appendix 59: Field production rates, BFIMRU model



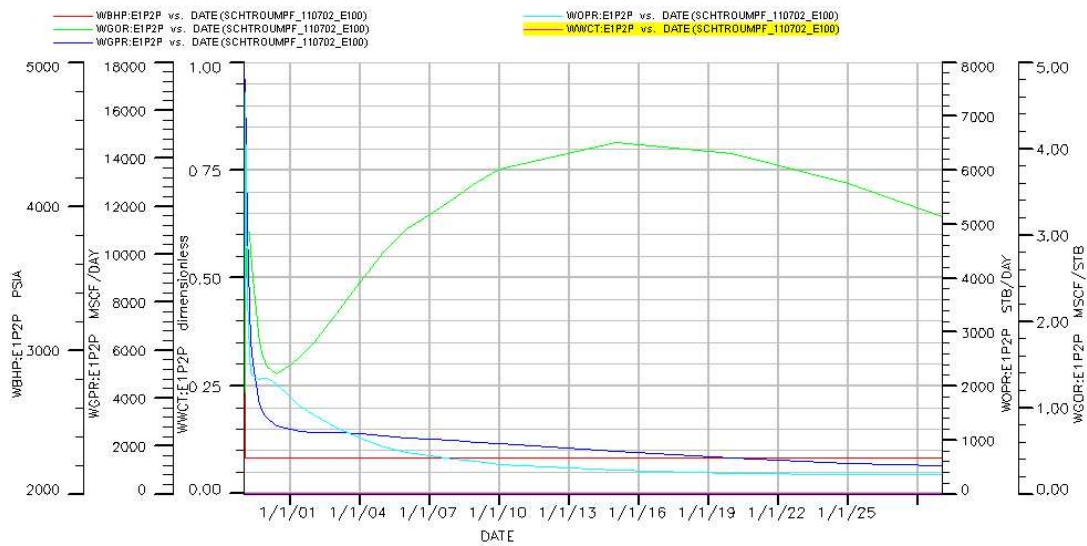
Appendix 60: Field cumulative fluid production, BFIMRU model



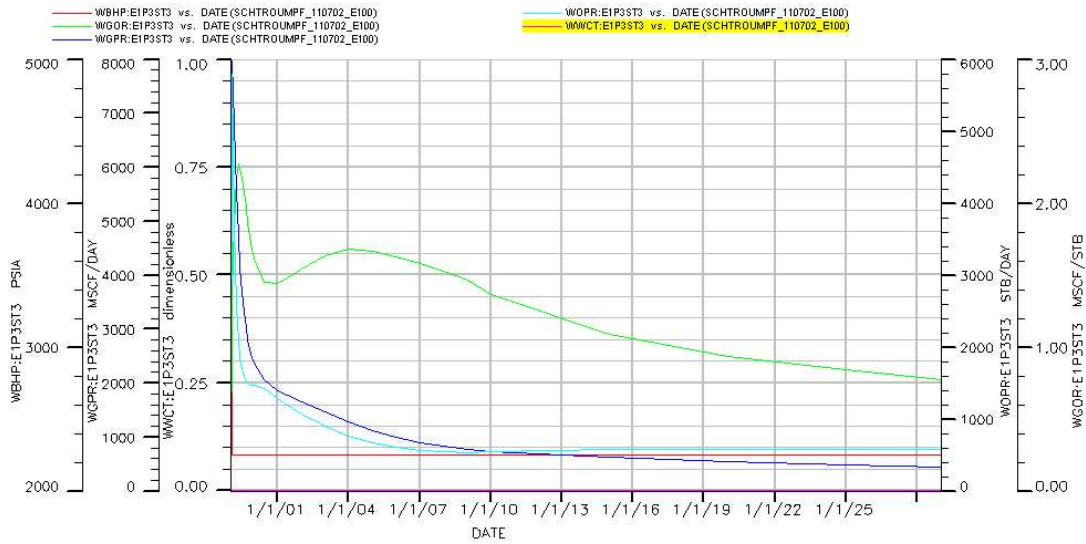
Appendix 61: Field water injection rate, BFIMRU model



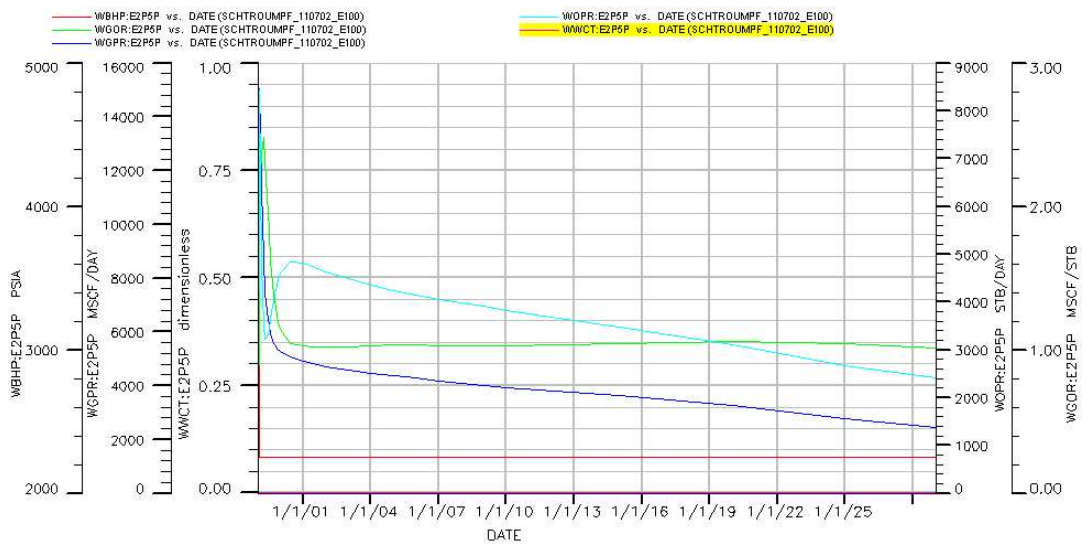
Appendix 62: WELL 1 well performances, BFIMRU model



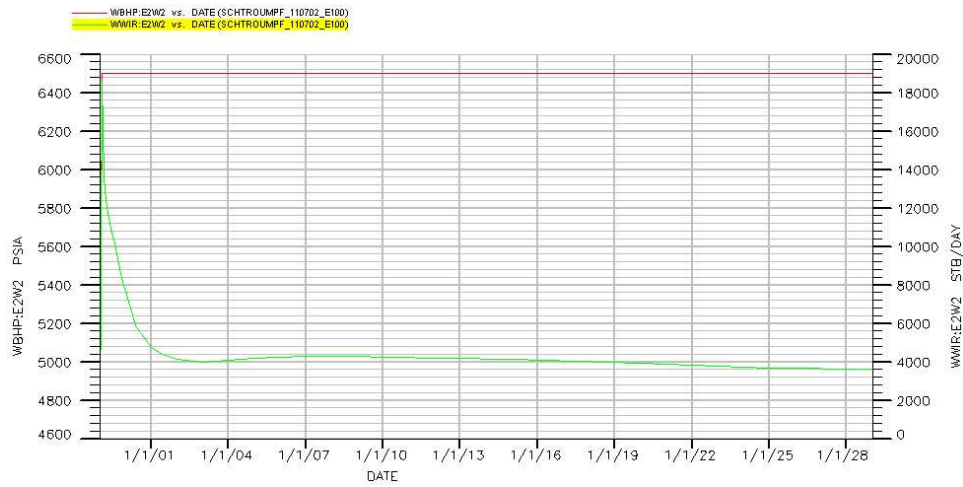
Appendix 63: WELL 2 well performances, BFIMRU model



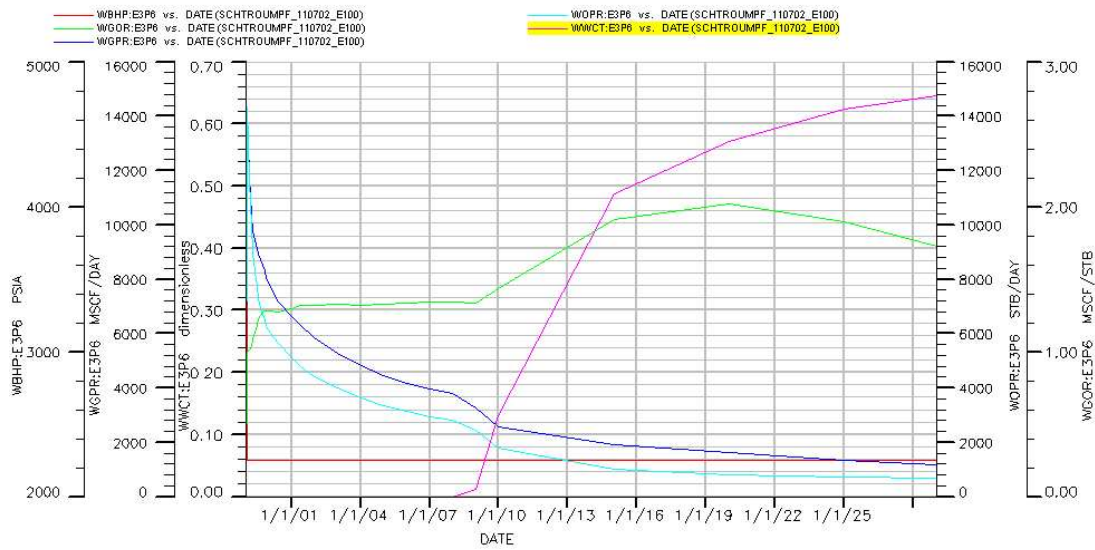
Appendix 64: WELL 6 well performances, BFIMRU model



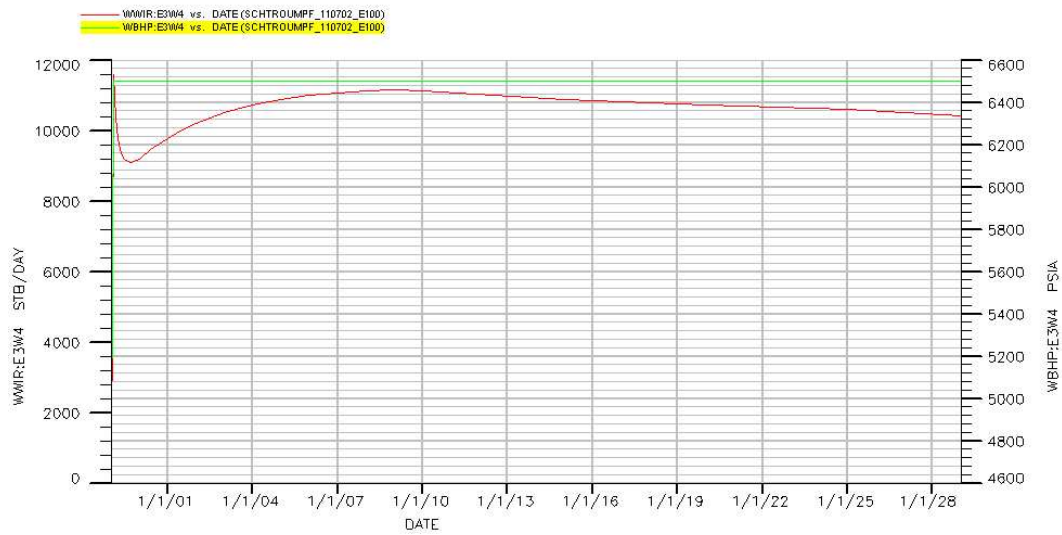
Appendix 65: WELL 16 well injection performances, BFIMRU model



Appendix 66: WELL 9 well performances, BFIMRU model



Appendix 67: WELL 18 well injection performances, BFIMRU model



Appendix 68: Symbols and abbreviations used in the text

Bo: Formation Volume Factor of oil. Ratio of quantity of produced oil at surface conditions over oil produced at reservoir conditions (STB/bbl)

DEX: Design of Experiment: a method to organize the combination of factors

GOR: Gas Oil Ratio: Quantity of gas produced over quantity of oil produced (Mscf/STB)

Gp: Cumulative gas produced after 30 years of production in this study, in MSCF/STB

Kv/Kh: permeability ratio: vertical permeability over horizontal permeability

MSCF: millions of square feet

MMSTB: Millions of stock tank barrels (surface conditions barrels)

Np: Cumulative oil produced after 30 years of production, in STB or MMSTB

OOIP: Original Oil In Place, original volume of oil in your reservoir, before production.

PVT: Pressure Volume Temperature fluid properties

Rec: recovery factor: ratio of oil produced over OOIP

STB: Stock tank barrels, volumetric unit

Wp: Cumulative water produced after 30 years of production

Appendix 69: Error factor computed for the 34 first models, for each response variable

Models	OOIP error	RF error	Np error	Wp/Np error	Gp/Np error
CAS MOYEN	10,71	0,0032	6,69	0,02	0,01
COARSE	-66,14	-0,0007	-14,96	-0,06	-0,03
AEIMQU	2,23	0,0105	3,99	1,14	-0,06
AEIMQV	10,28	-0,0014	-11,36	1,13	-0,04
AEIMRU	1,00	-0,0028	-9,33	1,15	-0,17
AEIMRV	5,66	0,0075	0,07	1,16	-0,07
AEINQU	0,09	-0,0065	0,67	1,15	0,09
AEINQV	-2,28	-0,0038	4,15	1,14	-0,02
AEINRU	1,01	-0,0067	0,14	1,14	0,19
AEINRV	3,24	-0,0063	2,61	1,15	0,09
AEJMQU	59,88	-0,0076	2,85	-1,20	-0,08
AEJMQV	55,53	-0,0064	0,77	-1,20	-0,19
AEJMRU	53,08	-0,0032	4,90	-1,20	0,01
AEJMRV	49,60	-0,0063	0,04	-1,19	-0,10
AEJNQU	-56,13	0,0070	0,32	-1,16	0,10
AEJNQV	-59,31	0,0088	0,69	-1,17	0,18
AEJNRU	-53,44	0,0091	2,27	-1,21	-0,01
AEJNRV	-62,00	0,0077	-0,91	-1,20	0,09
AFIMQU	-57,19	-0,0090	-0,29	-1,16	0,01
AFIMQV	-53,03	-0,0050	3,44	-1,17	0,11
AFIMRU	-63,98	-0,0091	-2,34	-1,15	-0,09
AFIMRV	-58,91	-0,0075	-0,62	-1,17	0,01
AFINQU	54,12	0,0073	-2,08	-1,19	0,00
AFINQV	58,45	0,0111	3,57	-1,20	-0,10
AFINRU	59,46	0,0013	-6,87	-1,13	0,10
AFINRV	63,01	0,0057	-2,12	-1,15	0,01
AFJMQU	2,63	0,0070	1,10	1,14	0,00
AFJMQV	2,15	0,0074	-1,85	1,13	-0,09
AFJMRU	-5,08	0,0126	4,07	1,14	0,08
AFJMRV	-3,94	0,0128	4,44	1,14	0,00
AFJNQU	-8,96	-0,0113	-3,97	1,15	-0,02
AFJNQV	-12,63	-0,0063	-0,45	1,13	0,08
AFJNRU	7,02	-0,0099	0,42	1,09	-0,09
AFJNRV	65,42	0,0029	11,83	-1,16	0,08

Appendix 70: Error factor computed for the 32 last models, for each response variable

Name	OOIP error	RF error	Np error	Wp/Np error	Gp/Np error
BEIMQU	-58,87	-0,0079	-15,03	-1,19	0,00
BEIMQV	-56,33	-0,0081	-14,78	-1,14	0,11
BEIMRU	-63,09	0,0001	-9,05	-1,16	-0,11
BEIMRV	-62,70	-0,0015	-6,88	-1,13	-0,03
BEINQU	57,22	0,0090	14,54	-1,12	-0,02
BEINQV	52,36	0,0065	12,09	-1,10	-0,09
BEINRU	58,87	0,0087	13,39	-1,12	0,11
BEINRV	57,90	0,0065	13,97	-1,11	0,00
BEJMQU	2,97	-0,0241	-13,39	1,18	0,01
BEJMQV	0,38	-0,0257	-16,95	1,16	-0,08
BEJMRU	-3,42	-0,0181	-9,85	1,11	0,08
BEJMRV	-4,41	-0,0211	-11,57	1,13	-0,02
BEJNQU	-1,15	0,0188	10,28	1,24	0,00
BEJNQV	-3,24	0,0176	7,18	1,22	0,10
BEJNRU	8,57	0,0201	13,20	1,22	-0,09
BEJNRV	6,38	0,0186	11,03	1,21	0,00
BFIMQU	-119,78	-0,0207	-13,24	1,15	-0,11
BFIMQV	-116,05	-0,0226	-13,76	1,16	0,00
BFIMRU	-119,73	-0,0265	-19,19	1,17	-0,18
BFIMRV	-118,34	-0,0238	-15,35	1,18	-0,10
BFINQU	115,69	0,0288	18,48	1,20	0,08
BFINQV	116,18	0,0271	19,82	1,23	0,04
BFINRU	117,02	0,0263	16,19	1,21	0,16
BFINRV	116,27	0,0232	15,18	1,24	0,08
BFJMQU	-48,57	-0,0112	-15,46	-1,18	-0,09
BFJMQV	-49,75	-0,0112	-17,91	-1,18	-0,18
BFJMRU	-56,31	-0,0061	-12,95	-1,19	0,00
BFJMRV	-54,74	-0,0094	-16,15	-1,20	-0,08
BFJNQU	57,16	0,0101	17,34	-1,14	0,07
BFJNQV	55,76	0,0105	19,18	-1,14	0,18
BFJNRU	58,22	0,0020	9,61	-1,11	0,03
BFJNRV	55,45	0,0031	9,93	-1,13	0,10

VITA

Name:

KARINE CHRYSTEL SCHEPERS

Permanent Address:

3 rue Gaston
94210 La Varenne, FRANCE

Education:

B.S., Geology 2001.
Institut Géologique Albert-de-Lapparent.
Cergy, France.

M.S., Geology 2003.
Texas A&M University.
College Station, Texas.